VOLTAGE HARMONIC ADJUSTMENT of CUK and SEPIC CONVERTERS

By MICHAEL K. JORDAN

For JACKSON COLLEGE OF GRADUATE STUDIES and

ENGINEERING and PHYSICS DEPARTMENT

AT UNIVERSITY OF CENTRAL OKLAHOMA

VOLTAGE HARMONIC ADJUSTMENT OF CUK AND SEPIC CONVERTERS

VOLTAGE HARMONIC ADJUSTMENT OF CUK AND SEPIC CONVERTERS

Thesis Title

Michael Jordan

Author's Name

May 7, 2020

Date

Jackson College of Graduate Studies at the University of Central Oklahoma

A THESIS APPROVED FOR

The Department of Engineering and Physics at the University of Central Oklahoma

By

Alaeddin Abuabed

Committee Chairperson

Evan Lemley Digitally signed by Evan Lemley Date: 2020.05.04 10:54:07 -05'00'

Committee Member

Weldon Wilson

Committee Member

Committee Member

Abstract

Voltage harmonics are present on electrical power lines today. These harmonics are voltage fluctuations which can be the result of dc to dc converters due to their high frequency switching called Pulse Width Modulation (PWM). PWM switch ON and OFF very quickly to control their output voltage. If harmonics are high enough, it can cause other equipment connected to that same power line to fail prematurely, due to the equipment operating outside its designed voltage margin.

This thesis shows that voltage harmonics can be adjusted by randomizing the PWM signal which is supplied to two dc to dc converters. The randomization technique applied is Random Pulse Width Modulation (RPWM), Random Phase Position Modulation (RPPM) and a combination of both RPWM and RPPM. These randomization techniques are applied to Single Ended-Primary Inductor Converter (SEPIC) and Cuk converters.

The results show that some randomization techniques can adjust the voltage harmonics if the applied PWM has enough time margin to randomize within each pulse. RPPM technique adjusted the voltage harmonics the most.

Table of Contents

LIST OF FIGURES

LIST OF TABLES

Chapter 1

BACKGROUND OF DC TO DC CONVERTERS

Direct Current (DC) to DC converters are commonly used today with cell phones, laptops, telecommunications, aerospace and medical equipment [Kazimierczuk]. A DC to DC converter is a device which changes a known input voltage, V_i and outputs a known voltage V_o which is usually higher or lower in magnitude than V_i. Dc to dc converters are used because of their high efficiency in voltage conversions. Efficiency is greatly desired when the converters are powered from a battery. A battery's power source capacity would be limited and the need to minimize wasted energy is highly encouraged. The efficiency of a converter, η, is defined by the following equation [Krein]:

$$\eta = \frac{P_{out}}{P_{in}}. \tag{1-1}$$

where P_{out} and P_{in} is the converter's real output and input power (Watts), respectively.

Why use DC to DC Converters?

Basic dc to dc converters can either increase or decrease the output voltage relative its supplied input voltage. When output voltage is reduced this is called a buck converter. When output voltage is increased, this is called a boost converter. But if a buck converter is being used, why not use a resistor to drop the voltage? If a resistor is connected in series to a load, the resistor can drop applied input voltage to a lower level and meet the output voltage requirement of a converter. The answer as to why a resistor isn't always used to reduce the applied input voltage resides with the converter's efficiency equation, which was provided earlier. The addition of resistors could be utilized to as shown in Figure 1.1.Voltage source is the input voltage which is the total voltage of the input resistor's voltage drop (8.13 volts) and the output resistor's voltage drop (3.87 volts). So the input voltage is 12 volts total and the output voltage is 3.87 volts. This circuit receives 12 volts and then drops it to 3.87 volts.

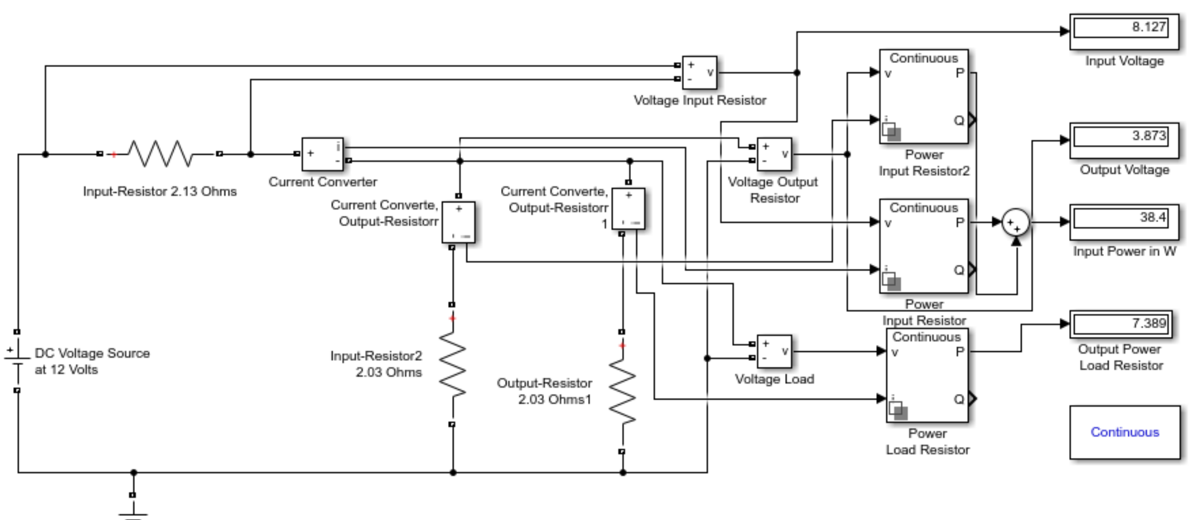

Figure 1.1, Voltage Reduction through Addition of Resistors [Krein], MATLAB model of Example 3.2.1

The power consumed by this converter shows that P_{in} = 38.4 Watts and P_{out}=7.39 Watts. The efficiency calculation of the circuit shows the following:

$$\eta = \frac{P_{out}}{P_{in}} = \frac{7.39\,Watts}{38.4\,Watts} = 19.2\%\text{ Efficient.} \tag{1-2}$$

The efficiency of this circuit is 19.2% which means 80.8% of the power supplied to the circuit is wasted as heat and not used for voltage conversion. Which means if this circuit was powered from a battery a lot of wasted energy would result and drain the battery quickly.

Now if a dc to dc buck converter is utilized, the voltage conversion's power efficiency is increased drastically by comparing the output and input power values as shown in Figure 1.2.

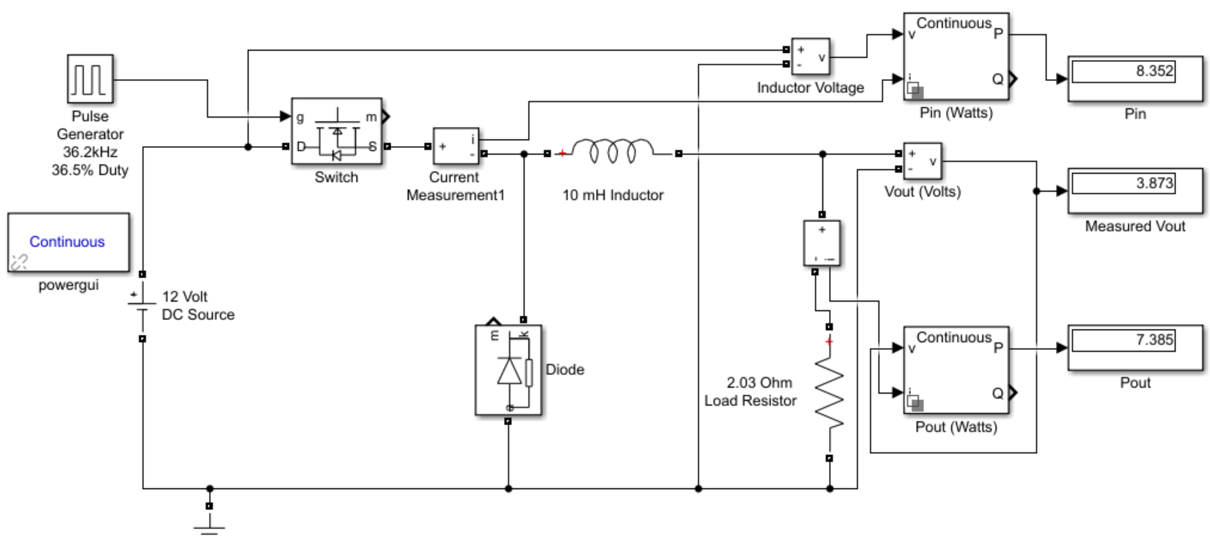

Figure 1.2, Buck Converter using same Voltage Input and Output Values

As a result of Figure 1.2 buck converter, the same output voltage conversion occurred 12 volts to 3.87 volts, but the input power now is 8.35 Watts while the output power is still 7.39 Watts. The buck converter's efficiency equation is shown as follows:

$$\eta = \frac{P_{out}}{P_{in}} = \frac{7.39\,Watts}{8.35\,Watts} = 88.5\%\text{ Efficient.} \tag{1-3}$$

This shows that the buck converter efficiency of 88.5% is losing 11.5% of that power to heat. The buck converter is a far better choice if the conversion occurs from a battery source, which would aid in extending the battery's life. So, converters can be very efficient from converting from one voltage level to another due to utilizing four major components:

1) Metal-Oxide Field Effect Transistor (MOSFET) transistor
2) Diode
3) Inductor
4) Capacitor.

A MOSFET transistor is a device which behaves as an electronic switch between its source and drain pins when a threshold voltage is exceeded on the gate pin [Aminian]. This MOSFET transistor connects the drain and source pins together during its ON state and then disconnects those pins during its OFF. The MOSFET IRF520, was used in this thesis, which was able to switch between ON and OFF very quickly at 36.2 kHz. The inductors and capacitors in the circuit behave differently during the high frequency switching as compared to normal steady state voltage. Inductors have the following behavior equation[Alexander]:

$$V_L = L\frac{di_L}{dt}. \tag{1-4}$$

The equation above shows that inductor's voltage can freely change but current does not change instantly. The inductor component, and its nature to not change current instantly, is used to control the current flow through the dc to dc converter. During high frequency switching, the inductor can behave similarly to a current source, for short durations between cycles [Krein]. Similar to the inductor, capacitors also behave differently when compared to steady state voltage. This time the capacitor's voltage does not change instantly, as shown below [Alexander]:

$$i = C\frac{dv}{dt}. \tag{1-5}$$

Capacitors change freely with current but voltage does not change instantaneously. So under really high switching frequencies the capacitor can behave like a voltage source, for short durations [Krein]. These components are able to behave in those conditions due to the inductors and capacitors are energy storing devices. During high frequencies conditions, the inductors and capacitors can adjust the input voltage to increase or decrease in magnitude due to their nature to resist changes in current and voltage instantly, respectively.

A diode behaves similarly to a switch in which it allows current to flow in one direction and when voltage drop across the diode is low enough, it switches to the OFF state and stops the flow of current. This is used to again to maximize the voltage and current sources coming from the inductor and capacitors. The diode used in this thesis was 1N5817 which utilizes a lower voltage drop value of 0.45 volts when turned ON.

Background: Basic Types of Converters

Using the high frequency switching of the MOSFET transistor and specifically arranging the inductor and capacitor components, the two basic converters are a buck converter and boost converter, as mentioned before. The buck converter output voltage will be lower in magnitude than the converter's input voltage. Likewise, a boost converter will result in an output voltage higher in magnitude than the converter's input voltage. An example of a buck converter is shown in Figure 1.3.

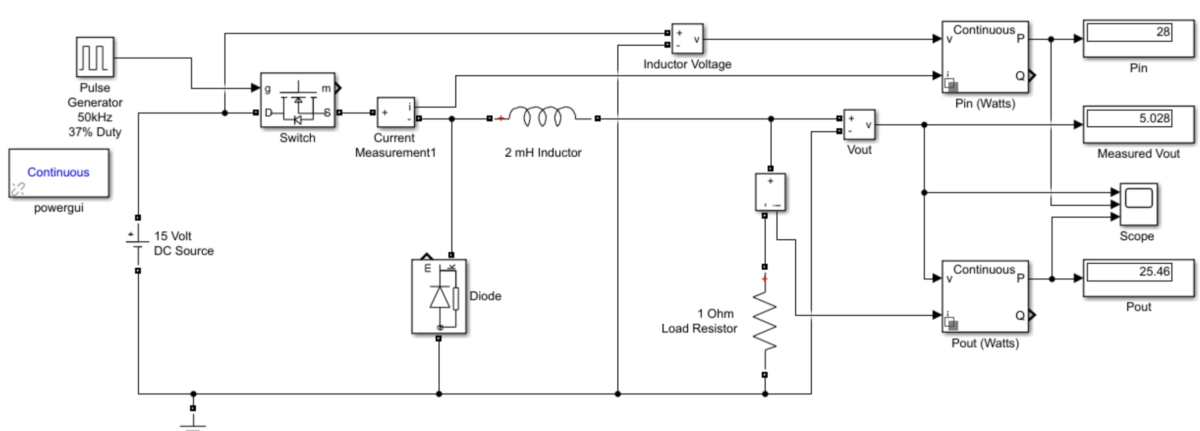

Figure 1.3, Buck Converter [Krein], from Example 3.4.1

The buck converter's inductor behaves like a current source to the resistor. The voltage remains constant as a result of both the MOSFET's and diode's high switching frequency and the current flowing from the inductor. The "Pulse Generator" as shown in Figure 1.3, includes a parameter of duty cycle, D, and switching frequency, f_s. Duty cycle is a ratio of time that the transistor is switched ON, T_{on}, during its full one cycle switching time, T_s. The switching time is derived from the switching frequency, f_s:

$$f_s = \frac{1}{T_s}. \tag{1-6}$$

Where T_s is the time for one cycle for the transistor. Duty cycle is then derived from:

$$D = \frac{T_{on}}{T_s}. \tag{1-7}$$

Duty cycle ratio, D, can also be expressed in terms of time OFF, T_{OFF}, as shown in Figure 1.4.

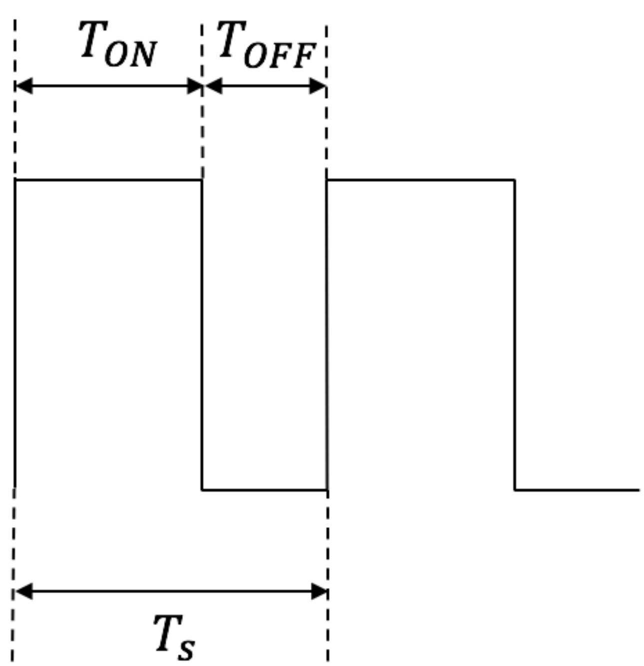

Figure 1.4, Duty Cycle Ratio, (Mohen)

The duty cycle is related to each applied signal to the transistor which can also be referred to as a Pulse Width Modulation (PWM) signal. This signal is called a PWM signal because the duty cycle could increase, which means T_{on} would increase, thus increasing the pulse width of that signal. The term PWM is used throughout this thesis.

The converters used for this thesis are the Single Ended Primary Inductor Converter (SEPIC) and Cuk converters. These converters are described in more detail in the following sections.

Background: SEPIC Converter

Single Ended Primary Inductor Converter (SEPIC) is a circuit type which has a different arrangement of inductors, capacitors and switches when compared to the basic buck and boost converters. The SEPIC circuit allows V_o to be either higher or lower in magnitude when compared to V_i depending on the duty cycle applied to the PWM signal. An example of the SEPIC converter [Hammerbauer] is shown in Figure 1.5.

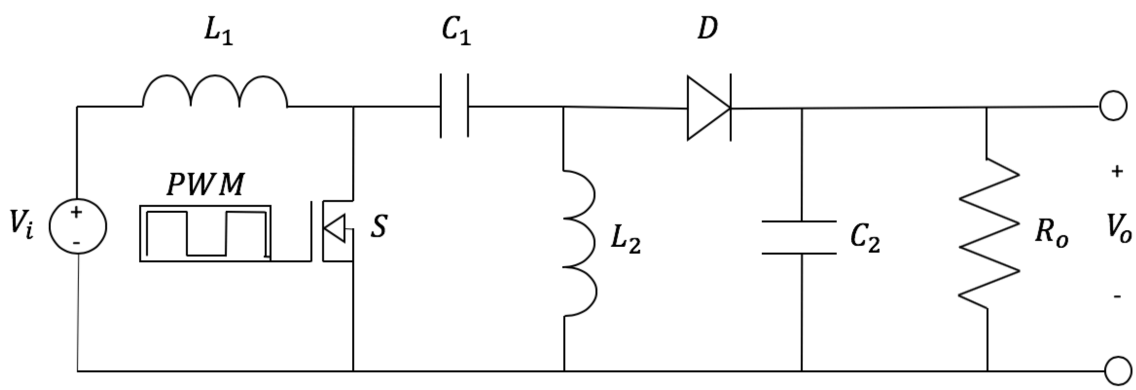

Figure 1.5, SEPIC Converter Example

The circuit in Figure 1.5 shows the overview of the power source, inductors, capacitors, transistor, diode and resistor locations. The transistor receives a PWM signal which turns the transistor ON or OFF very quickly. Figure 1.6 explains how the SEPIC operates in steady state conditions, which is where the converter has been operating for a while and there are no inrush currents as a result of turning the converter ON.

During steady state, Figure 1.6 shows the basic of how the SEPIC converter operates when the switch, S, is turned ON and the diode, D, is OFF. The diode is OFF because it is operating in the reverse voltage position which means that the diode prevent current to flow through it [Aminian]. When the SEPIC converter's transistor, S, is ON, and the diode, D, is OFF the converter is charging its inductors and discharging its capacitors. Inductor L_1 is charging from the power source V_i, Capacitor C_1discharges into inductor L_2, Capacitor C_2 discharges its energy into the output resistor, R_o [Zhang].

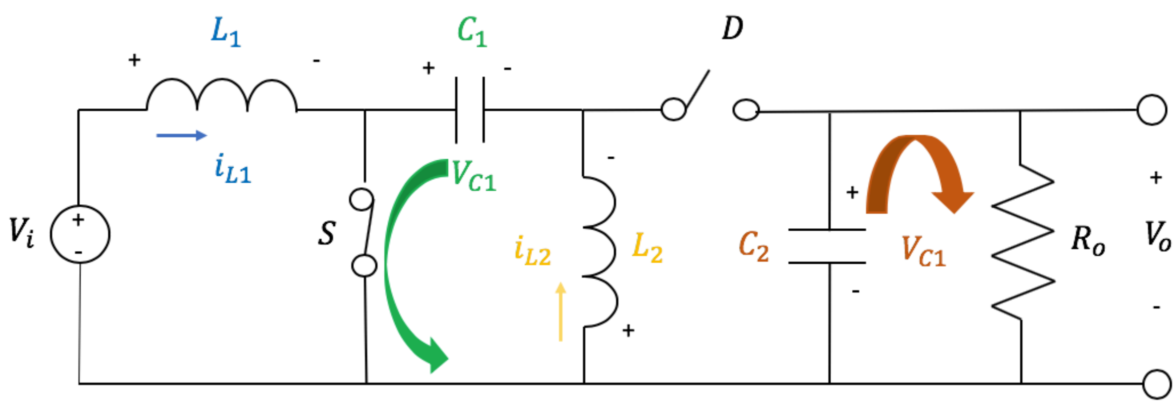

Figure 1.6, Switch ON and Diode Off, Explanation of SEPIC Operation [Zhang and Hammerbauer]

As shown in Figure 1.7, when the SEPIC's transistor is turned OFF and its diode is turned ON, the inductors' discharge and the capacitors' charge. The inductors, being previously charged, are now discharging to both the capacitors and load resistor. Inductor L_1 discharges to capacitor C_1, while inductor L_2, and some remaining current from inductor L_1, both discharge into both capacitor C_2 and resistor R_o [Hammerbauer].

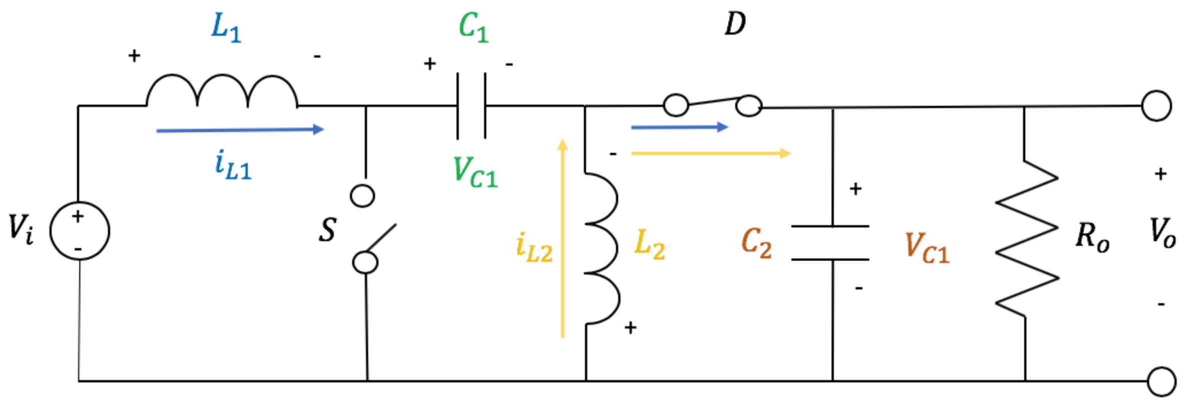

Figure 1.7, SEPIC Operation for Switch OFF and Diode ON [Hammerbauer]

As a result of this charging and discharging of both the inductors and the capacitors, the resistor receives energy from both component types and maintains a constant output voltage that is either higher or lower in magnitude than the input voltage.

Background: CUK Converter

A Cuk converter can also supply an output voltage, V_o, which is either higher or lower in magnitude than its input voltage, V_i; but the output voltage polarity is reversed. If V_i is positive then V_o would be negative as shown by Figure 1.8 [Kushwaha].

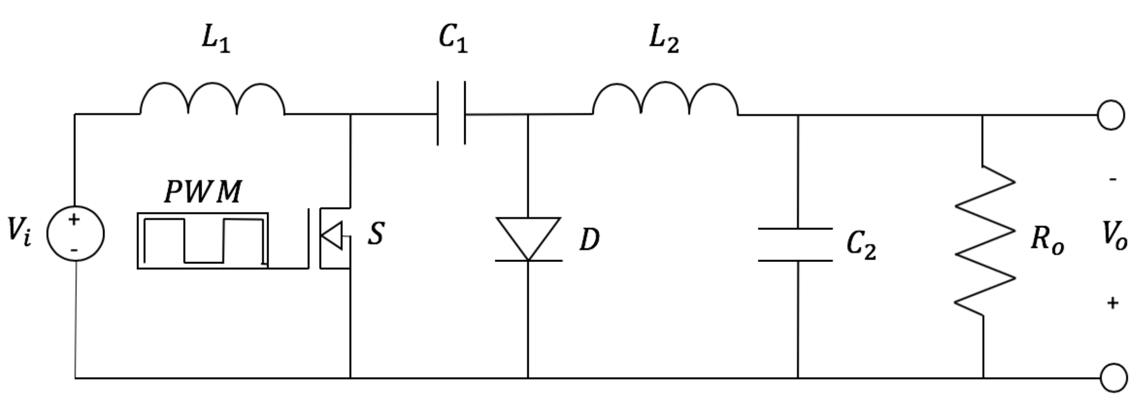

Figure 1.8, Basic Cuk Converter [Kushwaha]

When the transistor, S, is turned ON; the diode, D, is reversed biased and is turned OFF as shown in Figure 1.9 [Zhang and Kushwaha]. The capacitors discharge in this mode while the inductors are charging. The capacitor, C_1, discharges into inductor, L_2, through both C_2 and R_o and the inductor, L_1, is charging through the voltage source, V_i [Zhang].

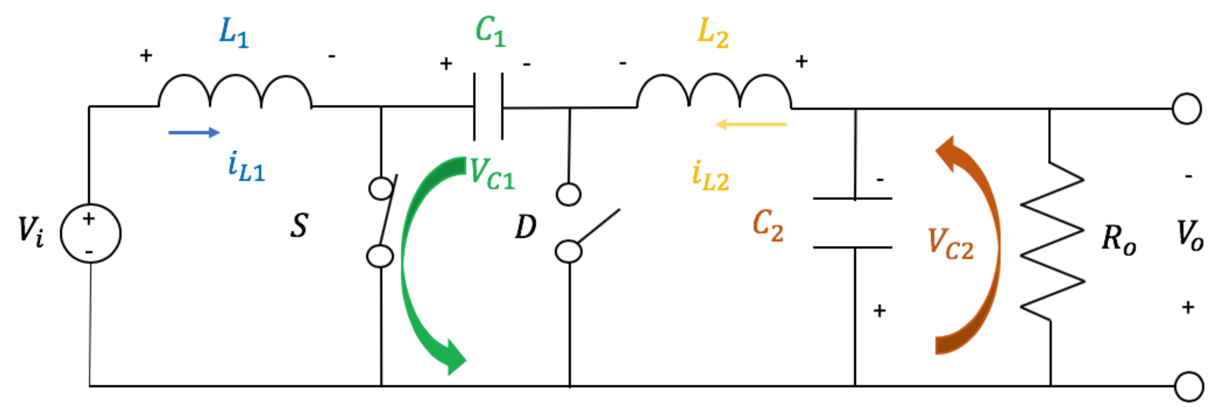

Figure 1.9, Cuk Converter with Switch ON and Diode OFF [Zhang and Kushwaha]

When the switch is OFF and the diode is ON, the inductors are discharging and the capacitors charging as shown by Figure 1.10. The L_1 inductor discharges into the C_1 capacitor, the L_2 inductor discharges into C_2 capacitor, and the output load, R_o [Zhang].

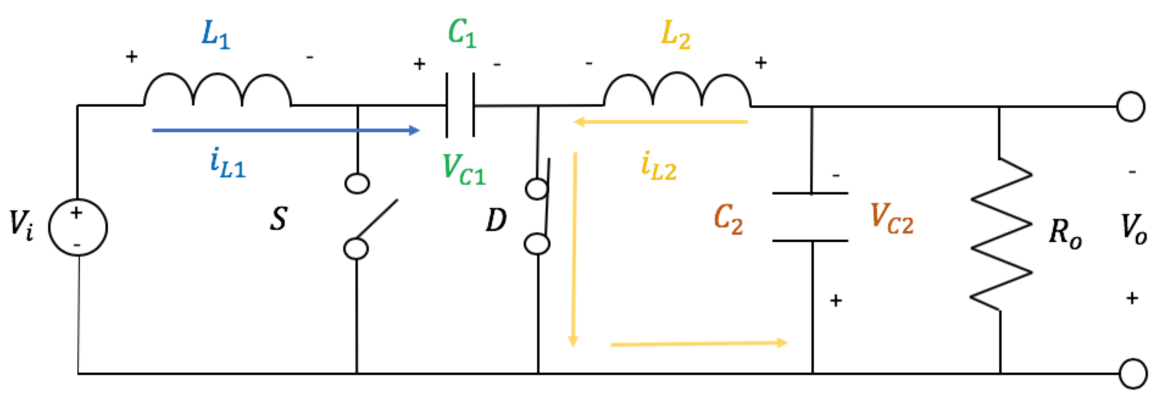

Figure 1.10, Cuk Converter with Switch ON and Diode OFF [Zhang and Kushwaha]

Background: Harmonics on a Power Line

Dc to dc converters can generate harmonics onto the power line it is connected too since the converters are switching ON and OFF very quickly. Harmonics can cause equipment, especially motors and transformers to fail prematurely [Santoso]. Harmonics add additional voltages, or current, on the power line but in multiples of the fundamental frequency. The total root-mean-squared (RMS) voltage is the square-root sum of the fundamental frequency voltage and the addition of the remaining voltages squared as shown by the equation provided below [Dugan]:

$$V_{rms} = \sqrt{\sum_{h=1}^{h_{max}} \left(\frac{1}{\sqrt{2}} V_h\right)^2} = \frac{1}{\sqrt{2}} \sqrt{V_1^2 + V_2^2 + V_3^2 + \cdots + V_{h_{max}}^2}. \tag{1-8}$$

This equation shows the harmonic voltages are portions which make up the total RMS voltage. The harmonic values, 1, 2, 3, etc. represent the multiplier of the fundamental frequency. For example, if 60 Hz is the fundamental frequency (h=1), the 2nd harmonic (h=2) would occur at 120 Hz, 3rd harmonic (h=3) would occur at 180 Hz, etc. Each frequency would have an RMS voltage assigned to it. Total Harmonic Distortion (THD) is a method to show the extent of harmonics on a power line. THD is defined by the equation below [Santoso]:

$$THD_V = \frac{V_{rms,h}}{V_{rms,1}} = \frac{\sqrt{\sum_{n=2}^{h_{max}} V_{rms,h}^2}}{V_{rms,1}}. \tag{1-9}$$

This equation shows the ratio of voltage distortion relative to the fundamental RMS voltage, $V_{rms,1}$. THD is used throughout this thesis to determine the overall impact on the power line.

Chapter 2

DERIVATION OF CUK AND SEPIC CONVERTERS USING STATE SPACE EQUATIONS

State space representation is a way to model a system which can have multiple inputs and multiple outputs. A system is derived using dynamic variables, or state space variables. These state space variables are constantly changing within the system. The state space system is defined with these changing variables in mind. State Space equations are defined as [Nise]:

$$\dot{x} = Ax + Bu, \tag{2-1}$$

$$\text{and } \dot{x} = Cx + Du. \tag{2-2}$$

where A is the system matrix in relation to the state variables, x. B is the system input matrix. C is the system output matrix and D is the feedforward matrix (which is 0). Each of the converters, SEPIC and Cuk are derived for when the switching MOSFET transistor is ON and OFF. There are two separate state space equations for the SEPIC and Cuk converter. this derivation is to provide a detailed understanding of the circuits operation each of their ON and OFF conditions

State Space Equation for Cuk Converter, Transistor is ON

The Cuk converter has the following diagram [Kushwaha]:

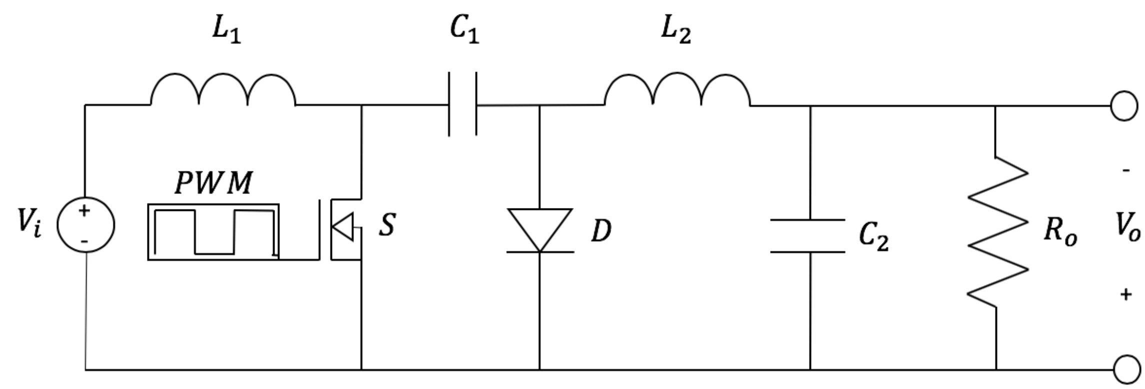

Figure 2.1, Cuk Basic Circuit

The state space variables are the energy storing passive devices from Figure 2.1, such as the inductors and capacitors. Since there are two of each component, this becomes a fourth order state space system and requires four state space equations to define each of those components. As shown in the previous chapter, inductors can be expressed in the following way:

$$V_L = L\frac{di_L}{dt}. \tag{2-3}$$

Where V_L is inductor's voltage and L is the inductance of the inductor. $\frac{di_L}{dt}$ is the inductor's change in current with respect to time which means that i_L is a state variable. Also recalled from the previous chapter is the equation for a capacitor is:

$$I_C = C\frac{dV_C}{dt}. \tag{2-4}$$

Where I_C is capacitor's current and C is the capacitance value of the capacitor. $\frac{dV_C}{dt}$ is the capacitor's change in voltage with respect to time which results in V_C is the other state variable. The state space equations also include assumed current and voltage values of the diode (i_D and

V_D) when turned ON and the equivalent series resistive elements of the inductors and capacitors, which are defined by R_L and R_C. The state space variables are shown below that need to derived from both Kirchhoff's Voltage (KVL) [Alexander] and Kirchhoff's Current (KCL) Laws [Alexander]:

$$x_1 = I_{L1}, x_2 = I_{L2}, x_3 = V_{C1}, \text{ and } x_4 = V_{C2}. \tag{2-5}$$

When the transistor is turned ON, apply KVL to find the state variable of I_{L1} to Figure 2.1. Starting with the input voltage and moving to the transistor the following equation results:

$$-V_i + V_{L1} + V_{RL1} = 0. \tag{2-6}$$

Which the equation becomes after rearranging:

$$V_{L1} = V_i - V_{RL1}. \tag{2-7}$$

Apply the inductor equation and the result is as follows:

$$\left(L_1 \frac{dI_{L1}}{dt}\right) = V_i - V_{RL1}. \tag{2-8}$$

With $V = IR$ the equation results in the first derived state equation:

$$\boldsymbol{\frac{dI_{L1}}{dt} = \frac{V_i}{L_1} - \frac{I_{L1}R_{L1}}{L_1}}. \tag{2-9}$$

Now to find I_{L2}, apply KVL again and start at capacitor C1 and move towards second capacitor which results in the following equation:

$$V_{C1} + V_{RC1} - V_{L2} - V_{RL2} - V_{C2} - V_{RC2} = 0. \tag{2-10}$$

Rearrange equation for V_{L2} results in the following equation:

$$V_{L2} = V_{C1} + V_{RC1} - V_{RL2} - V_{C2} - V_{RC2}. \tag{2-11}$$

With $V = IR$ the equation now becomes:

$$V_{L2} = V_{C1} + (I_{RC1}R_{C1}) - (I_{RL2}R_{L2}) - V_{C2} - (I_{RC2}R_{C2}). \tag{2-12}$$

Now, applying KCL results in $I_{RC2=}I_{L2} + \frac{V_o}{R_o}$. Additionally, $V_o = V_{C2} + V_{RC2}$ which results in the equation now as:

$$I_{RC2=}I_{L2} + \frac{V_{C2} + V_{RC2}}{R_o}. \tag{2-13}$$

After some rearranging the equation now becomes:

$$I_{RC2=}\frac{I_{L2}R_o + V_{C2}}{R_o - R_{C2}}. \tag{2-14}$$

Since $I_{RC1} = I_{RL2}$ and the result of $I_{RC2=}\frac{I_{L2}R_o+V_{C2}}{R_o-R_{C2}}$, the V_{L2} equation now becomes:

$$V_{L2} = V_{C1} + I_{L2}\left(R_{C1} - R_{L2} - \frac{R_o R_{C2}}{R_o - R_{C2}}\right) + V_{C2}\left(\frac{R_{C2}}{R_o - R_{C2}} - 1\right). \tag{2-15}$$

Applying the inductor equation, the resulting state equation is:

$$\boldsymbol{\frac{dI_{L2}}{dt} = \frac{V_{C1}}{L_2} + \frac{I_{L2}}{L_2}\left(R_{C1} - R_{L2} - \frac{R_o R_{C2}}{R_o - R_{C2}}\right) + \frac{V_{C2}}{L_2}\left(\frac{R_{C2}}{R_o - R_{C2}} - 1\right)}. \tag{2-16}$$

Now to find V_{C1} start by using KCL and focused on the node between the first capacitor and second inductor. The current equation is:

$$I_{C1} = -I_{L2}. \tag{2-17}$$

After applying the capacitor equation, the equation is now:

$$\left(C_1 \frac{dV_{C1}}{dt}\right) = -I_{L2}. \tag{2-18}$$

After some rearranging, the resulting state equation is:

$$\boldsymbol{\frac{dV_{C1}}{dt} = -\frac{I_{L2}}{C_1}}. \tag{2-19}$$

Now to find V_{C2} by using KCL and focused on the node between output resistor, second capacitor and inductor. The current equation is:

$$I_o + I_{C2} = I_{L2}. \tag{2-20}$$

With $I = \frac{V}{R}$ and $V_o = V_{C2} + V_{RC2}$ the equation becomes:

$$I_{C2} = I_{L2} - \frac{V_{C2}}{R_o} - \frac{V_{RC2}}{R_o}. \tag{2-21}$$

With V=IR the equation result is shown:

$$I_{C2}(R_o) = I_{L2}R_o - V_{C2} - I_{RC2}R_{C2}. \tag{2-22}$$

With $I_{RC2} = I_{C2}$ and combining like terms the equation is now:

$$I_{C2}(R_o + R_{C2}) = I_{L2}R_o - V_{C2}. \tag{2-23}$$

After rearranging the state space equation is:

$$I_{C2} = \frac{I_{L2}R_o}{R_o + R_{C2}} - \frac{V_{C2}}{R_o + R_{C2}}. \tag{2-24}$$

Applying the capacitor equation, the resulting state equation is:

$$\boldsymbol{\frac{dV_{C2}}{dt} = \frac{1}{C_2}\left(\frac{I_{L2}R_o}{R_o + R_{C2}} - \frac{V_{C2}}{R_o + R_{C2}}\right)}. \tag{2-25}$$

With the state variables derived, the state space equation for Cuk during transistor being turned ON is:

$$\begin{bmatrix} \dot{I_{L1}} \\ \dot{I_{L2}} \\ \dot{V_{C1}} \\ \dot{V_{C2}} \end{bmatrix} = \begin{bmatrix} -\frac{R_{L1}}{L_1} & 0 & 0 & 0 \\ 0 & \frac{1}{L_2}\left(R_{C1} - R_{L2} - \frac{R_oR_{C2}}{R_o - R_{C2}}\right) & \frac{1}{L_2} & \frac{1}{L_2}\left(\frac{R_{C2}}{R_o - R_{C2}} - 1\right) \\ 0 & -\frac{1}{C_1} & 0 & 0 \\ 0 & \frac{1}{C_2}\left(\frac{R_o}{R_o + R_{C2}}\right) & 0 & \frac{1}{C_2}\left(\frac{-1}{R_o + R_{C2}}\right) \end{bmatrix} \begin{bmatrix} I_{L1} \\ I_{L2} \\ V_{C1} \\ V_{C2} \end{bmatrix} + \begin{bmatrix} \frac{1}{L_1} \\ 0 \\ 0 \\ 0 \end{bmatrix} V_i. \tag{2-26}$$

The output equation for when the transistor is ON is shown below:

$$[\boldsymbol{V_o}] = \left[\boldsymbol{0} \quad \frac{(\boldsymbol{V_{C2}R_o})}{\boldsymbol{R_o + R_{C2}}} \quad \boldsymbol{0} \quad \left(\frac{\boldsymbol{R_{C2}R_o}}{\boldsymbol{R_o + R_{C2}}}\right)\right] \begin{bmatrix} \boldsymbol{I_{L1}} \\ \boldsymbol{I_{L2}} \\ \boldsymbol{V_{C1}} \\ \boldsymbol{V_{C2}} \end{bmatrix}. \tag{2-27}$$

Cuk Circuit State Space Derivation for Transistor OFF

Now to derive the Cuk converter when the transistor is turned OFF. To find the state variable of I_{L1} apply KVL to the Figure 2.2 [Kushwaha].

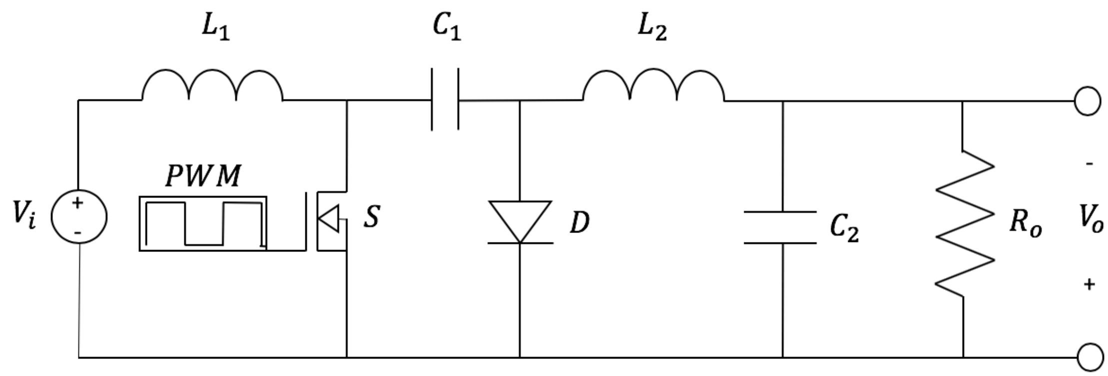

Figure 2.2, Cuk Basic Circuit

Starting from the source and moving towards the diode the equation is:

$$-V_i + V_{L1} + V_{RL1} + V_{C1} + V_{RC1} = 0. \tag{2-28}$$

Which becomes after rearranging the equation:

$$V_{L1} = V_i - V_{RL1} - V_{C1} - V_{RC1}. \tag{2-29}$$

Applying the state variable equation for the inductor results in:

$$\left(L_1 \frac{dI_{L1}}{dt}\right) = V_i - V_{RL1} - V_{C1} - V_{RC1}, \tag{2-30}$$

which becomes:

$$\boldsymbol{\frac{dI_{L1}}{dt} = \frac{V_i}{L_1} - \frac{V_{RL1}}{L_1} - \frac{V_{C1}}{L_1} - \frac{V_{RC1}}{L_1}}. \tag{2-31}$$

Now to find I_{L2}, apply KVL again from the diode to the second capacitor:

$$-V_d - V_{L2} - V_{RL2} - V_{C2} - V_{RC2} = 0. \tag{2-32}$$

Rearrange the equation and it simplifies to the following:

$$V_{L2} = -V_d - V_{RL2} - V_{C2} - V_{RC2}. \tag{2-33}$$

With $V = IR$ the equation becomes:

$$V_{L2} = -V_d - (I_{RL2}R_{L2}) - V_{C2} - (I_{RC2}R_{C2}). \tag{2-34}$$

With $I_{RC1} = I_{RL2}$ and $I_{RC2=}\frac{I_{L2}R_o+V_{C2}}{R_o-R_{C2}}$, the above equation becomes:

$$V_{L2} = -V_d - I_{L2}\left(R_{L2} + \frac{R_oR_{C2}}{R_o - R_{C2}}\right) - V_{C2}\left(\frac{R_{C2}}{R_o - R_{C2}} + 1\right). \tag{2-35}$$

Applying the inductor equation, the state space equation is now:

$$\boldsymbol{\frac{dI_{L2}}{dt} = -\frac{V_d}{L_2} - \frac{I_{L2}}{L_2}\left(R_{L2} + \frac{R_oR_{C2}}{R_o - R_{C2}}\right) + \frac{V_{C2}}{L_2}\left(\frac{R_{C2}}{R_o - R_{C2}} + 1\right)}. \tag{2-36}$$

Now to find V_{C1} by using KCL at the node between C1, L2 and the diode results in the following:

$$I_{C1} + I_{L2} = I_d. \tag{2-37}$$

Applying the state variable equation for the capacitor results in the following:

$$\left(C_1\frac{dV_{C1}}{dt}\right) = I_d - I_{L2}. \tag{2-38}$$

Simplifying the equation, the result is:

$$\boldsymbol{\frac{dV_{C1}}{dt} = \frac{I_d}{C_1} - \frac{I_{L2}}{C_1}}. \tag{2-39}$$

Now to find V_{C2} by using KCL at the output between the second capacitor, second inductor and the output resistor results in the following:

$$I_o + I_{C2} = I_{L2}. \tag{2-40}$$

With $I = \frac{V}{R}$ and $V_o = V_{C2} + V_{RC2}$ the equation becomes:

$$I_{C2} = I_{L2} - \frac{V_{C2}}{R_o} - \frac{V_{RC2}}{R_o}. \tag{2-41}$$

and multiply R_o to both sides results in:

$$I_{C2}(R_o) = I_{L2}R_o - V_{C2} - I_{RC2}R_{C2}. \tag{2-42}$$

With $I_{C2} = I_{RC2}$ and simplifying, results in:

$$I_{C2}(R_o + R_{C2}) = I_{L2}R_o - V_{C2}. \tag{2-43}$$

After simplifying the equation for just I_{C2}, the equation is now:

$$I_{C2} = \frac{I_{L2}R_o}{R_o + R_{C2}} - \frac{V_{C2}}{R_o + R_{C2}}. \tag{2-44}$$

Applying the state variable equation for the inductor results in the following:

$$\frac{dV_{C2}}{dt} = \frac{1}{C_2}\left(\frac{I_{L2}R_o}{R_o + R_{C2}} - \frac{V_{C2}}{R_o + R_{C2}}\right). \tag{2-45}$$

With the state variables derived, the state space equation for Cuk during transistor is turned ON is:

$$\begin{bmatrix} \dot{I}_{L1} \\ \dot{I}_{L2} \\ \dot{V}_{C1} \\ \dot{V}_{C1} \end{bmatrix} = \begin{bmatrix} -\frac{(R_{L1} + R_{C1})}{L_1} & 0 & -\frac{1}{L_1} & 0 \\ 0 & -\frac{V_d}{L_2} - \frac{\left(R_{L2} + \frac{R_o R_{C2}}{R_o - R_{C2}}\right)}{L_2} & 0 & -\frac{1}{L_2}\left(1 + \frac{R_{C2}}{R_o - R_{C2}}\right) \\ 0 & \frac{i_d - 1}{C_1} & 0 & 0 \\ 0 & \frac{1}{C_2}\left(\frac{R_o}{R_o + R_{C2}}\right) & 0 & -\frac{1}{C_2}\left(\frac{1}{R_o + R_{C2}}\right) \end{bmatrix} \begin{bmatrix} I_{L1} \\ I_{L2} \\ V_{C1} \\ V_{C2} \end{bmatrix} + \begin{bmatrix} \frac{1}{L_1} \\ 0 \\ 0 \\ 0 \end{bmatrix} V_i. \tag{2-46}$$

And the output equation is:

$$[V_o] = \begin{bmatrix} 0 & \frac{(V_{C2}R_o)}{R_o + R_{C2}} & 0 & \left(\frac{R_{C2}R_o}{R_o + R_{C2}}\right) \end{bmatrix} \begin{bmatrix} I_{L1} \\ I_{L2} \\ V_{C1} \\ V_{C2} \end{bmatrix}. \tag{2-47}$$

SEPIC State Space Derivation for Transistor ON

To derive the equations for state space during transistor is turned ON, KCL and KVL are utilized. The same state variables are defined below:

$$x_1 = I_{L1}, x_2 = I_{L2}, x_3 = V_{C1}, \text{ and } x_4 = V_{C2}. \tag{2-48}$$

To find the state variable of I_{L1} apply KVL to Figure 2.3.

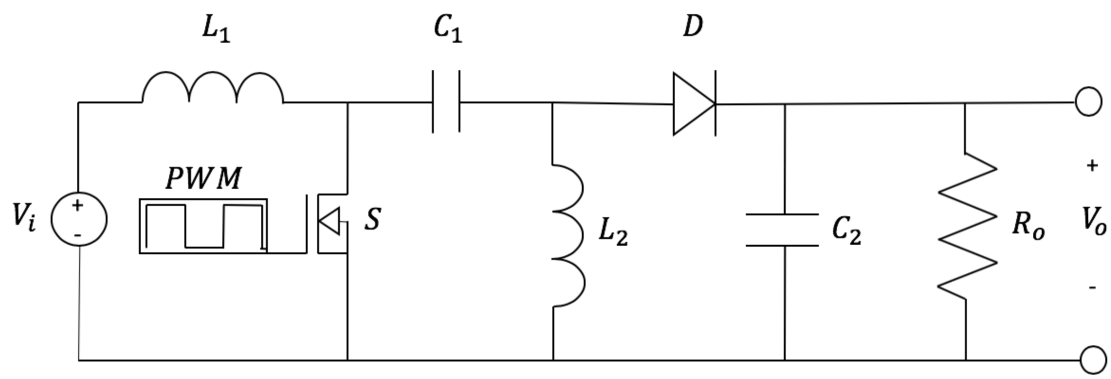

Figure 2.3, SEPIC Basic Circuit

Starting from the source and moving to the transistor, the KVL equation is

$$-V_i + V_{L1} + V_{RL1} = 0. \tag{2-49}$$

Which results after some rearranging:

$$V_{L1} = V_i - V_{RL1}. \tag{2-50}$$

With $V = IR$ and applying the inductor equation, the equation now becomes:

$$\left(L_1 \frac{dI_{L1}}{dt}\right) = V_i - (I_{RL1} R_{L1}). \tag{2-51}$$

After simplifying, the state space equation is now:

$$\boldsymbol{\frac{dI_{L1}}{dt} = \frac{V_i}{L_1} - \frac{I_{RL1} R_{L1}}{L_1}}. \tag{2-52}$$

Now to find I_{L2}, apply KVL between first capacitor and second inductor which results in the following:

$$V_{C1} + V_{RC1} - V_{L2} - V_{RL2} = 0. \tag{2-53}$$

After rearranging the equation:

$$V_{L2} = V_{C1} + V_{RC1} - V_{RL2}. \tag{2-54}$$

With $V = IR$, the equation becomes:

$$V_{L2} = V_{C1} + (I_{RC1}R_{C1}) - (I_{RL2}R_{L2}). \tag{2-55}$$

With $I_{RC1} = I_{RL2} = I_{L2}$ the above equation becomes:

$$V_{L2} = V_{C1} + I_{L2}(R_{C1} - R_{L2}). \tag{2-56}$$

After applying the inductor equation results in the following:

$$\boldsymbol{\frac{dI_{L2}}{dt} = -\frac{V_{C1}}{L_2} - \frac{I_{L2}}{L_2}(R_{C1} - R_{L2}).} \tag{2-57}$$

Now to find V_{C1} by using KCL between the first capacitor and the second inductor, the equation results:

$$I_{C1} = -I_{L2}. \tag{2-58}$$

Applying the state variable equation for the capacitor results in the following:

$$\left(C_1 \frac{dV_{C1}}{dt}\right) = -I_{L2}. \tag{2-59}$$

After simplifying, the state space equation is:

$$\boldsymbol{\frac{dV_{C1}}{dt} = -\frac{I_{L2}}{C_1}.} \tag{2-60}$$

Now to find V_{C2} by using KCL on the node between the second capacitor and the output resistor results:

$$I_{C2} = I_o. \tag{2-61}$$

With $I = \frac{V}{R}$ and $V_o = V_{C2} + V_{RC2}$, the equation now becomes:

$$I_{C2} = \frac{V_{C2}}{R_o} + \frac{V_{RC2}}{R_o}. \tag{2-62}$$

Multiply R_o to both sides results in the following equation:

$$I_{C2}(R_o) = V_{C2} + I_{RC2}R_{C2}. \tag{2-63}$$

With $I_{C2} = I_{RC2}$, the equation now becomes:

$$I_{C2}(R_o - R_{C2}) = V_{C2}. \tag{2-64}$$

After simplifying, the equation now becomes:

$$I_{C2} = \frac{V_{C2}}{R_o - R_{C2}}. \tag{2-65}$$

Applying the state variables for the capacitor results in the following equation:

$$\boldsymbol{\frac{dV_{C2}}{dt} = \frac{1}{C_2}\left(\frac{V_{C2}}{R_o - R_{C2}}\right)}. \tag{2-66}$$

With the state variables derived, the state space equation for SEPIC during transistor is turned ON is:

$$\begin{bmatrix} \dot{I_{L1}} \\ \dot{I_{L2}} \\ \dot{V_{C1}} \\ \dot{V_{C2}} \end{bmatrix} = \begin{bmatrix} -\frac{\boldsymbol{R_{L1}}}{L_1} & 0 & 0 & 0 \\ 0 & -\frac{\boldsymbol{1}}{L_2}(\boldsymbol{R_{C1}} - \boldsymbol{R_{L2}}) & \frac{1}{L_2} & 0 \\ 0 & -\frac{\boldsymbol{1}}{\boldsymbol{C_1}} & 0 & 0 \\ 0 & 0 & 0 & \frac{1}{C_2}\left(\frac{\boldsymbol{1}}{\boldsymbol{R_o} + \boldsymbol{R_{C2}}}\right) \end{bmatrix} \begin{bmatrix} I_{L1} \\ I_{L2} \\ V_{C1} \\ V_{C2} \end{bmatrix} + \begin{bmatrix} \frac{1}{L_1} \\ 0 \\ 0 \\ 0 \end{bmatrix} V_i. \tag{2-67}$$

And the output equation is:

$$[V_o] = \begin{bmatrix} 0 & \frac{(\boldsymbol{V_{C2}R_o})}{R_o + R_{C2}} & 0 & \left(\frac{\boldsymbol{R_{C2}R_o}}{\boldsymbol{R_o} + \boldsymbol{R_{C2}}}\right) \end{bmatrix} \begin{bmatrix} I_{L1} \\ I_{L2} \\ V_{C1} \\ V_{C2} \end{bmatrix}. \tag{2-68}$$

SEPIC State Space Derivation for Transistor OFF

With the transistor OFF, to find the state variable of I_{L1} apply KVL to the Figure 2.4.

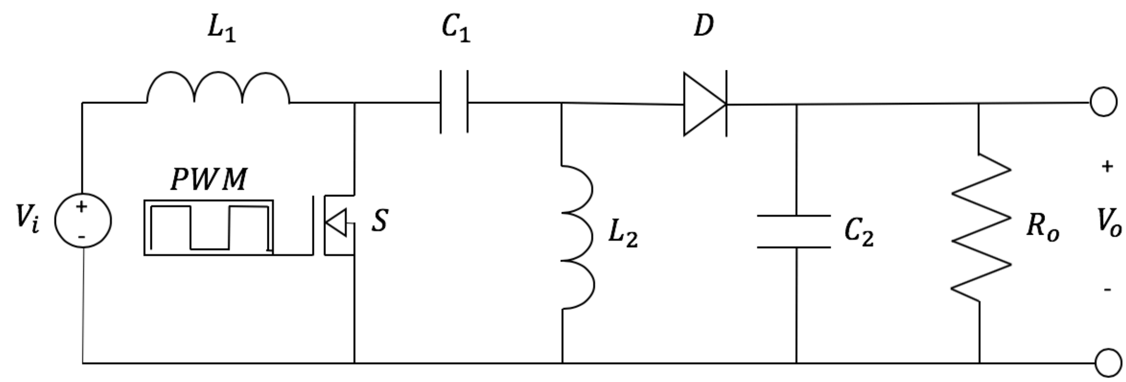

Figure 2.4, SEPIC Basic Circuit

Start at the power source going through the first inductor, first capacitor, diode and second capacitor, results in the following equation:

$$V_{L1} = V_i + V_{RL1} + V_{C1} + V_{RC1} + V_d + V_{C2} + V_{RC2}. \tag{2-69}$$

With $I = \frac{V}{R}$ and $I_{L1} = -I_{C1}$, and applying the state variable equation for the inductor, the equation now becomes:

$$\left(L_1 \frac{dI_{L1}}{dt}\right) = V_i + I_{L1}(R_{L1} - R_{C1}) + V_{C1} + V_d + V_{C2} + I_{RC2}R_{C2}. \tag{2-70}$$

With $I_{RC2} = \frac{V_{C2} - I_d R_o}{R_o - R_{C2}}$ the equation becomes:

$$\left(L_1 \frac{dI_{L1}}{dt}\right) = V_i + I_{L1}(R_{L1} - R_{C1}) + V_{C1} + V_d + V_{C2} + \frac{V_{C2}R_{C2}}{R_o - R_{C2}} - \frac{I_d R_o R_{C2}}{R_o - R_{C2}}. \tag{2-71}$$

After combining like terms the resulting equation is now:

$$\boldsymbol{\frac{dI_{L1}}{dt} = \frac{V_i}{L_1} + \frac{I_{L1}}{L_1}(R_{L1} - R_{C1}) + \frac{V_{C1}}{L_1} + \frac{V_d}{L_1} + \frac{V_{C2}}{L_1}\left(1 + \frac{R_{C2}}{R_o - R_{C2}}\right) - \frac{I_d}{L_1}\left(\frac{R_o R_{C2}}{R_o - R_{C2}}\right)}. \tag{2-72}$$

Now to find I_{L2}, apply KVL from diode to second capacitor and the second inductor, which results in the following equation:

$$V_d + V_{C2} + V_{RC2} - V_{L2} - V_{RL2} = 0. \tag{2-73}$$

After rearranging the equation, the equation is now:

$$V_{L2} = V_{RL2} - V_d + V_{C2} + V_{RC2}. \tag{2-74}$$

With $V = IR$ the equation becomes:

$$V_{L2} = (I_{RC1}R_{C1}) - V_d + V_{C2} + (I_{RC2}R_{C2}). \tag{2-75}$$

With $I_{RC2} = \frac{V_{C2} - I_d R_o}{R_o - R_{C2}}$ the above equation becomes:

$$V_{L2} = I_{RC1}R_{C1} - V_d + V_{C2} + \frac{V_{C2}R_{C2}}{R_o - R_{C2}} - \frac{I_d R_o R_{C2}}{R_o - R_{C2}}. \tag{2-76}$$

Applying the inductor equation and combining like terms the equation result is:

$$\boldsymbol{\frac{dI_{L2}}{dt} = \frac{I_{RC1}R_{C1}}{L_1} - \frac{V_d}{L_1} + \frac{V_{C2}}{L_1}\left(1 + \frac{R_{C2}}{R_o - R_{C2}}\right) - \frac{I_d}{L_1}\left(\frac{R_o R_{C2}}{R_o - R_{C2}}\right).} \tag{2-77}$$

Now to find V_{C1} by using KCL between the first capacitor and the second inductor, which results in the following equation:

$$I_{C1} = I_{L2}. \tag{2-78}$$

Applying the capacitor equation results in the following equation:

$$\left(C_1 \frac{dV_{C1}}{dt}\right) = I_{L2}. \tag{2-79}$$

After some simplifying, the state space equation is now:

$$\boldsymbol{\frac{dV_{C1}}{dt} = \frac{I_{L2}}{C_1}} \tag{2-80}$$

Now to find V_{C2} by using KCL between the node of second capacitor, the diode and the output resistor; the equation results as follows:

$$I_{C2} + I_d = I_o. \tag{2-81}$$

With $I = \frac{V}{R}$ and $V_o = V_{C2} + V_{RC2}$ the equation becomes:

$$I_{C2}R_o = V_{C2} + I_{C2}R_{C2} - I_d R_o. \tag{2-82}$$

Solving for I_{C2}, the equation is now:

$$I_{C2} = \frac{V_{C2} - I_d R_o}{R_o - R_{C2}}. \tag{2-83}$$

Applying the capacitor equation has the following equation:

$$\frac{d\boldsymbol{V_{C2}}}{d\boldsymbol{t}} = \frac{\mathbf{1}}{\boldsymbol{C_2}}\left(\frac{\boldsymbol{V_{C2}} - I_d R_o}{\boldsymbol{R_o} - \boldsymbol{R_{C2}}}\right). \tag{2-84}$$

The state space equation for SEPIC when the circuit’s transistor is OFF is shown below:

$$\begin{bmatrix} \dot{I_{L1}} \\ \dot{I_{L2}} \\ \dot{V_{C1}} \\ \dot{V_{C1}} \end{bmatrix} = \begin{bmatrix} -\frac{(\boldsymbol{R_{L1}} + \boldsymbol{R_{C1}})}{L_1} & -\frac{I_d}{I_{L2}L_1}\left(\frac{\boldsymbol{R_o R_{C2}}}{\boldsymbol{R_o} - \boldsymbol{R_{C2}}}\right) & \frac{V_d}{V_{C1}L_1} + \frac{1}{L_1} & \frac{\left(1 + \frac{\boldsymbol{R_{C2}}}{\boldsymbol{R_o} - \boldsymbol{R_{C2}}}\right)}{L_1} \\ -\frac{I_d}{I_{L1}L_1}\left(\frac{\boldsymbol{R_o R_{C2}}}{\boldsymbol{R_o} - \boldsymbol{R_{C2}}}\right) & -\frac{\boldsymbol{V_d}}{I_{L2}L_2} - \frac{\left(\boldsymbol{R_{L2}} + \frac{\boldsymbol{R_o R_{C2}}}{\boldsymbol{R_o} - \boldsymbol{R_{C2}}}\right)}{L_2} & 0 & -\frac{1}{L_2}\left(\mathbf{1} - \frac{\boldsymbol{V_{C2} R_{C2}}}{\boldsymbol{R_o} - \boldsymbol{R_{C2}}}\right) \\ 0 & \frac{\mathbf{1}}{\boldsymbol{C_1}} & 0 & 0 \\ 0 & -\frac{1}{I_{L2}C_2}\left(\frac{\boldsymbol{i_d R_o}}{\boldsymbol{R_o} - \boldsymbol{R_{C2}}}\right) & 0 & \frac{1}{C_2}\left(\frac{\mathbf{1}}{\boldsymbol{R_o} + \boldsymbol{R_{C2}}}\right) \end{bmatrix} \begin{bmatrix} I_{L1} \\ I_{L2} \\ V_{C1} \\ V_{C2} \end{bmatrix} + \begin{bmatrix} \frac{1}{L_1} \\ 0 \\ 0 \\ 0 \end{bmatrix} V_i \tag{2-85}$$

The output equation for when the transistor is OFF is shown below:

$$[V_o] = \left[0 \quad \frac{(\boldsymbol{V_{C2} R_o})}{R_o + R_{C2}} \quad 0 \quad \left(\frac{\boldsymbol{R_{C2} R_o}}{\boldsymbol{R_o} + \boldsymbol{R_{C2}}}\right)\right] \begin{bmatrix} I_{L1} \\ I_{L2} \\ V_{C1} \\ V_{C2} \end{bmatrix}. \tag{2-86}$$

Chapter 3

MICROCONTROLLER GENERATION OF RANDOMIZED PWM

Dc to dc converters have a constant PWM applied to them so the converters can achieve the desired output voltage. But if the PWM signal to the converter was randomized, the harmonics on the input line can appear differently. Randomization of the PWM was accomplished by utilizing different states of randomness of a pulsed width modulation which have been utilized before [Faisal]. These randomizations were able to adjust the discrete harmonics to spread to the other frequencies when applied to the buck and boost converters [Mihalič and Tse]. PWM has a constant switching time, T_s, and time ON value, α. If α changes its duration randomly and or changes its start time by a random value ϵ the result of these techniques were previously used [Mihalič and Tse]. When α changes in time duration, that is called Randomized Pulse Width Modulation (RPWM). When α's starting time is delayed by an amount of time, ϵ, that is refered to as Random Phase Position Modulation (RPPM). Table 3.1 shows the different techniques of randomizing that were accomplished before [Mihalič and Tse].

Table 3.1, Randomization Technique Types Utilized from other Examples [Mihalič and Tse

Randomized Technique	Switching Time, T_s	Time ON Duration, α	Phase Position, ϵ	Time Remaining, β	Utilized in Thesis
PWM	Fixed	Fixed	Zero	Fixed	Yes
RPWM	Fixed	Random	Zero	Random	Yes
RPPM	Fixed	Fixed	Random	Random	Yes
RPWM and RPPM	Fixed	Random	Random	Random	Yes
RCFMFD	Random	Random	Zero	Random	No
RCFMVD	Random	Fixed	Zero	Random	No

Other techniques which were used previously adjusted the switching frequency, T_s, but that was not utilized in this thesis since the switching frequency was already low and making it lower would require higher inductors. Those techniques were referred to as Random Carrier-frequency modulation with fixed duty cycle (RCFMFD) and with variable duty cycle (RCFMVD). Again, those two techniques weren't utilized in this thesis. The last variable in the randomization technique utilized in this thesis is time remaining, β. This was used to ensure the switching frequency remained constant even with all the randomization occuring between each cycle. Time remaining will always be random when either time ON duration and/or Phase Position duration variables are randomized. Switching Time, T_s can be expressed in terms of duty cycle, phase position and time remaining are shown by Figure 3.1. The equation which relates switching time, time ON, phase position time and remaining time is shown below:

$$T_s = \epsilon + \alpha + \beta. \tag{3-1}$$

Duty cycle, D, is also defined as:

$$D = \frac{\alpha}{T_s}. \tag{3-2}$$

The physical representation of these variables in relation to the PWM is shown in Figure 3.1.

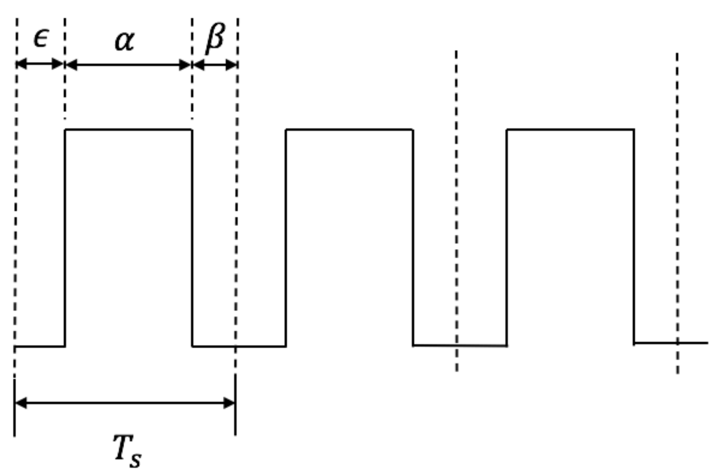

Figure 3.1, Explanation of Switching Parameters [Tse]

Microcontroller: Arduino Due Generation of PWM, RPWM and RPPM

Randomness was performed by an Arduino Due [Arduino, Due] since that board has a higher operating frequency than the Arduino Uno board [Arduino, Uno]. The Arduino Due can utilizes a random function which is shown below:

$$random(min, max - 1). \tag{3-3}$$

The random function would return random numbers between a defined minimum and maximum number minus one [Arduino random()].

The code to accomplish the different random schemes is shown below in Figure 3.2.

```
/*
 * Code for Random Pulse Width Modulation
 */

 long randNumber_Time;
 long randNumber_Alpha;
 long randNumber_Epsilon;
 long randNumber_Beta;

void setup() {

  pinMode(8, OUTPUT); //declare pin 5 to be an output:
  randomSeed(0);
  randNumber_Time = 0;
  randNumber_Alpha = 0;
  randNumber_Epsilon = 0;
  randNumber_Beta = 0;

void loop() {
  randNumber_Time = 0;     //set randNumber_Time to zero
  randNumber_Alpha = 0;    //set randNumber_Alpha to zero
  randNumber_Epsilon = 0; //set randNumber_Epsilon to zero
  randNumber_Beta = 0;     //set randNumber_Beta to zero

//Set Switching Time, Ts
  randNumber_Time = random(16,17); //Fixed value but still execute Random() function.

//Add Randomness for Alpha (aka Duty Cycle)
  randNumber_Alpha = random(4,5);  //Fixed value but still execute Random() function.

//Add Randomness for Epsilon
  randNumber_Epsilon = random(0,4); //Select a random number between 0 and 3 (4 minus 1).

//Add Randomness for Beta (Remaining time after Epsilon and Alpha)
 randNumber_Beta = randNumber_Time - randNumber_Alpha - randNumber_Epsilon;

  delayMicroseconds(randNumber_Epsilon); //Delay Epsilon microseconds.

  digitalWrite(8,HIGH);
  delayMicroseconds(randNumber_Alpha);   //delay HIGH Alpha microseconds.

  digitalWrite(8,LOW);
  delayMicroseconds(randNumber_Beta);   //delay LOW Beta microseconds
}
```

Figure 3.2, Randomization Execution Code

The code utilized another function called delayMicroseconds [Arduino, delayMicroseconds()]. This function would pause the code execution so if a High or Low pulse was generated, the pulse would stay in that position for a number of microseconds. This function was used control the randomization of ON and OFF values during specific time durations. The digitalWrite function is setting pin 8 to output a HIGH or LOW value depending on if the value within digitalWrite is “HIGH” or “LOW” [Arduino, digitalWrite()].

The MOSFET transistor operated at a constant switching frequency of 36.2 kHz when T_s was set to value of 16 microseconds. Throughout the experiment, the switching time, T_s, was set to 16 microseconds. This was determined in order to maintain consistency so when α, ϵ, and β values changed it could be determined that randomization was impacting the input voltage’s harmonics or not. When the random function was executed it was discovered there was a difference between both the expected switching time and duty cycle of the Arduino Due’s code than the measured switching time and duty cycle experienced on the Arduino Due. If T_s, was set to 16 microseconds, α was set to 4 microseconds, and ϵ was zero the expected duty cycle was 25%. The expected switching time was 16 microseconds but the measured time was 27.6 microseconds (36.2 kHz) and α was measured at 6.4 microseconds. The duty cycle was then measured at 23%. This is probably due to the code executing the random and digitalWrite functions. But even with the differences between expectation and measurement the importance was to have this difference be repeatable for all measurements, which it was repeatable.

During each randomized PWM cycle, there was a small region within the PWM which was actually controllable. This controllable region is shown in Figure 3.3.

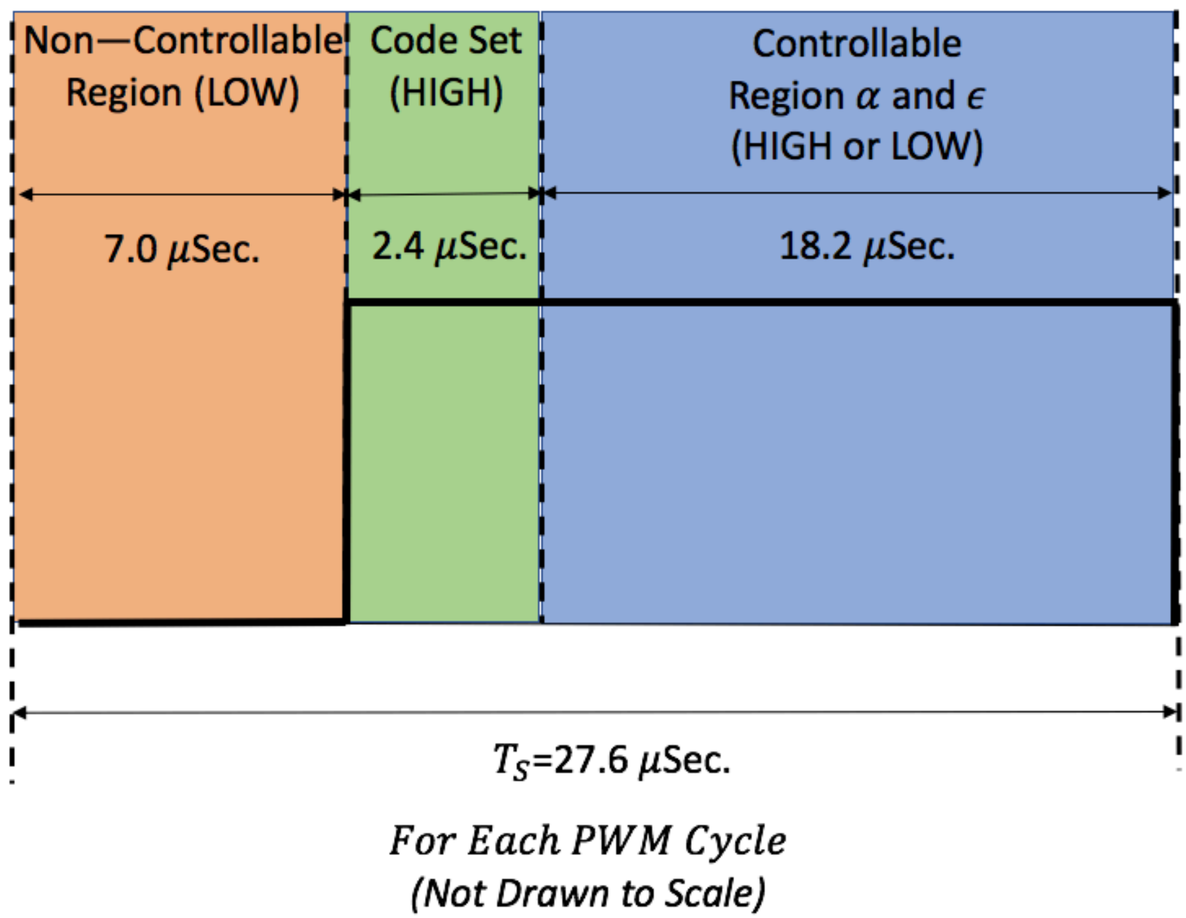

Figure 3.3, Physical Representation of PWM Controllable Region

During each cycle, the PWM had a duty cycle range of 23% to 63%. So, randomization can occur within that region. The maximum time to which randomization could occur is 18.2 microseconds. This means if α is 4 microseconds, the remaining value of ϵ can range anywhere from 0 to 16.2 microseconds. 2.4 microseconds was dedicated to HIGH value from the code's digitalWrite function. 7 microseconds was dedicated towards code execution of the randomization values and performing the calculations of the LOW value in the Controllable region.

Measurement and PWM Equipment Setup

Figure 3.4 shows the Arduino Due connected to the Cuk or SEPIC converter and the Arduino Due generates the needed randomized and non-randomized PWM. A power supply, oscilloscope and the Arduino Due are shown connected.

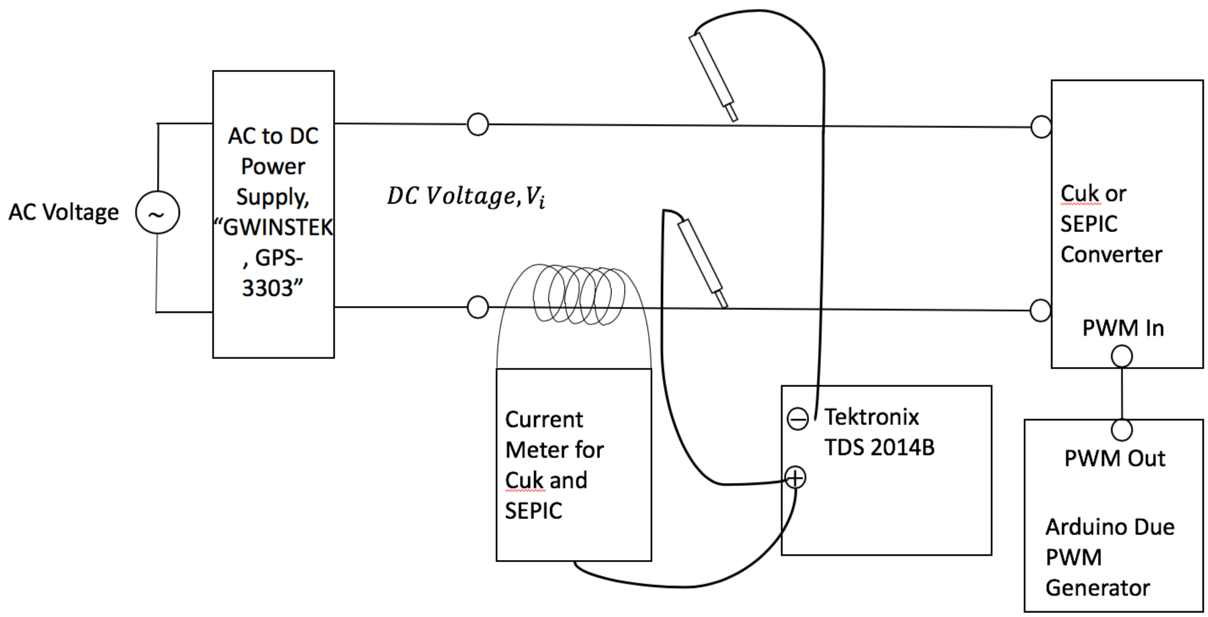

Figure 3.4, PWM Generation and Experimentation Measurement of Cuk and SEPIC Converter

The Arduino Due's connection is shown below in Figure 3.5.

The wire colors on the circuit have a specific meaning as shown in Figure 3.5. Green was used to measure current through the inductor to understand if the converter is operating in Continuous Conduction Mode (CCM) or Discontinuous Conduction Mode (DCM). Red wires is where the positive DC power supply is connected too. The orange wire indicates the PWM signal, grey wires indicates nodal connections and ground connections and finally blue wires indicates points of voltage measurements with the voltage probe.

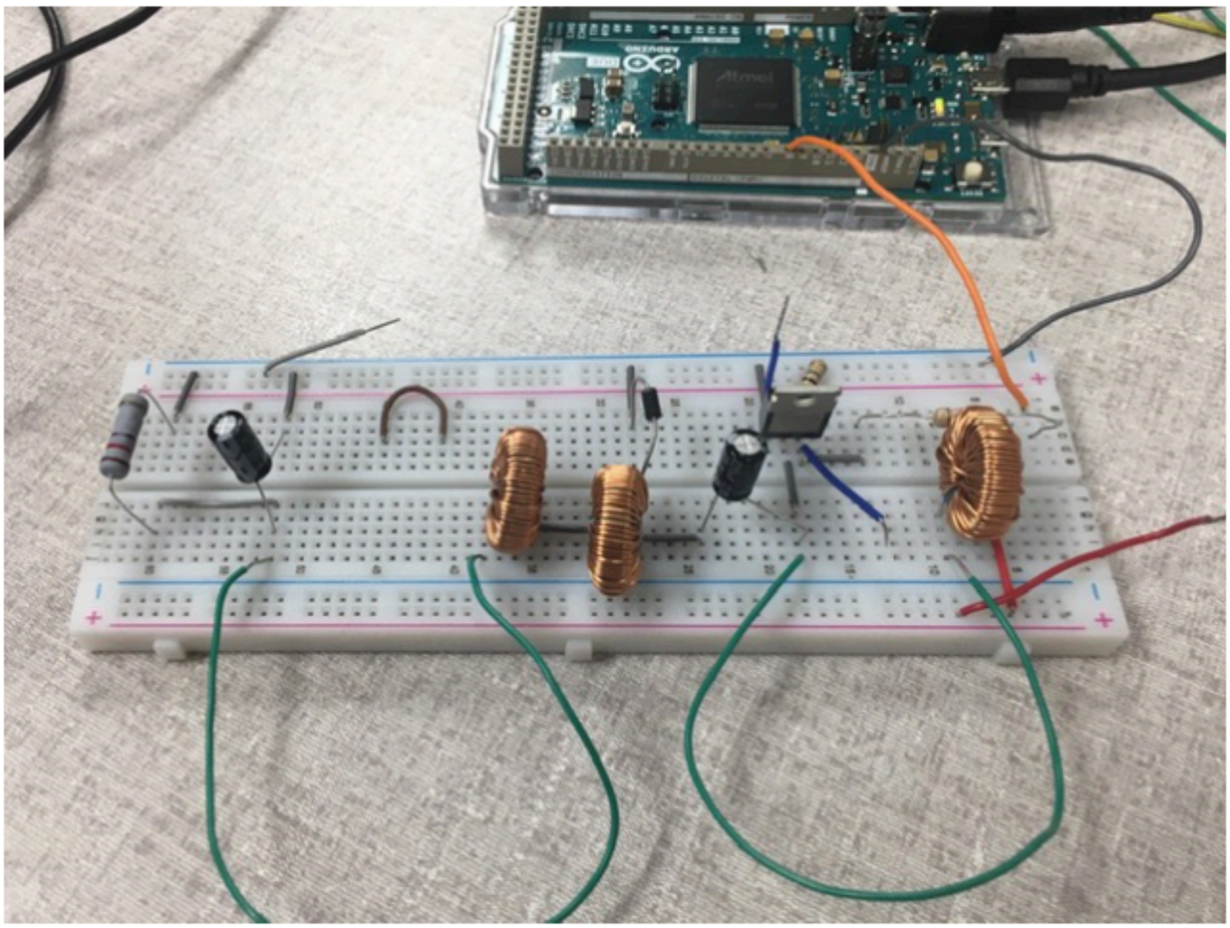

Figure 3.5, Cuk Converter's Connection to the Arduino Due

The inductor's current was measured with a 200 kHz current probe as shown in Figure 3.6. The probe is connected to an oscilloscope and current flowing through the current probe would be displayed on the oscilloscope during the converter's operation.

Figure 3.6, Current Probe used for Measuring Inductor Current

An example of the connection to the DC Power Supply, the current probe and the Arduino Due is shown in Figure 3.7.

Figure 3.7 shows the DC power supply, Arduino Due, current probe connected together.

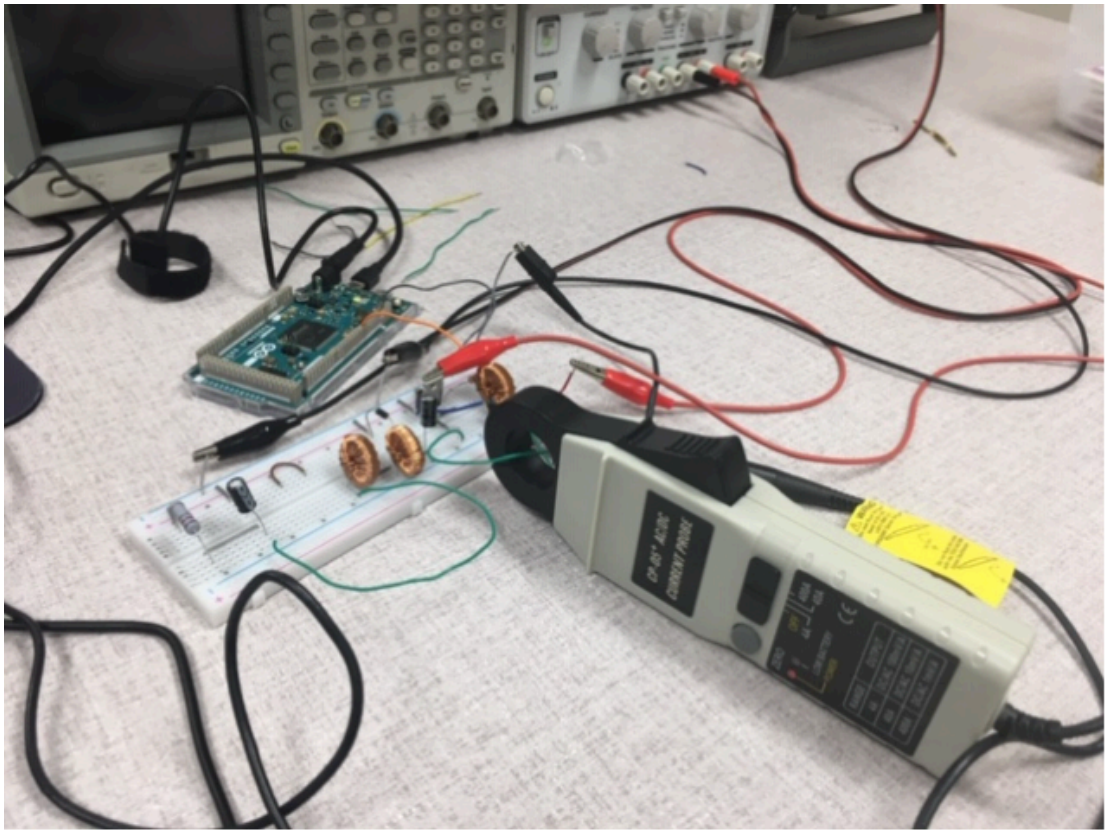

Figure 3.7, Set up Example of Cuk with DC Power Supply, Current Probe and Arduino Due

The SEPIC converter is shown in Figure 3.8.

The SEPIC converter utilized the same wiring color scheme as the Cuk converter as shown in Figure 3.8.

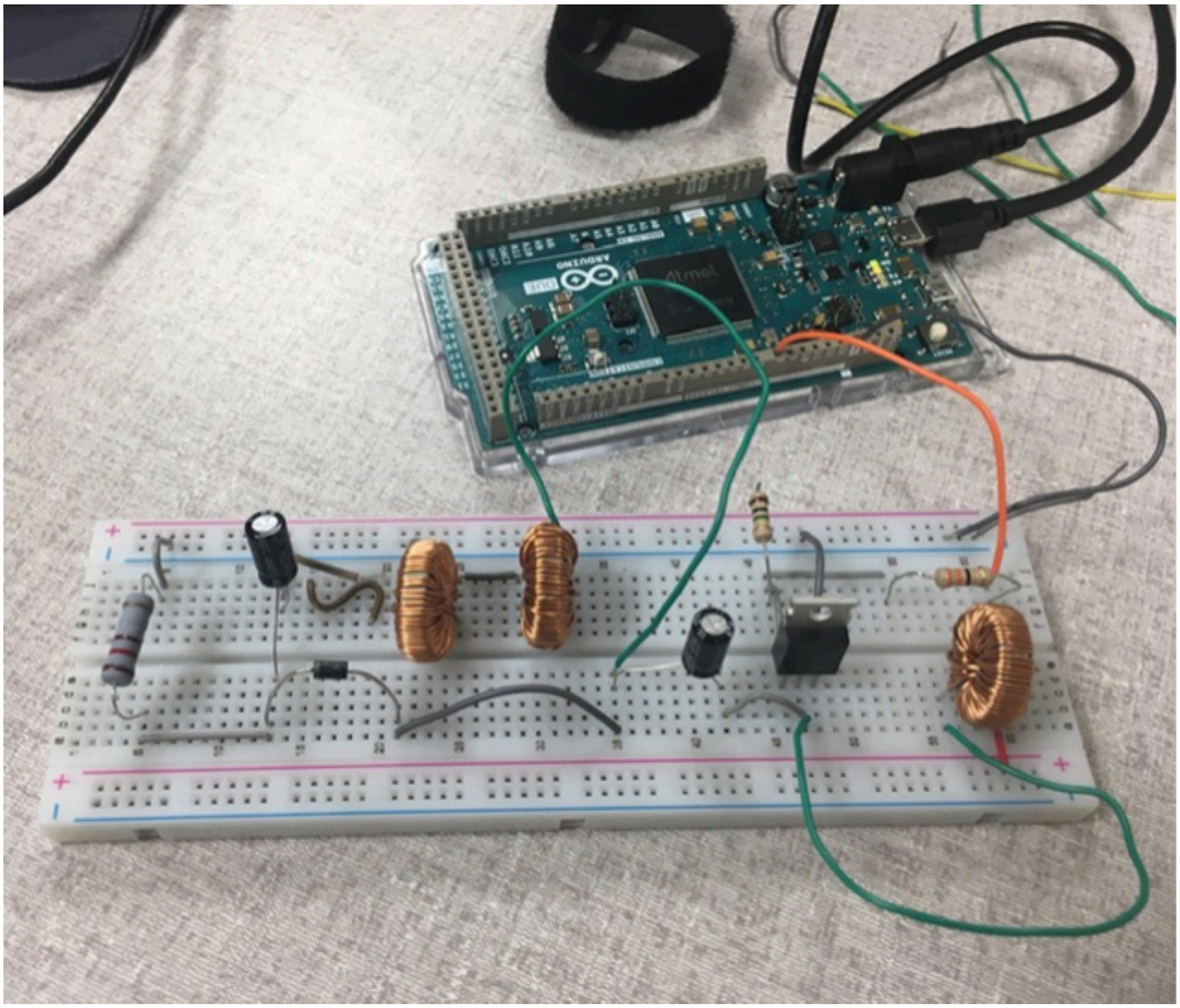

Figure 3.8, SEPIC Converter Connection to the Arduino Due

Converter Current Measurements

The PWM duty cycle range used for both circuits was from 23% to 63%. For 23% the first inductor measurement for the SEPIC converter which had a measurement of 53.2 mA as shown in Figure 3.9

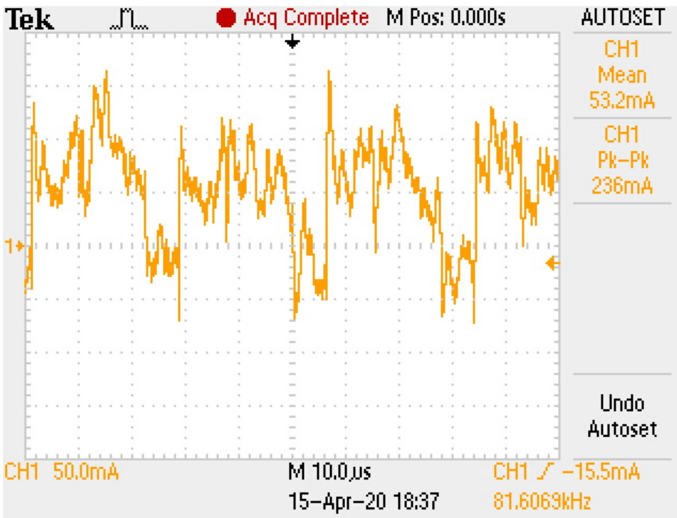

Figure 3.9, Current Measurement through SEPIC for First Inductor at 23% Duty Cycle

The second inductor under the same duty cycle measured 47.6 mA as shown in Figure 3.10. The converter is expected to be in DCM due to the current dropping below zero.

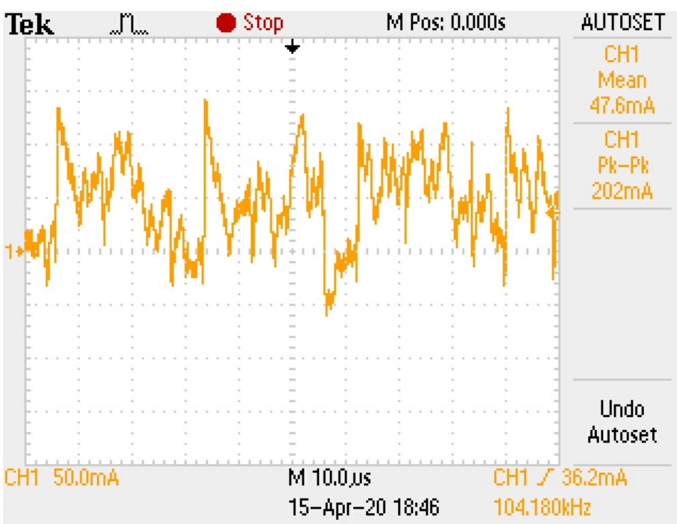

Figure 3.10, Current Measurement through SEPIC for Second Inductor at 23% Duty Cycle

For the higher duty cycle of 52% the SEPIC converter's first inductor measured 176 mA as shown by Figure 3.11.

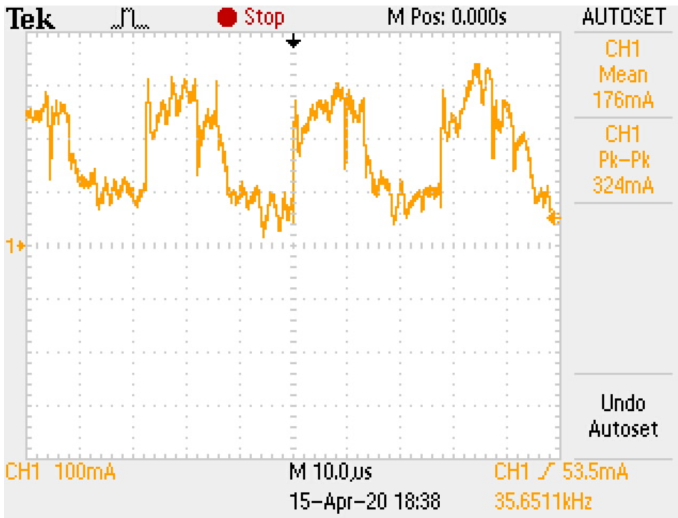

Figure 3.11, Current Measurement through SEPIC's for First Inductor at 52% Duty Cycle

The current measurement for the second inductor at 52% duty cycle measured 95.4 mA as shown by Figure 3.12. Due to the second inductor's current is below zero the converter is still in DCM.

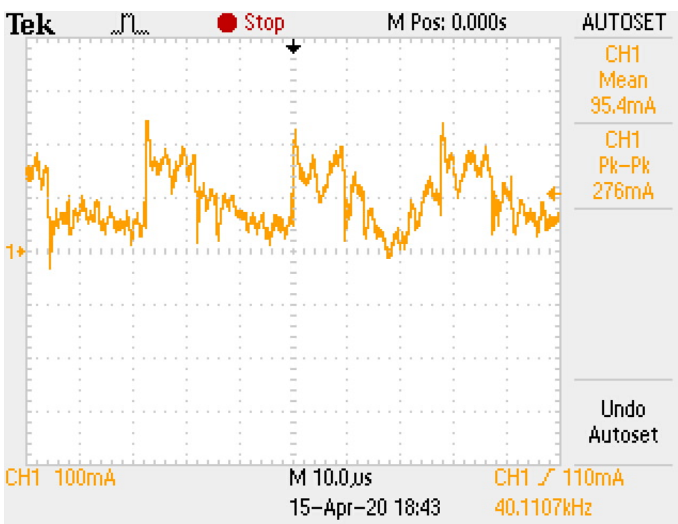

Figure 3.12, Current measurement through SEPIC's for Second Inductor at 52% Duty Cycle

When the duty cycle is increased to 63% the current measured through the first inductor of the SEPIC converter is 264 mA as shown by Figure 3.13.

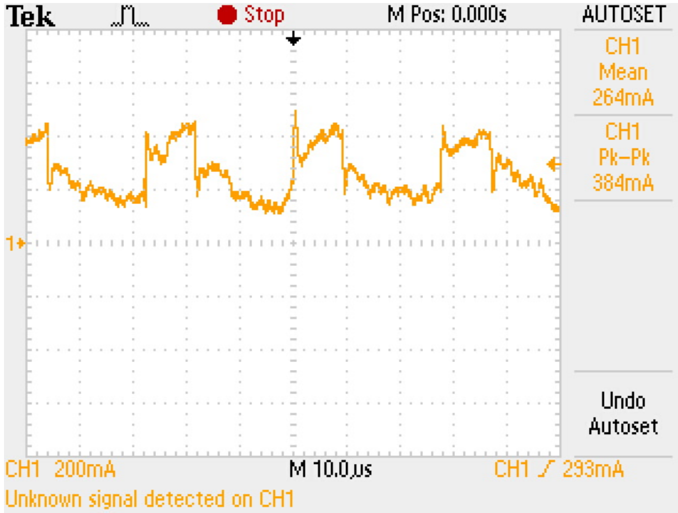

Figure 3.13, Current Measurement through SEPIC's for First Inductor with 63% Duty Cycle

The current measured for SEPIC's second inductor at 63% duty cycle is 97.9 mA as shown by Figure 3.14.

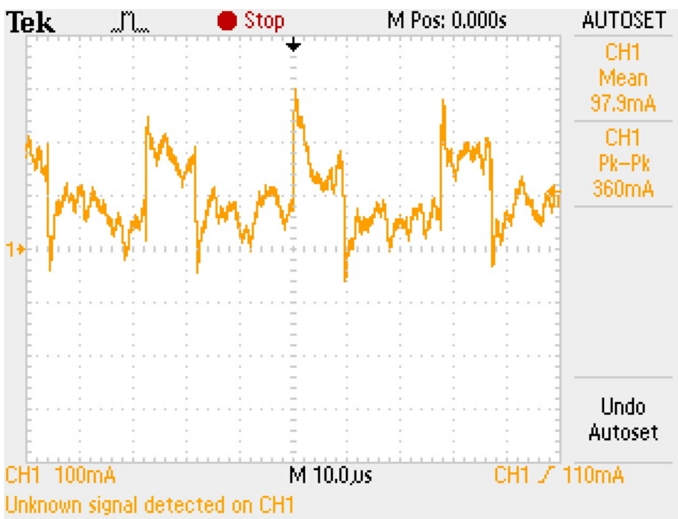

Figure 3.14, Current Measurement through SEPIC's for Second Inductor with 63% Duty Cycle

The Cuk converter has the same results as SEPIC circuit except at 63% duty cycle. The inductors for the Cuk converter appear to be operating in CCM. Figure 3.15 shows the Cuk's first inductor current measurement of 284 mA.

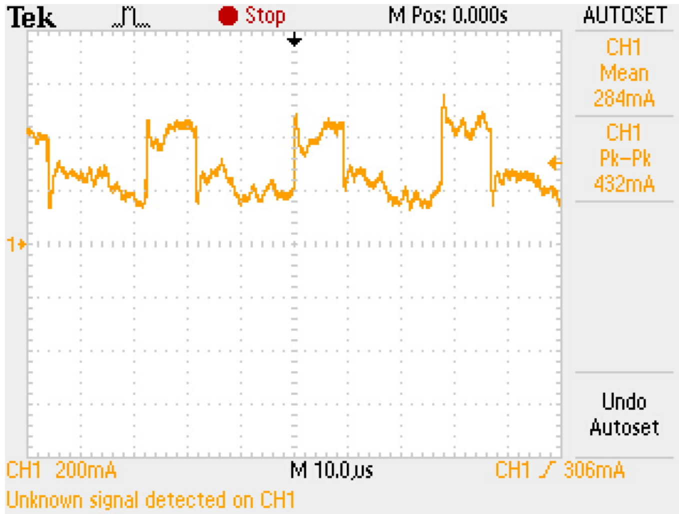

Figure 3.15, Current Measurement through Cuk's for First Inductor with 63% Duty Cycle

The second inductor was measured at 141 mA as shown by Figure 3.16. As a result of both inductors outputting current above zero amps the converter is operating in CCM.

Figure 3.16, Current measurement through Cuk's for Second Inductor with 63% Duty Cycle

Chapter 4

RANDOMIZATION SIMULATION ON CUK AND SEPIC CONVERTERS

Each section of this chapter is divided into different categories, Cuk or SEPIC converter type, High or Low Vout voltages, and randomization techniques (PWM, RPWM, RPPM and both RPWM and RPPM). Each technique starts with no randomization or PWM in order to show the impact of randomization performed on it. Again, the randomization techniques utilized from Table 3.1 are PWM, RPPM, RPWM and a combination of both RPPM and RPWM.

MATLAB's Simulink FFT Function

MATLAB's Simulink has a built-in Fast Fourier Transfer (FFT) tool [MathWorks, powergui] which performs a Discrete Fourier Transform (DFT) from scope measurements received in Simulink [MathWorks, powerscope_fft]. The DFT is defined at the beginning with the periodic expansion Fourier Series [Mutagi]:

$$\tilde{x}(t) = a_0 + \textstyle\sum_{n=0}^{\infty}[a_n \cos(n\omega_0 t) + b_n \sin(n\omega_0 t)]. \tag{4-1}$$

Where $\tilde{x}(t)$ is a periodic signal, a_0 is the amplitude at the fundamental frequency ω_0, and a_n and b_n are the amplitudes of discrete frequencies. ω_0 can also be written as:

$$\omega_0 = 2\pi f_0. \tag{4-2}$$

The Fourier Series can also be expressed in exponential form [Mutagi] during a time period, T:

$$\tilde{x}(t) = \sum_{n=0}^{\infty} c_n e^{jn\omega_0 t}, \tag{4-3}$$

where the value of c_n can be expressed as:

$$c_n = \frac{1}{T} \int_{\frac{-T}{2}}^{\frac{T}{2}} \tilde{x}(t) e^{-jn\omega_0 t} dt. \tag{4-4}$$

The period, T, is defined by:

$$T = \frac{1}{f_0}. \tag{4-5}$$

To discretize the exponential form of the Fourier Series, the number of signal samples, N, occur within the period, T. The signal within a defined window discretizes the signal between -T/2 and T/2. Simulink's DFT formula is shown below [MathWorks, fft]:

$$Y(k) = \sum_{j=1}^{n} X(j)\, W_n^{(j-1)(k-1)}. \tag{4-6}$$

Where $W_n = e^{\frac{(-2\pi i)}{n}}$, X(j) is the input dataset, n is the transform length, and Y(k) is the output vector of X(j) in the frequency domain. The j and k values are the indices for X and Y vectors, respectively.

For example of performing an DFT in MATLAB Simulink, a Cuk converter has a voltage measurement at its input of about 7.23 volts, which has an output voltage of -23.07 volts as shown by the circuit Figure 4.1.

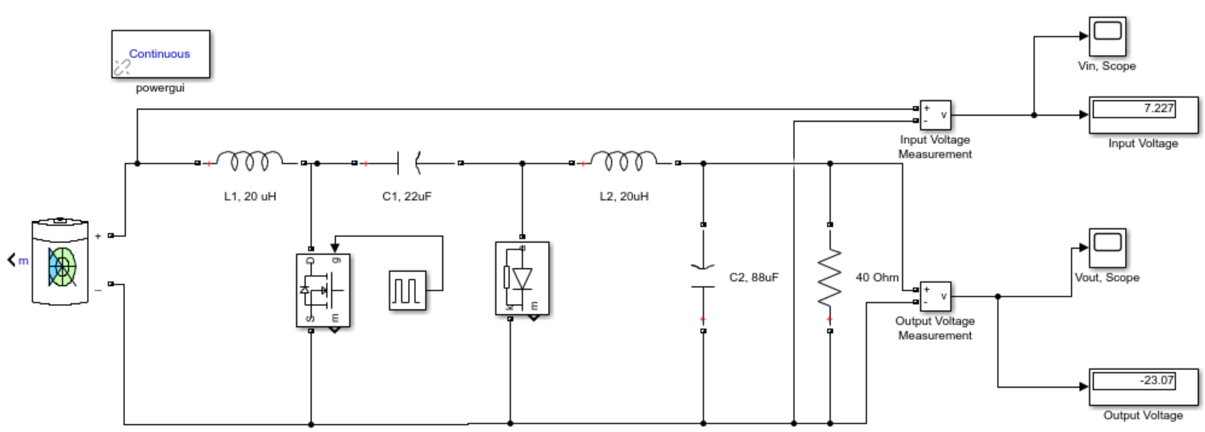

Figure 4.1, Cuk Circuit for FFT Example by MATLAB Simulink

The input voltage scope captures the input voltage data in time and stores that data for FFT analysis. The input voltage measurement is shown by Figure 4.2.

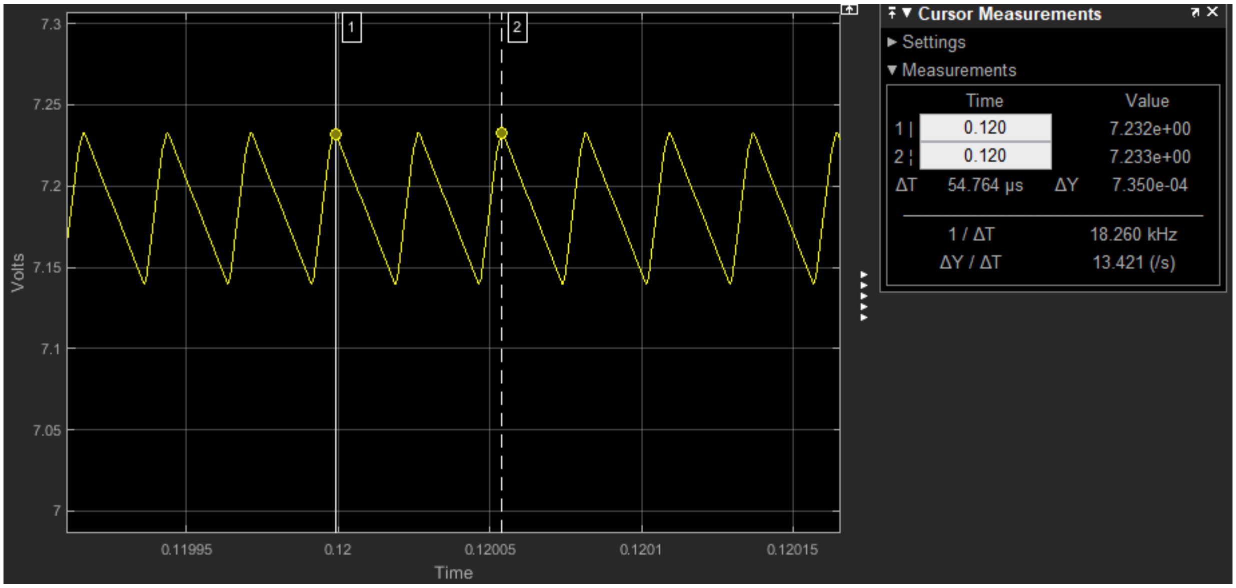

Figure 4.2, Input Voltage Measurement used for FFT Analysis

Simulink's FFT analysis function shows the FFT window, which depends on the number of cycles per Figure 4.3. The number of cycles would then be used in the FFT analysis. For this example, the number of cycles analyzed were 2 cycles. The FFT window shows 5435 cycles possible cycles from the simulation performed.

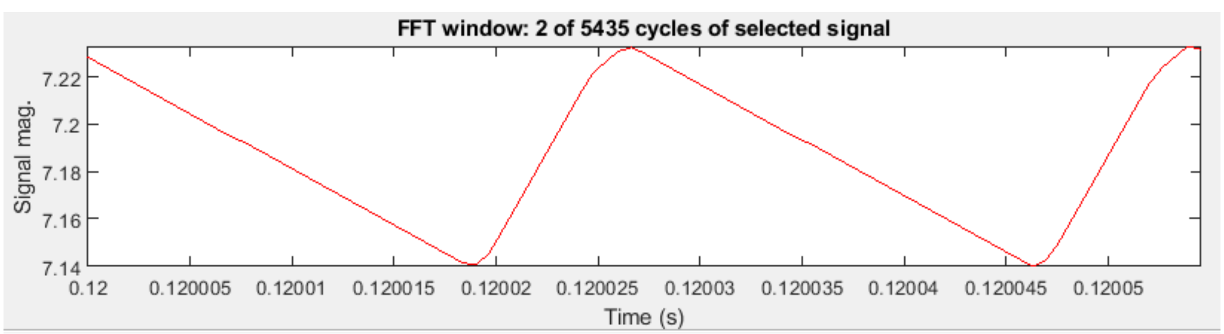

Figure 4.3, FFT Window for Cuk Example (2 Cycles)

The FFT function takes the values shown in Figure 4.3 and outputs the values as shown in Figure 4.4 by discretizing the FFT window and summing the frequencies together.

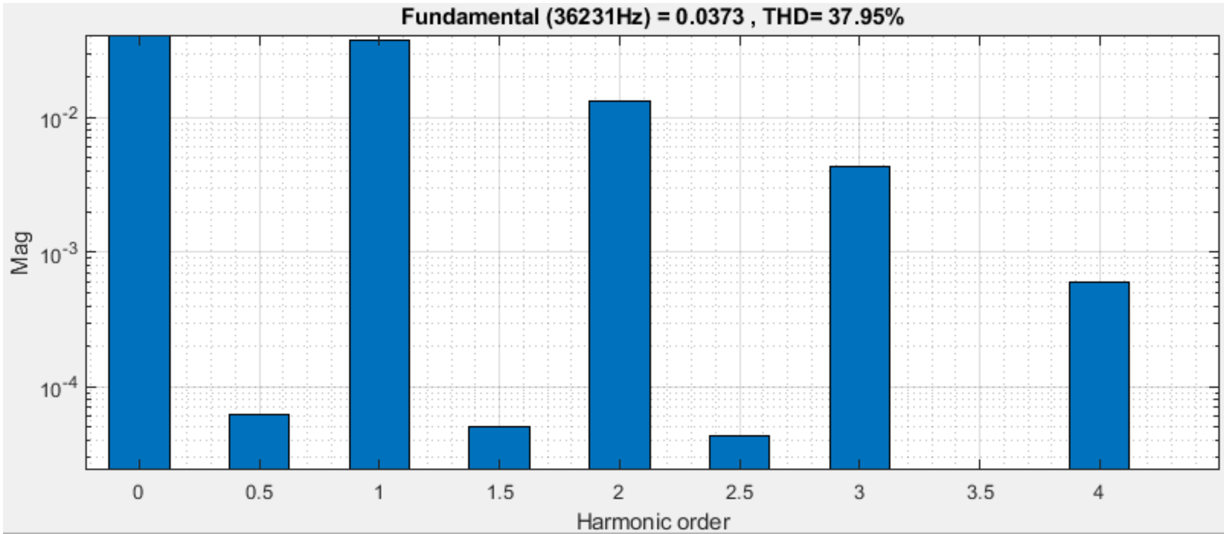

Figure 4.4, FFT Results from Cuk Example (2 Cycles)

For the remainder of the simulation, the process is the same for showing the FFT results, but the selected cycles is 42 cycles. The randomized PWM technique for Low Vout, RPWM and RPPM had 42 different possible combinations for randomized PWM signal. This was the most possible combinations available to allow all randomized pulses be executed. So the other converters and techniques performed their FFT analysis against the same number of 42 cycles to ensure FFT windows were compared similarly.

CUK Simulation, Vout Lower than Vin

<u>CUK Simulation, Low Vo, PWM Measurements (Baseline)</u>

The Cuk circuit is shown below in Figure 4.5 which occurs at a 36 kHz switching frequency and 23% duty cycle. The circuit includes the Equivalent Series Resistance (ESR) value of the capacitor and inductors [Kushwaha]. These resistance values was included to provide a more realistic approach towards the circuit modeling.

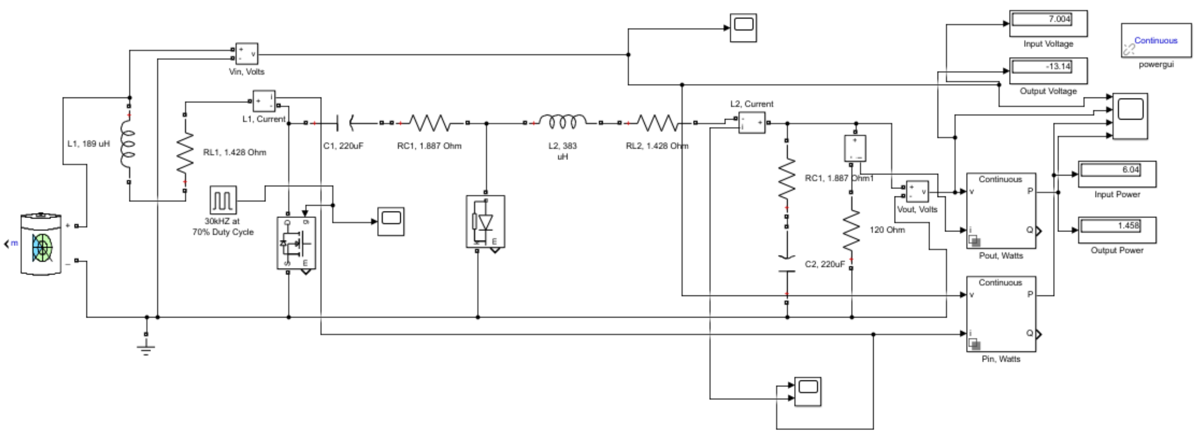

Figure 4.5, Cuk MATLAB Simulink Model Simulation, No Randomized PWM, Low Voltage Output

As mentioned before, to show the harmonics on the input power line, the Fast Fourier Transform (FFT) function was used from MATLAB's Simulink. The PWM measurement can be seen from Figure 4.6 as shown below. The switching frequency is shown to be about 36 kHz and PWM have a duty cycle of 23%.

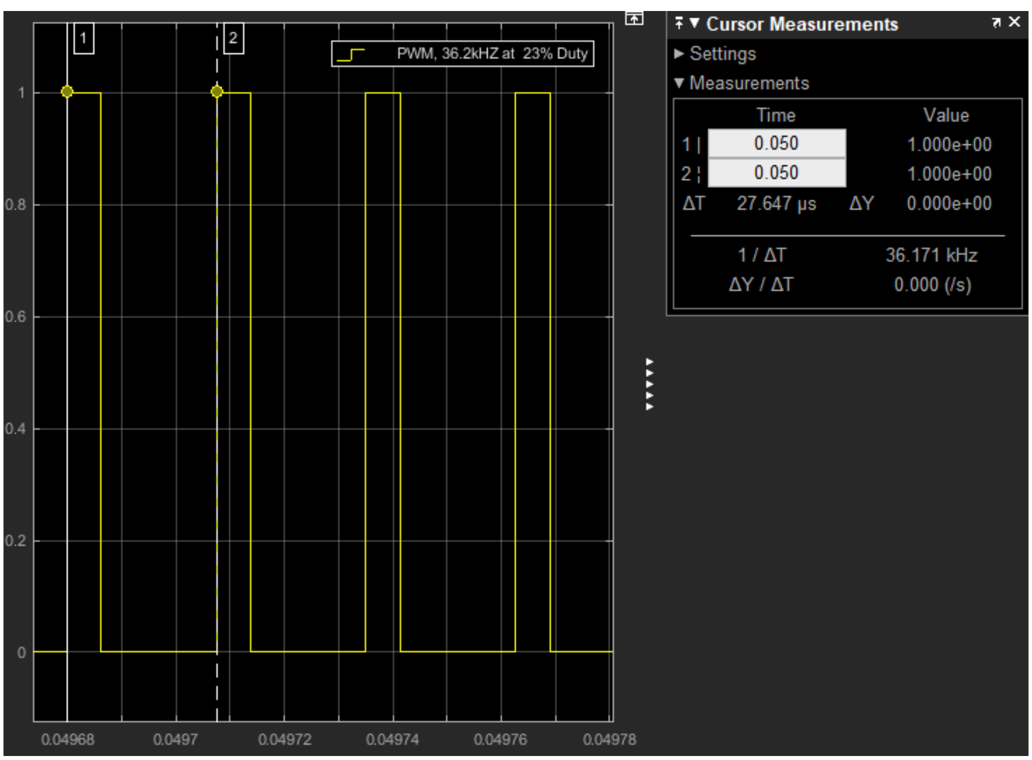

Figure 4.6, Cuk Simulation with No Randomized PWM Result, Low Voltage Output

CUK Simulation, Low Vo, PWM FFT and Voltage Measurements

The simulation results are shown below of the input and output voltage and the FFT results. The expectant input and output voltage is 7.2 Volts and -6.5 Volts, respectively, as shown by Figure 4.7.

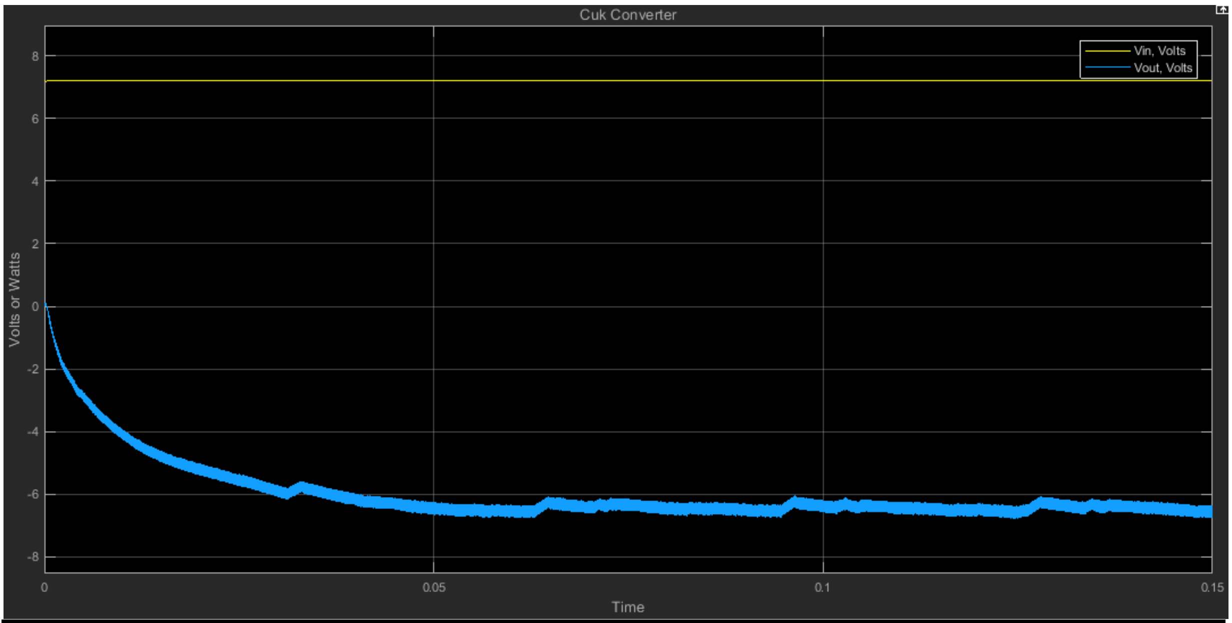

Figure 4.7, Cuk Simulation, PWM, Input and Output Voltage Results, Low Vout

As a result of the frequency switching about 36.2 kHz. The input voltage of 7.2 volts resulted in the following FFT spectrum as shown below in Figure 4.8. The frequencies displayed is a ratio against 1 Volt and displayed logarithmically.

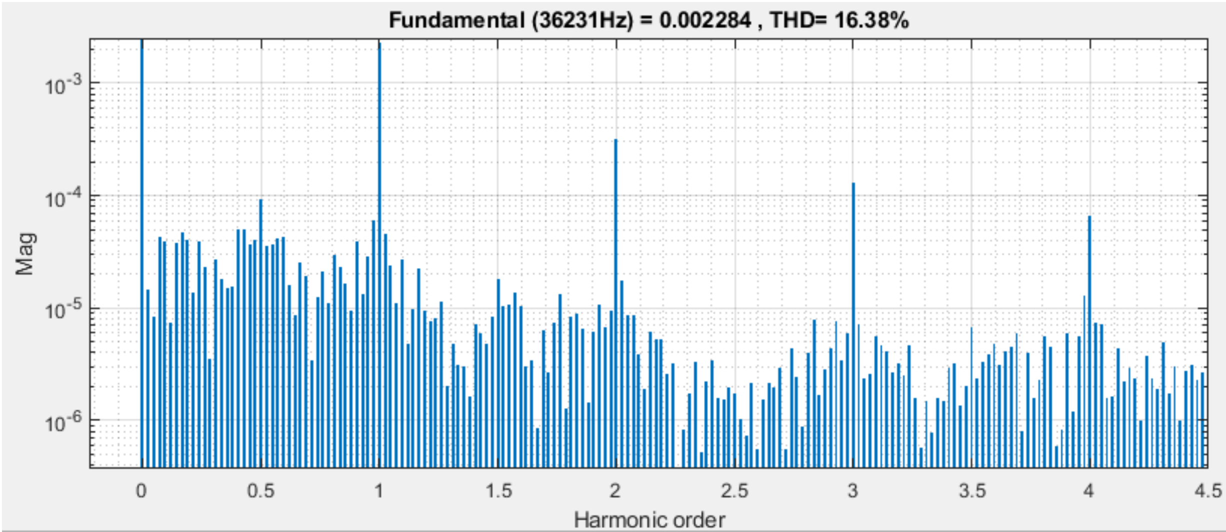

Figure 4.8, Cuk Simulation, PWM, Simulink FFT Analysis, Low Vout

CUK Simulation, Low Vout, Added RPWM

<u>CUK Simulation, Low Vout, Add RPWM, PWM Measurement</u>

The simulation for RPWM of the PWM is shown by Figure 4.9. The figure shows two graphs. The top graph is the output of the randomized integer generator from Simulink which randomly selects values between 0 and 11. Each value is tied to specific PWM duty cycle. The duty cycles range from 23% to about 63%. The switching time between each cycle is constant at 36 kHz.

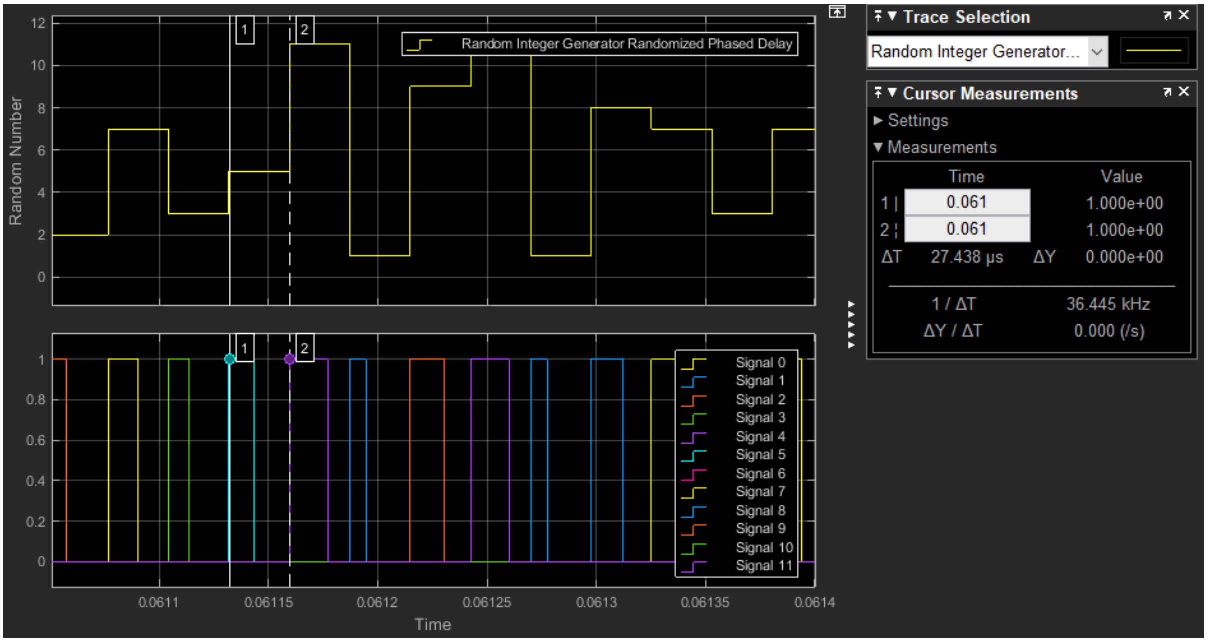

Figure 4.9, Cuk Simulation, RPWM Result, Low Vout

The Simulink program to accomplish the PWM selection with different duty cycles is shown below in Figure 4.10. The output values of the randomized integer generator and the PWM with different duty cycles are shown in Figure 4.9.

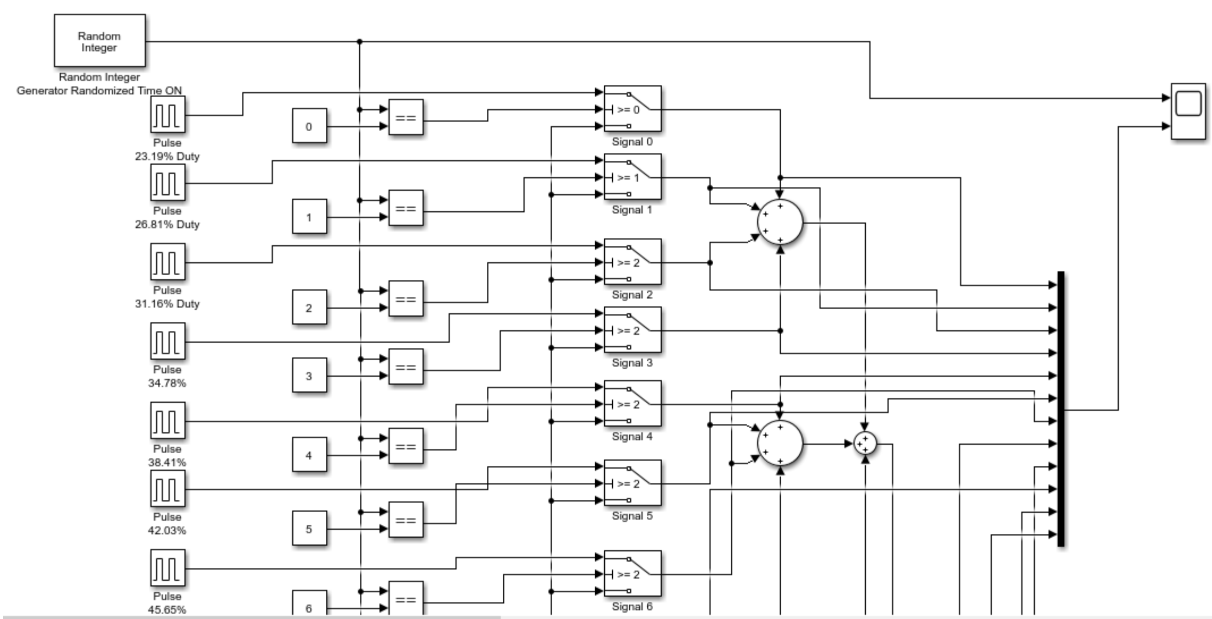

Figure 4.10, Cuk MATLAB Simulink Simulation of RPWM during Low Vout

CUK Simulation, Low Vout, RPWM, FFT and Voltage Measurements

The FFT results from the randomized PWM is shown in Figure 4.11. The results show that compared to the FFT measurements of PWM of Figure 4.8, the discrete harmonics are still shown but THD has increased.

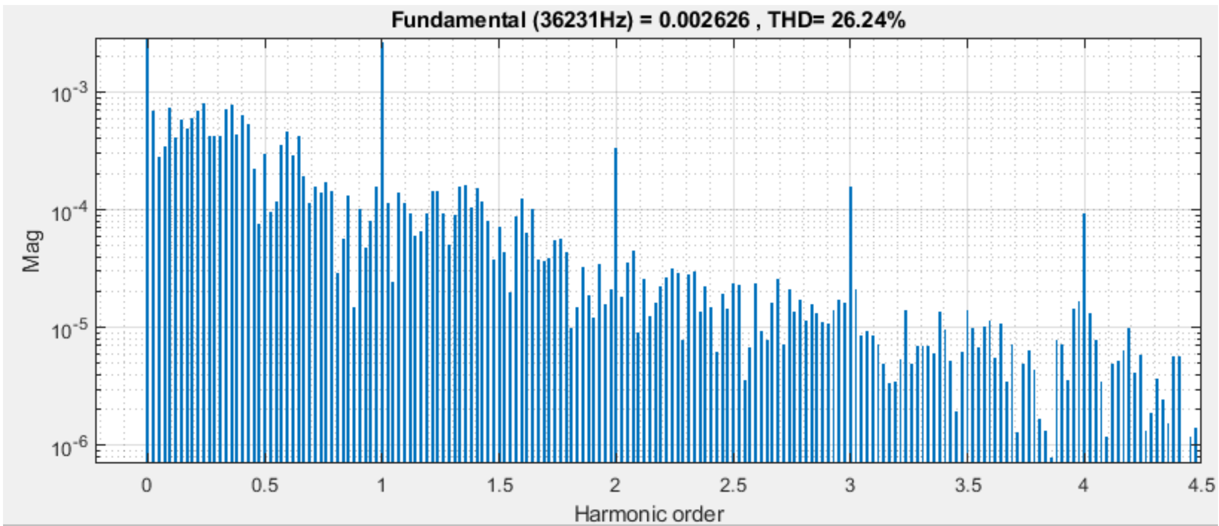

Figure 4.11, Cuk Simulation, RPWM, FFT Results, Low Vout

The input and output voltage measurements are shown in Figure 4.12. the expectant input voltage is 7.2 volts while the output voltage is expected to be -9.034 Volts.

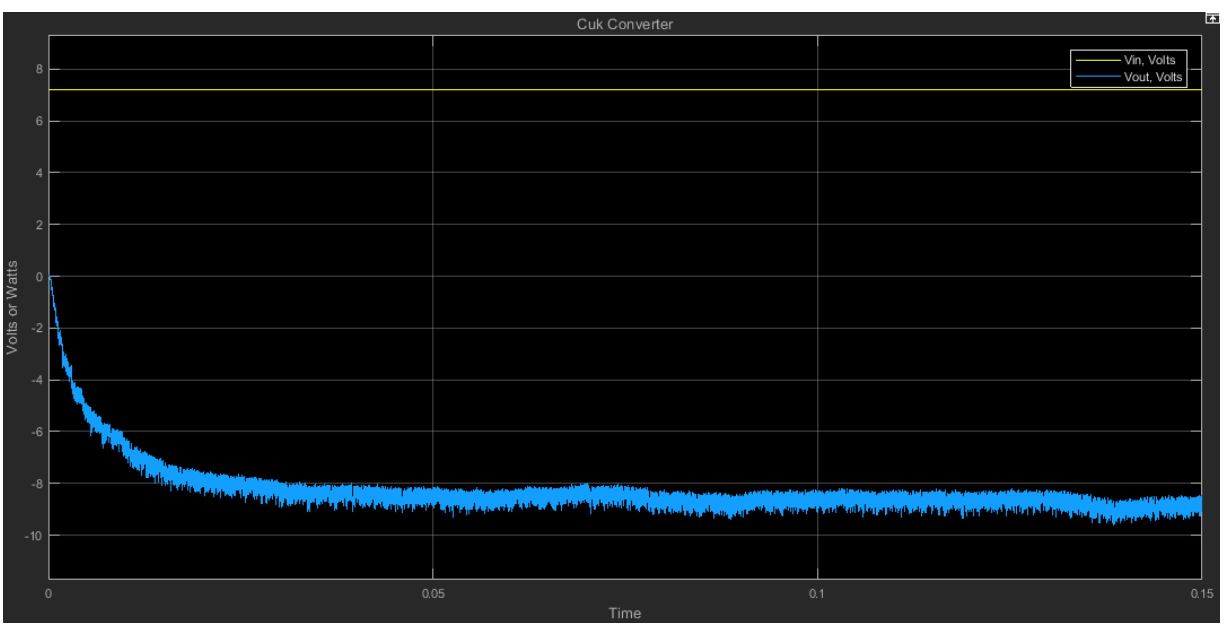

Figure 4.12, Cuk Simulation, RPWM, Input and Output Voltages Measurements for Low Vout

Cuk Simulation, Added RPWM and RPPM for Low Vout

Cuk Simulation, RPWM and RPPM, PWM Measurements

Simulated RPWM and RPPM utilizes both randomness of duty cycle, α, and the phase position, ϵ of PWM. To simulate this, each combination of randomization for 23% to 45% duty and phase position delay from 0 to 5 microseconds, corresponded to 42 possible combinations. With each combination provided an assigned random number. The result of each random number is a distinct duty cycle and phase delay at 27.6 microseconds. Figure 4.13 shows the simulation architecture of how this RPWM and RPPM was accomplished. The architecture shows duty cycle changing which is the result of RPWM.

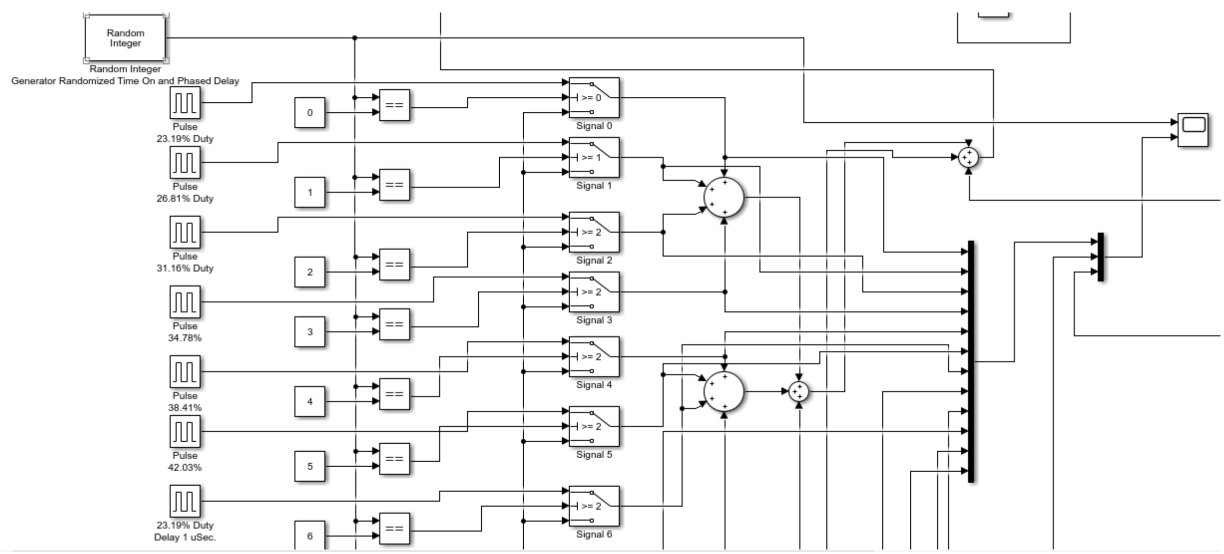

Figure 4.13, Cuk MATLAB Simulink Simulation of RPWM and RPPM, Low Vout

The duty cycles shown in Figure 4.13 is also delayed between 0 to 5 microseconds. This delay accounts for the RPPM. The full diagram is shown below in Figure 4.14 which includes all 42 PWM combinations of RPWM and RPPM.

Figure 4.14, Cuk's Full MATLAB Simulink Simulation Diagram of RPWM and RPPM for Low Vout

The PWM results of accomplishing both RPWM and RPPM is shown in Figure 4.15. It can be seen that the duty cycles and its position are changing with each random number generation.

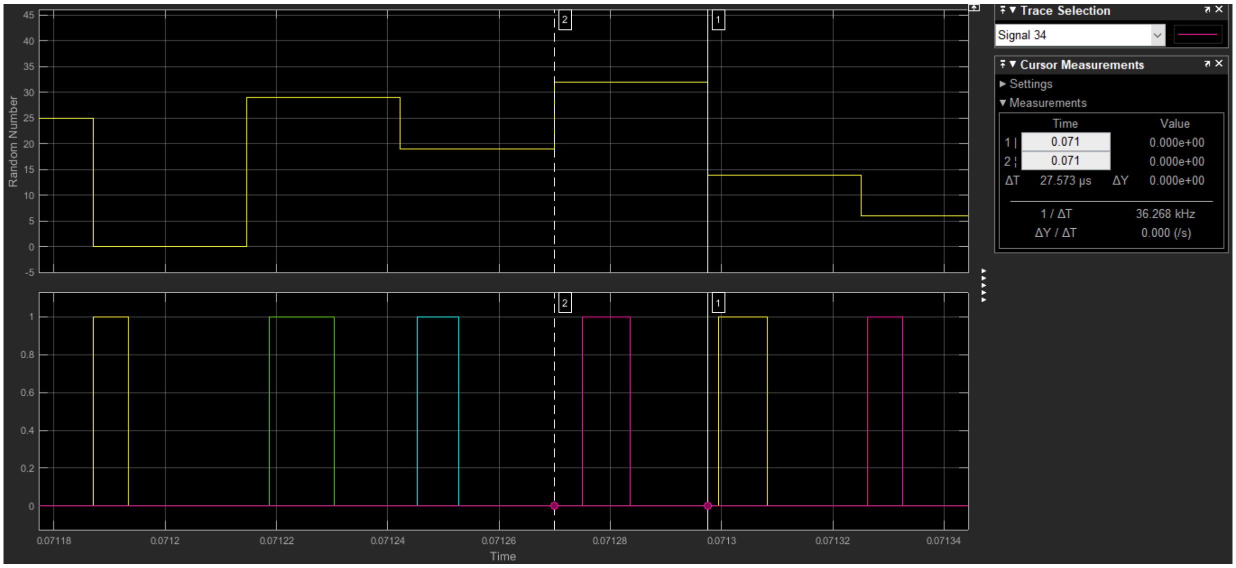

Figure 4.15, Cuk Simulation, RPWM and RPPM Result, Low Voltage Output

Cuk Simulation, RPWM and RPPM, FFT and Voltage Measurements Low Vout

FFT results of accomplished both RPWM and RPPM are shown in Figure 4.16. The figure shows that the discrete harmonics are adjusted when compared to the PWM baseline Figure 4.8. But THD also increased as a result of the RPWM and RPPM.

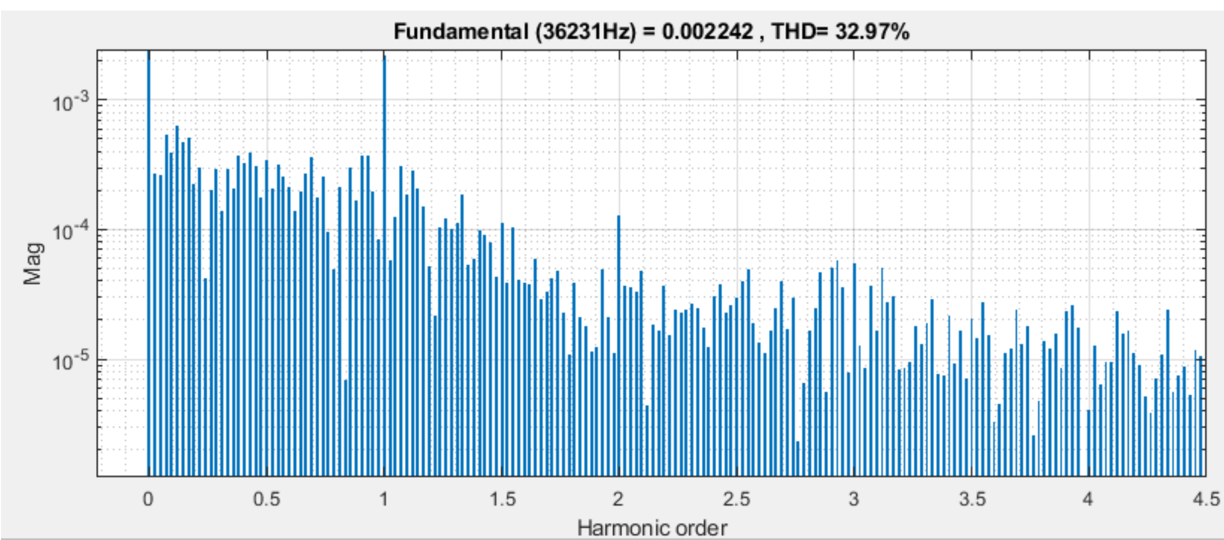

Figure 4.16, Cuk Simulation, RPWM and RPPM FFT Results, Low Vout

The input and output voltages are shown in Figure 4.17. The input voltage is 7.2 Volts while the output voltage is -5.974 Volts.

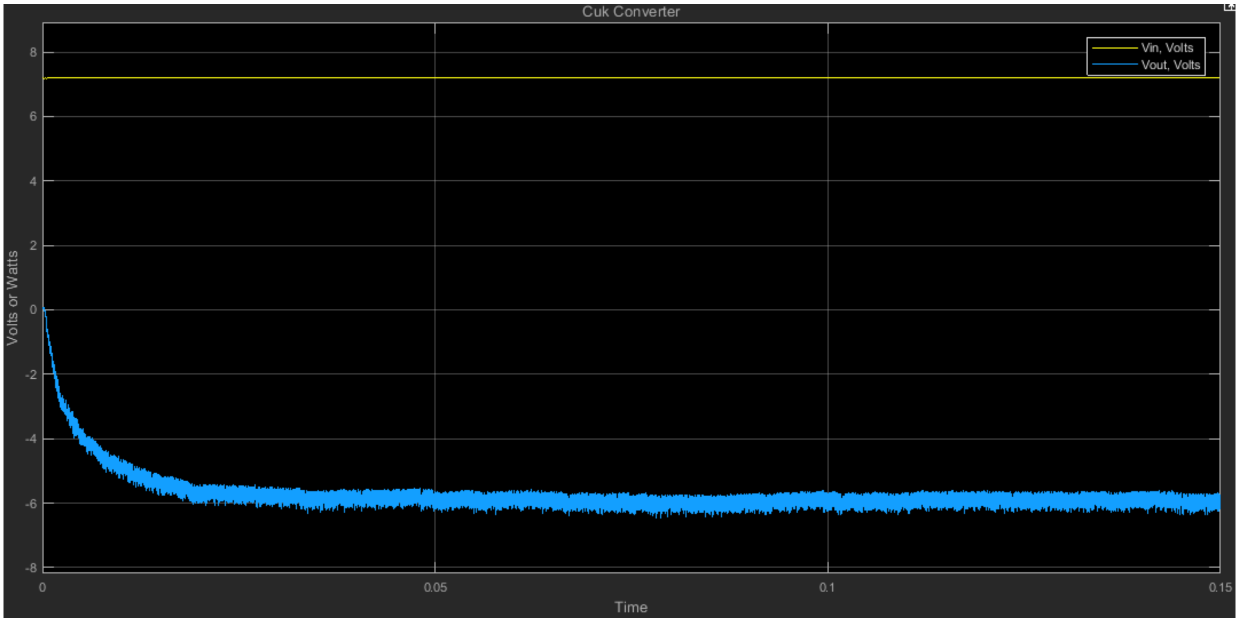

Figure 4.17, Cuk Simulation, RPWM and RPPM, Input and Output Voltages Measurements for Low Vout

Cuk Simulation, Added RPPM for Low Vout

<u>CUK Simulation, RPPM for Low Vout, PWM Measurements</u>

The randomized PWM which was now applied against the Cuk converter was phased position delayed between 0 and 11 microseconds. The PWM is shown in Figure 4.18 shows the results of that phase position randomization (RPPM). It is shown that the pulse have different switching times and the result is the randomization of phase position.

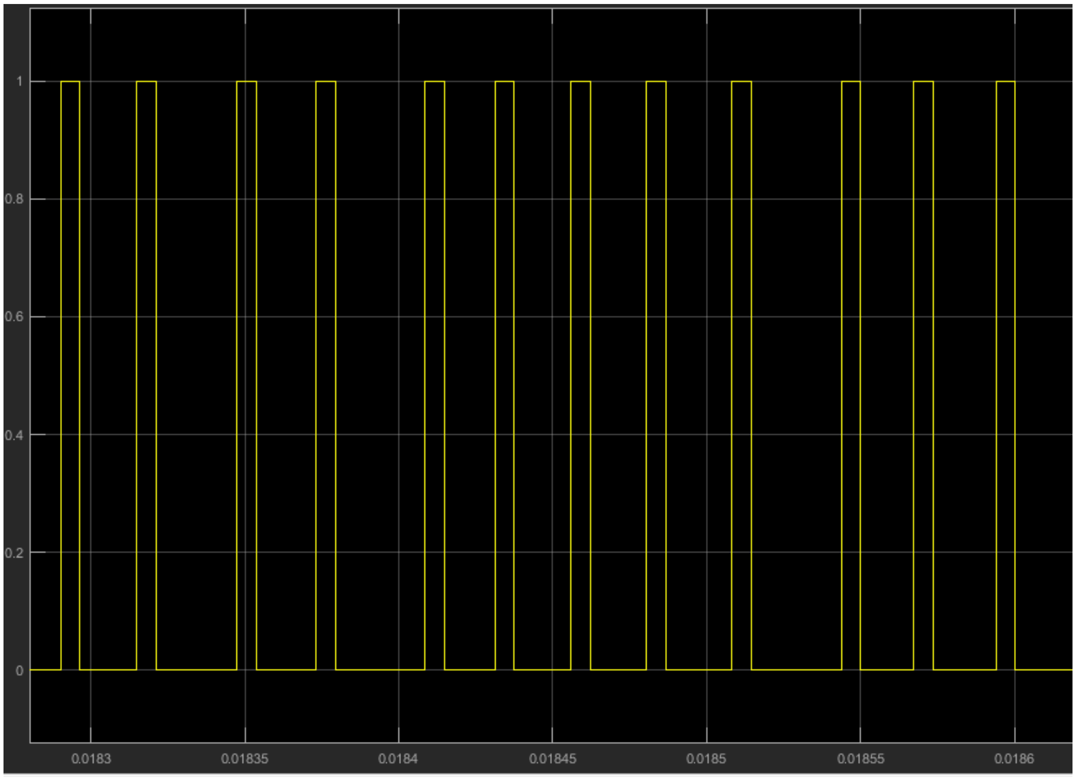

Figure 4.18, Randomized Modulation Phase Position Delay between 0 and 11 Microseconds

<u>Cuk Simulation, FFT and Voltage Measurements for RPPM, Low Output Voltage</u>

The FFT measurements with the maximum phase position delay of 11 microseconds between switching shows that the harmonic peaks are reduced but other frequencies are higher in magnitude. Additionally, the THD increased when compared to the baseline measurement. As shown in Figure 4.19 are the expectant input and output voltages, which are 7.2 and -4.3 Volts, respectively.

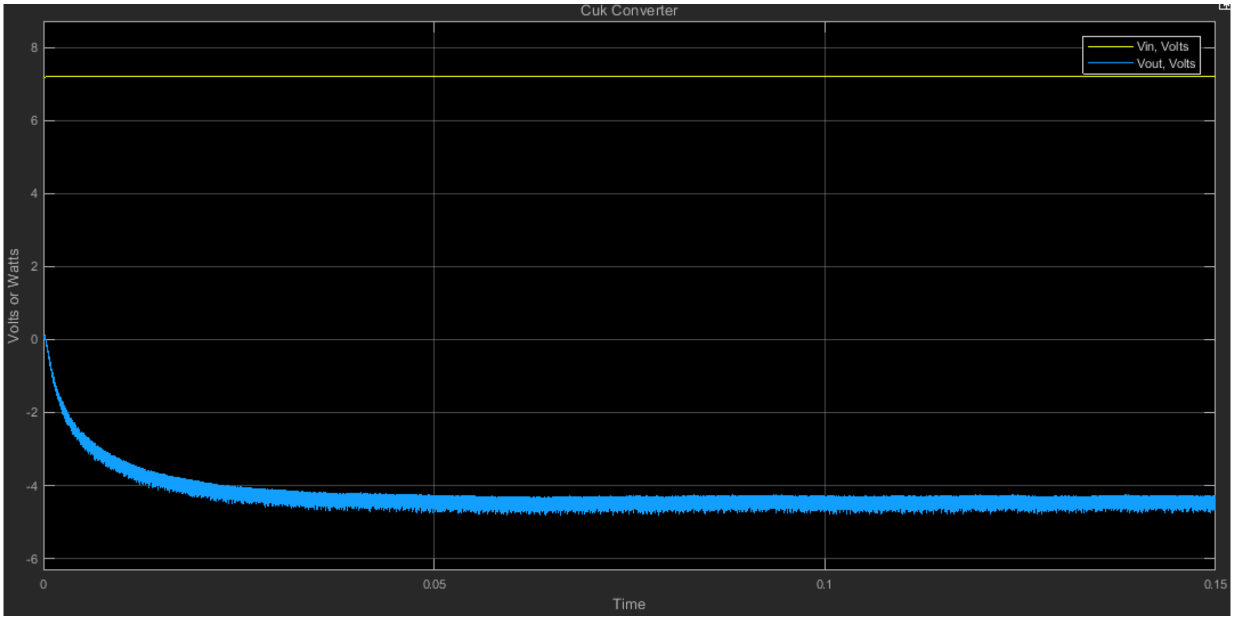

Figure 4.19, Cuk Simulation, RPPM Results, Low Output Voltage

The FFT results are shown in Figure 4.20 below. The discrete harmonics are adjusted to other frequencies especially towards the lower frequencies when compared to the PWM FFT Figure 4.8. THD has also increased as a result of the RPPM when compared to PWM FFT.

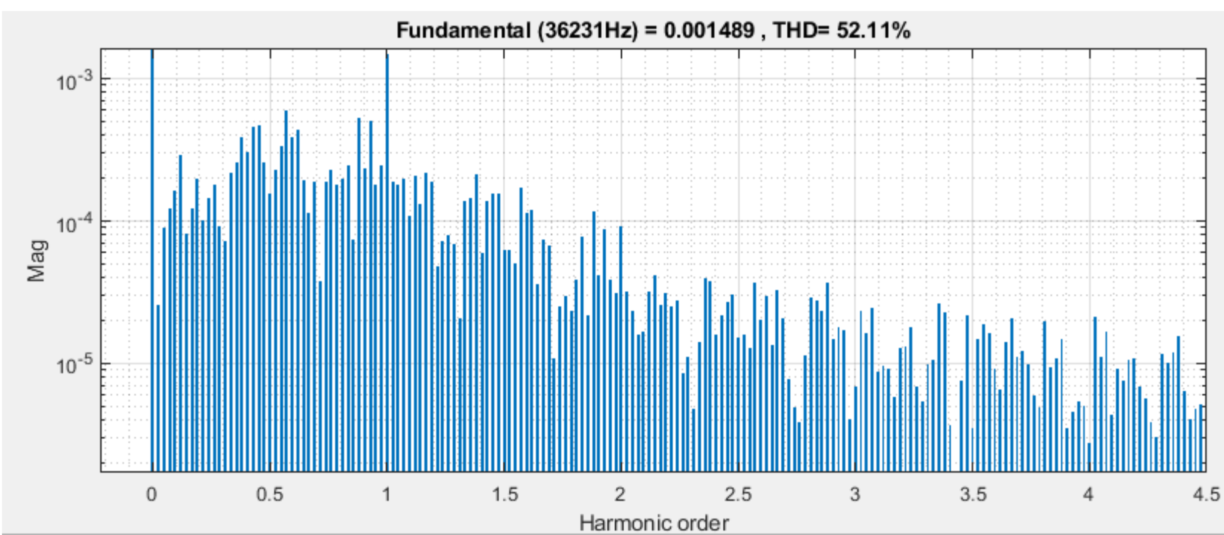

Figure 4.20, Cuk Simulation FFT Result of RPPM with Low Voltage Output

CUK Converter Vout Higher than Vin

Simulation Cuk Converter, High Vout, PWM

<u>Cuk Converter, High Vout, PWM Measurements</u>

Pulse width modulation measurements with no randomization is shown below in Figure 4.21. The duty cycle of the PWM is 52%. The switching frequency is shown to be 36 kHz. This PWM is the baseline for which randomization would be compared too.

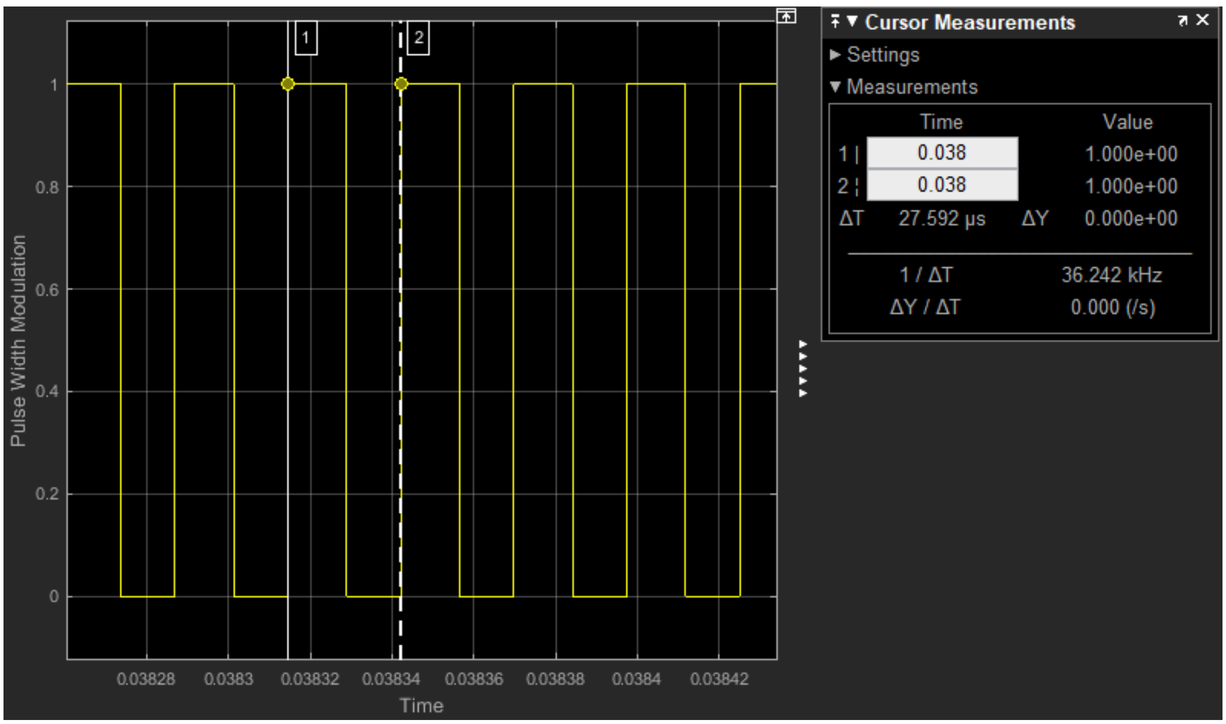

Figure 4.21, Cuk Simulation, PWM Results with no Randomization, High Vout

<u>CUK Simulation, High Vout, PWM, FFT and Voltage Measurements</u>

FFT measurement of PWM, or no randomization, is shown below in Figure 4.22 for the Cuk converter.

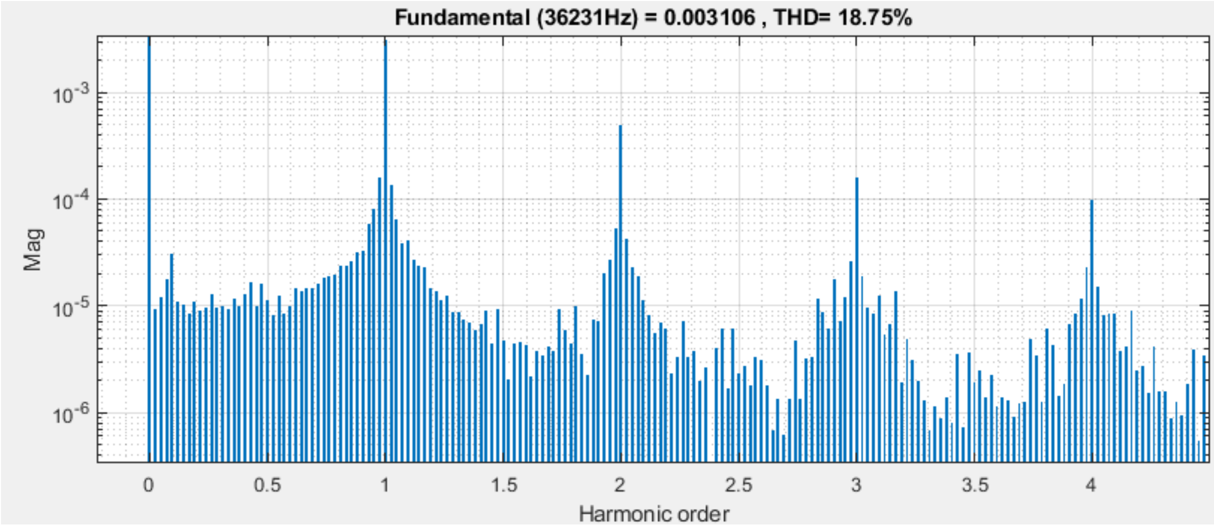

Figure 4.22, Cuk Simulation FFT Result, PWM, High Vout

The input and output measurement is shown below in Figure 4.23. The input voltage is 7.2 volts while the output voltage is about -10.0 volts.

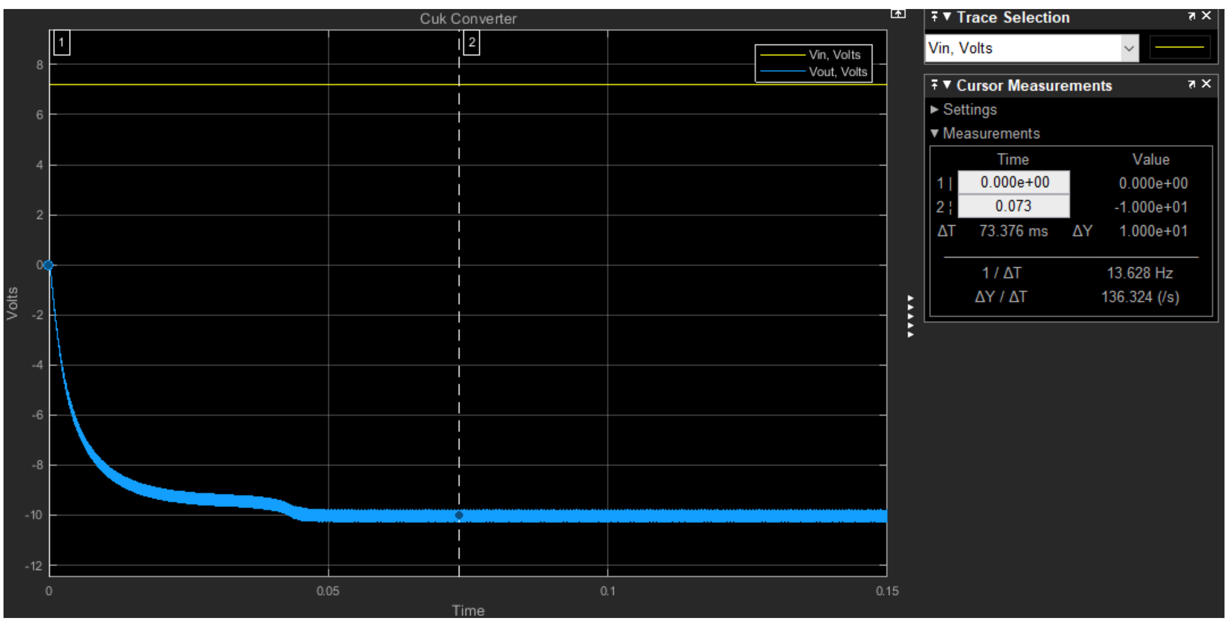

Figure 4.23, Cuk Simulation, Input and Output Voltage for PWM, High Vout

Simulation Cuk Converter, High Vout, Add RPWM

Simulation Cuk Converter, High Vout, Add RPWM, PWM Measurements

RPWM was added to the Cuk converter and resulted in the following PWM randomization as shown in Figure 4.24. The bottom PWM graph shows that different PWM duty cycles were used. The duty cycles ranged from 52% to 63%. The number of different duty cycles was four.

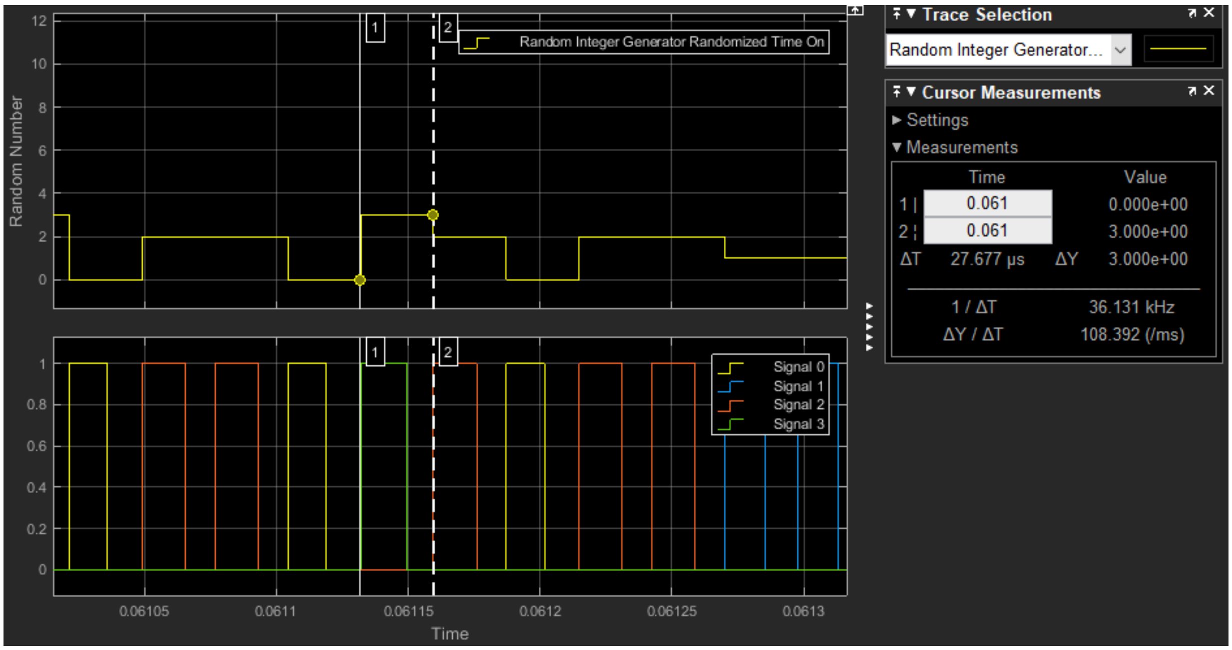

Figure 4.24, Cuk Simulation, RPWM Result, High Vout

Simulation, Cuk High Vout, FFT and Voltage Measurements

FFT results of the RPWM are shown in Figure 4.25. Based off of the PWM FFT in Figure 4.22, the RPWM still shows the discrete harmonics, and increases the THD.

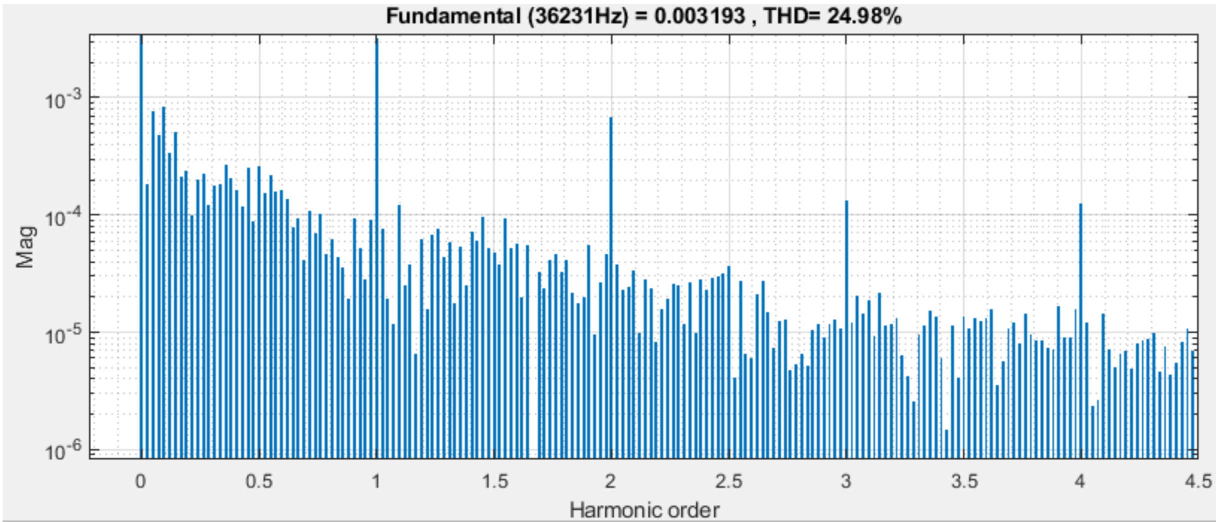

Figure 4.25, Cuk Simulation, FFT Results of RPWM, High Vout

The input and voltage measurements are shown in Figure 4.26. The input voltage is 7.21 volts while the output voltage is -11.51 volts.

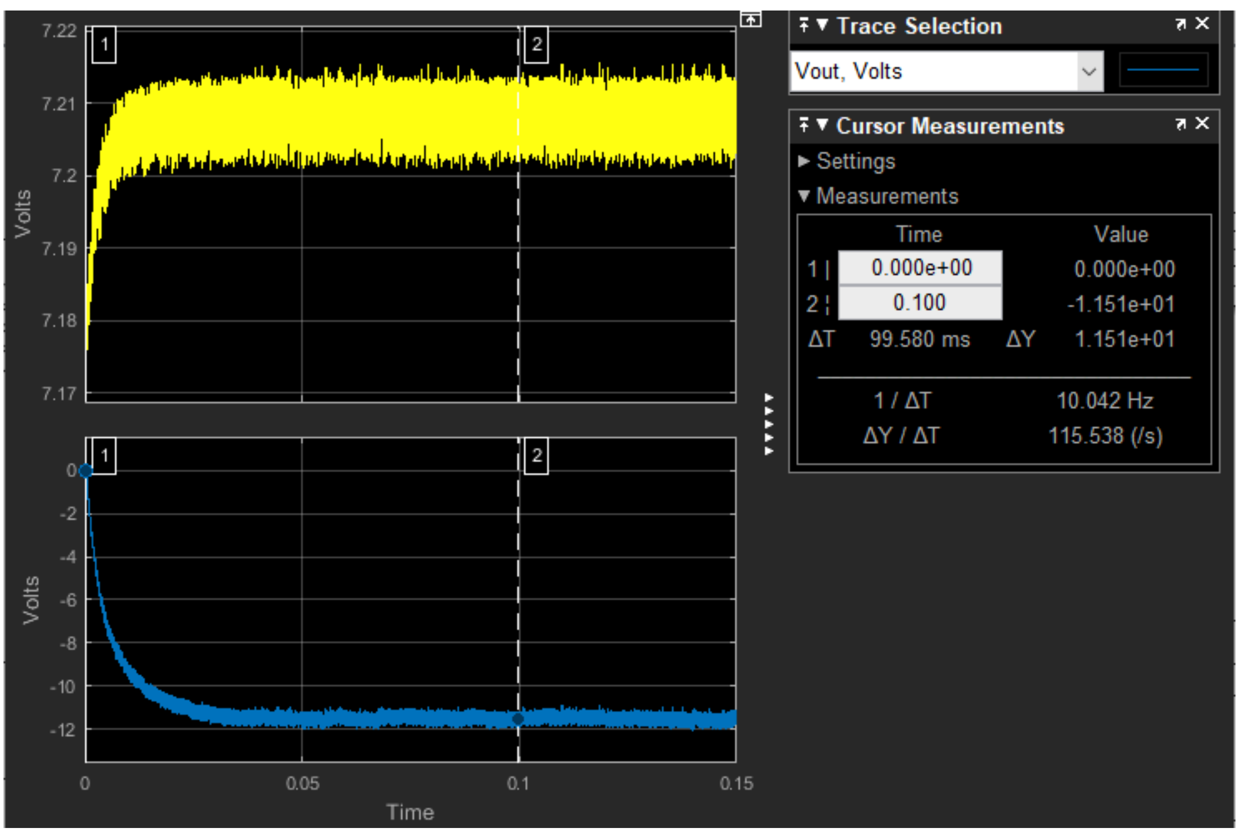

Figure 4.26, Cuk Simulation Input and Output Voltage Results, RPWM, High Vout

Cuk Simulation, High Vout, Add RPWM and RPPM

Cuk Simulation, High Vout, Add RPWM and RPPM, PWM Measurements

For RPWM and RPPM there were 6 different combinations used during the randomization. The architecture diagram of the simulation is shown below in Figure 4.27. As a result of the PWM randomization the duty cycles were change between 52% to 55% randomly and also have a time delay of 0 to 2 microseconds.

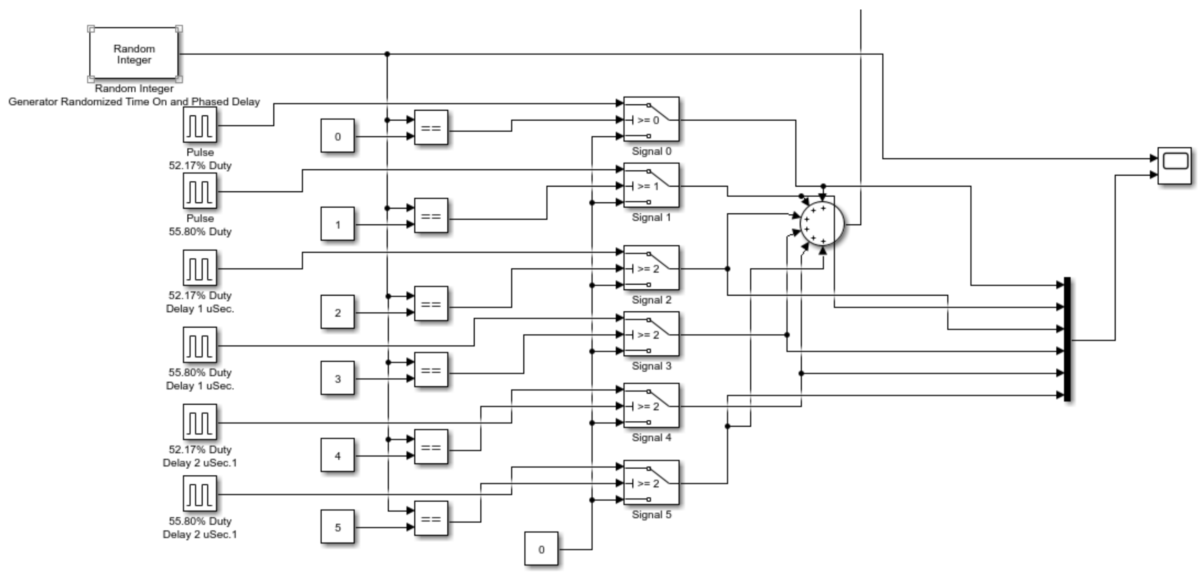

Figure 4.27, Cuk Simulation Architecture for RPWM and RPPM for High Vout

The results of the PWM simulation is shown in Figure 4.28. The top graph shows the random number to which each PWM randomization combination is assigned too. The bottom shows some of the PWMs randomized with either an increase in duty cycle or a phase position delay.

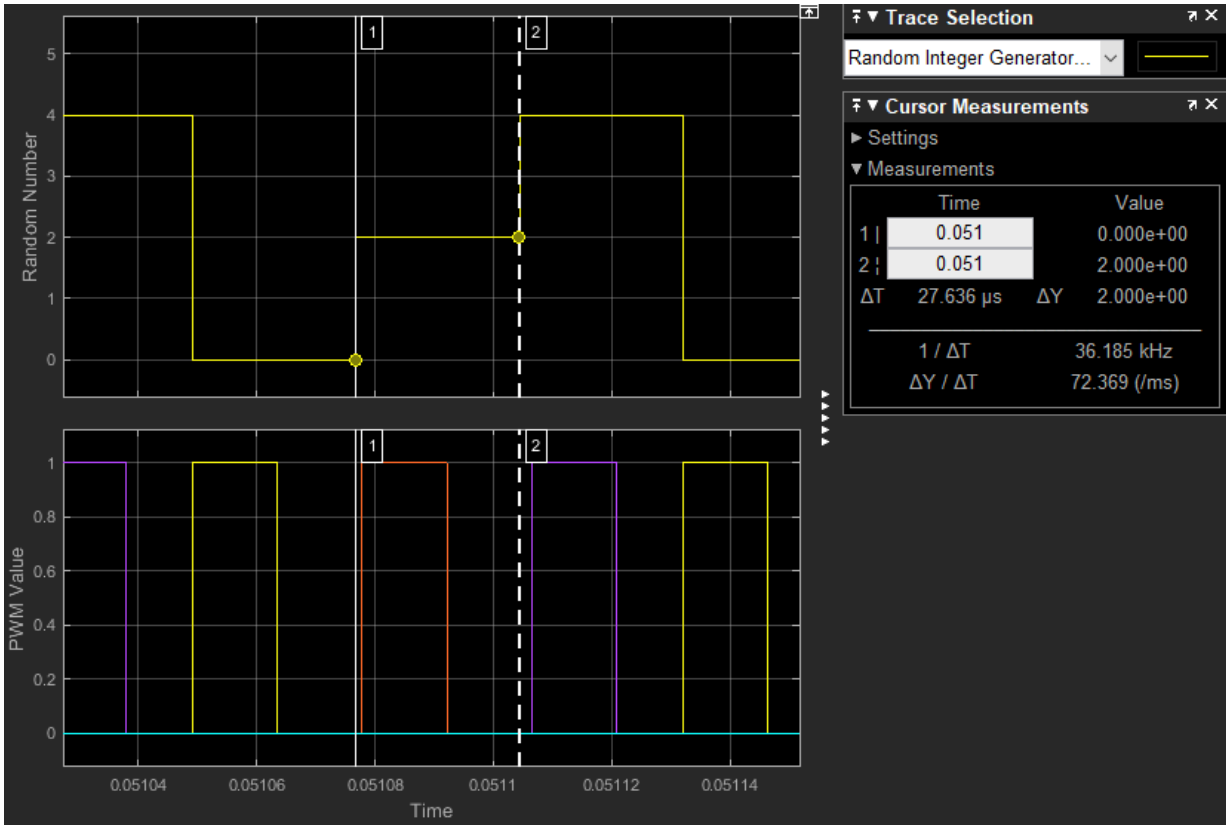

Figure 4.28, Cuk Simulation, RPWM and RPPM Results, High Vout

<u>Cuk Simulation, RPWM and RPPM, High Vout, FFT and Voltage Measurements</u>

The FFT results of RPWM and RPPM are shown in Figure 4.29. The discrete harmonics appear the same and the THD is slightly higher as a result of both RPWM and RPPM when compared to the PWM FFT result found in Figure 4.22.

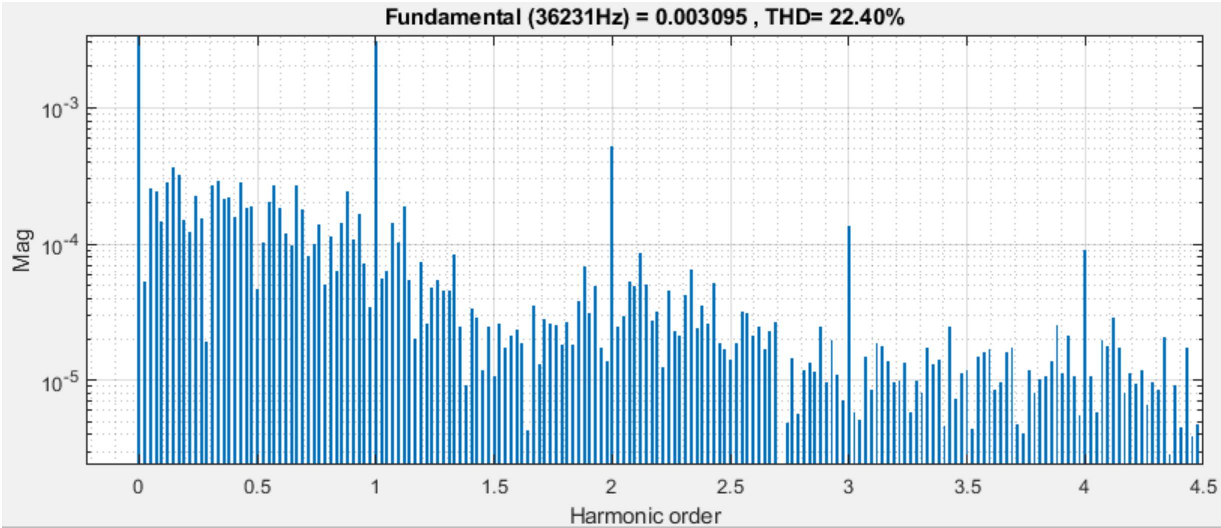

Figure 4.29, Cuk Simulation, FFT Results for RPWM and RPPM, High Vout

The input and output voltage results are shown in Figure 4.30. Input voltage is about 7.2 volts while the output voltage is -10.48 volts.

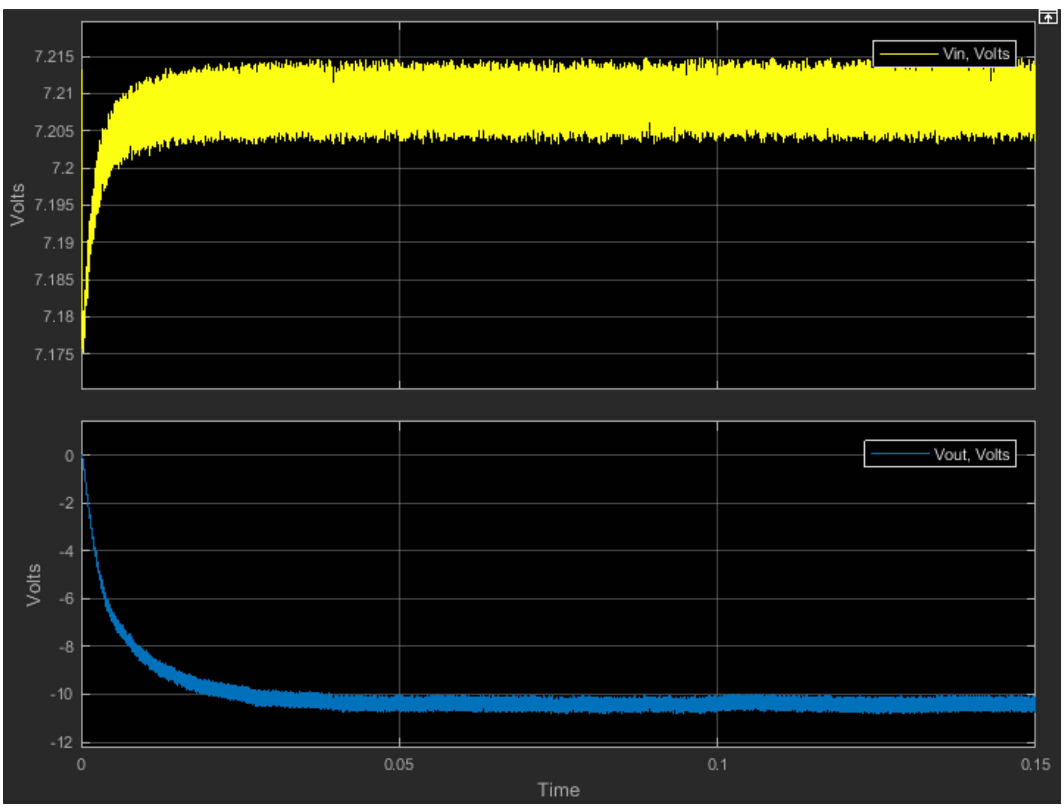

Figure 4.30, Cuk Simulation, Input and Output Voltage Results, RPWM and RPPM, High Vout

Cuk Simulation, Add RPPM for High Vout

Cuk Simulation, Add RPPM for High Vout, PWM Measurements

The PWM phase position was delayed between 0 and 3 microseconds. The result of the delay is shown in Figure 4.31 where some pulses are closer to the starting time than other pulses. The switching frequency is about 36 kHz.

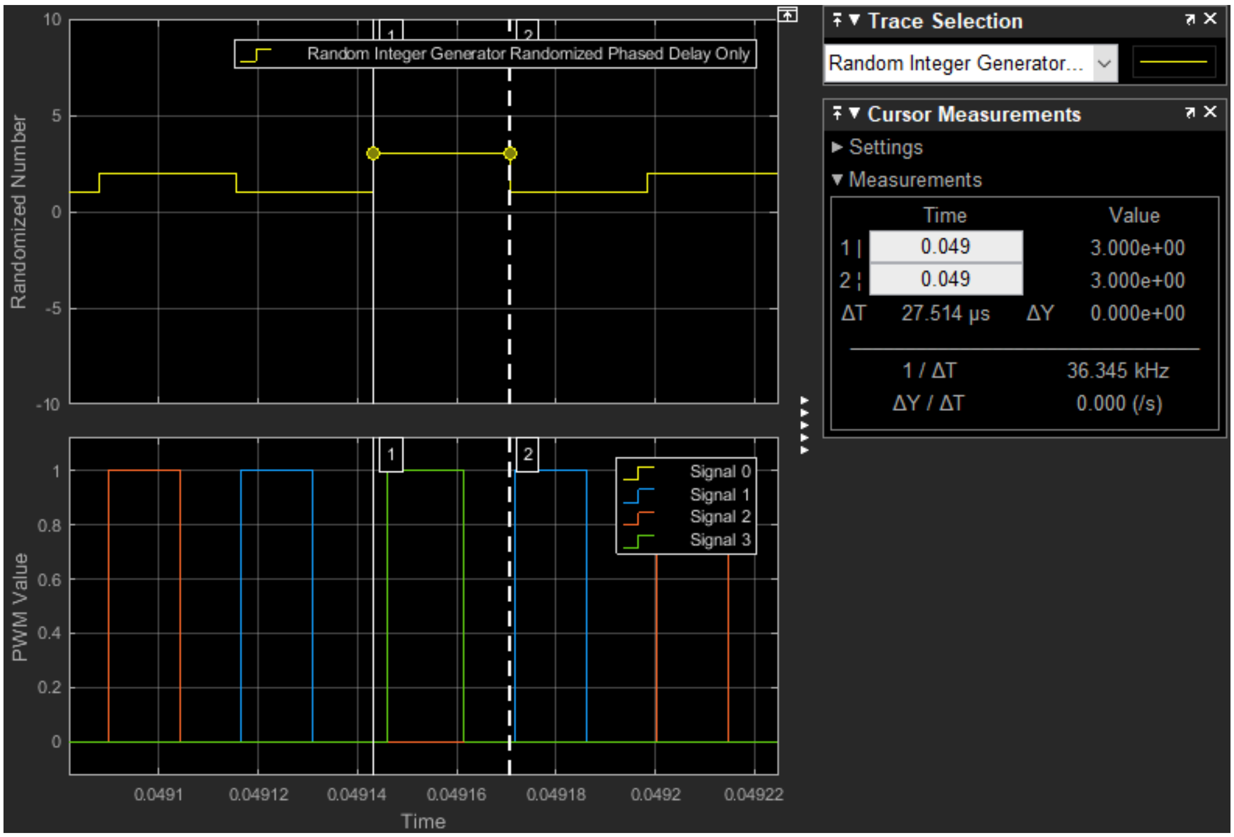

Figure 4.31, Cuk Simulation, RPPM Results, High Vout

Cuk Simulation, Add RPPM for High Vout, FFT and Voltage Measurements

Typically, the RPPM would result in harmonic adjustment but since the randomization margin is between 0 and 3 microseconds there isn't much harmonic adjustment due to the small time adjustment when compared to the PWM FFT result as shown in Figure 4.22. The result of the RPPM FFT is shown in Figure 4.32.

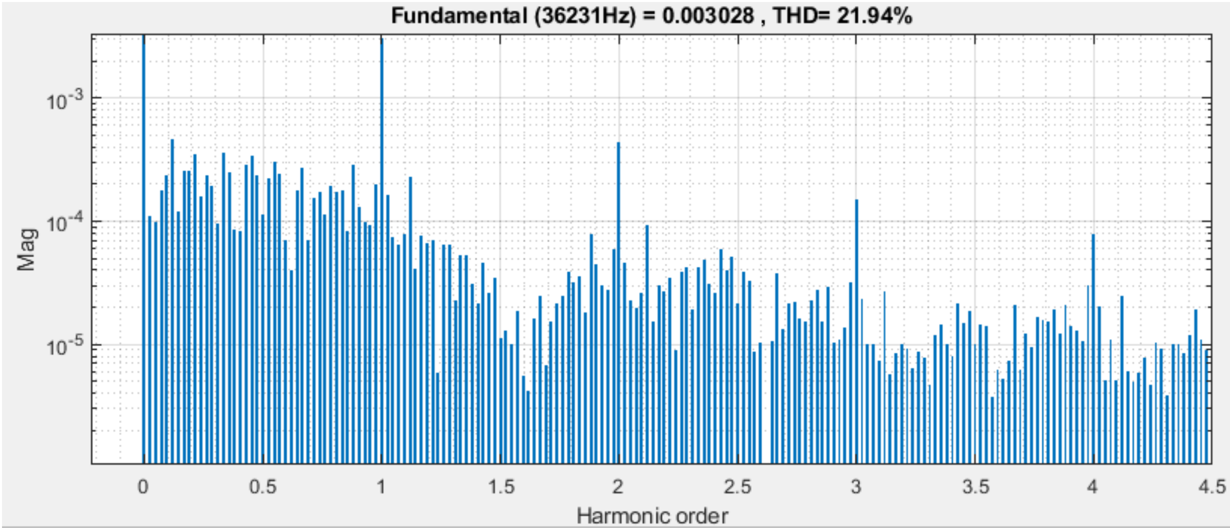

Figure 4.32, Cuk Simulation, FFT Results, RPPM, High Vout

Voltage results are shown below Figure 4.33. The input voltage is 7.21 volts while the output voltage is about -10.07 volts.

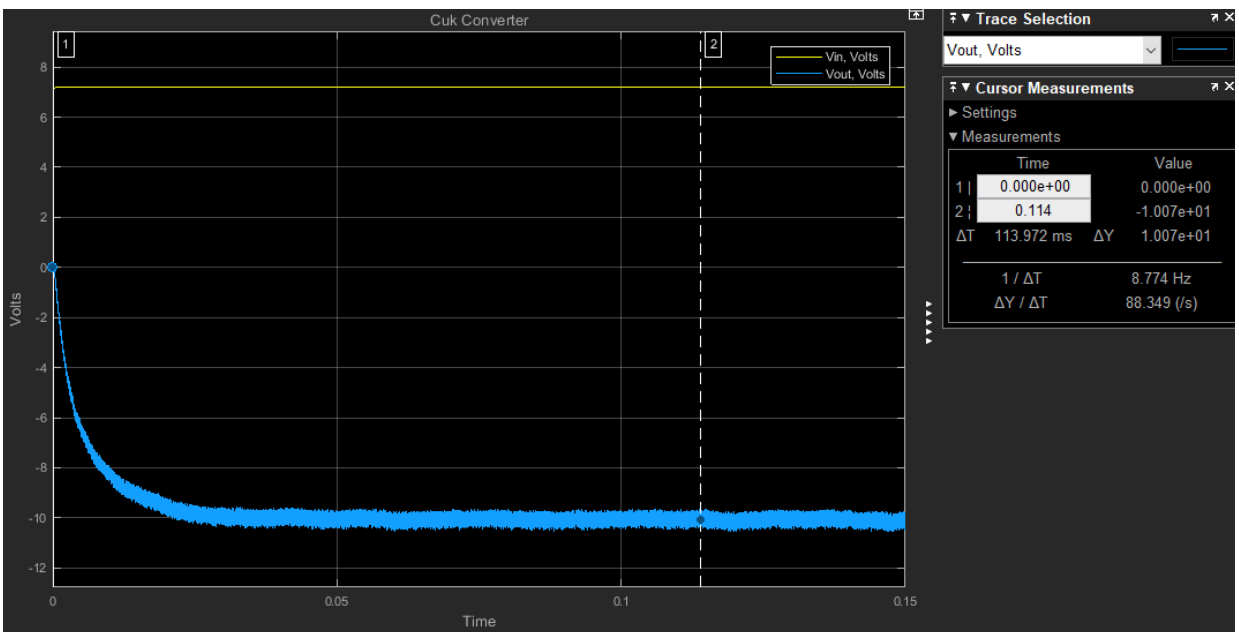

Figure 4.33, Cuk Simulation, Input and Output Voltage Results, RPPM, High Vout

SEPIC Converter Vout Lower than Vin

SEPIC Converter, No Randomization, Low Vout

<u>SEPIC Converter, PWM Measurements, Low Vout</u>

The SEPIC Simulation is shown below in Figure 4.34. The converter looks similar to the Cuk converter but the second inductor and the diode have switched locations. This results in a SEPIC converter architecture with an output the same polarity as the input voltage.

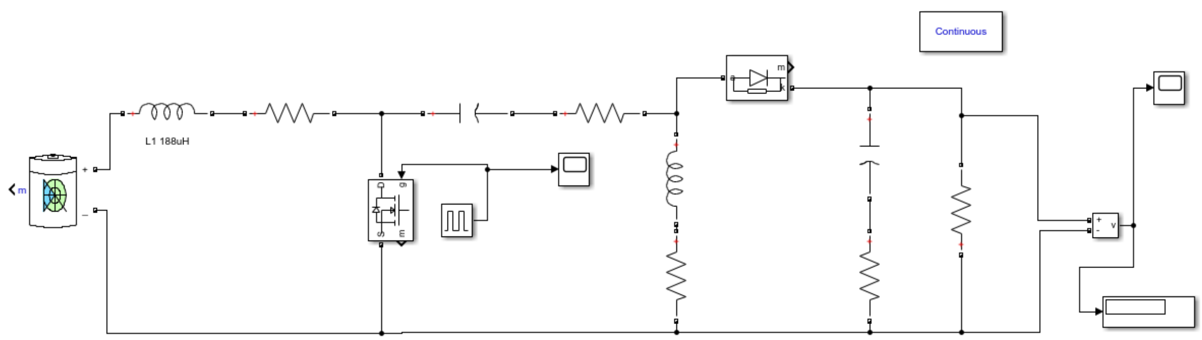

Figure 4.34, SEPIC Simulation Converter

PWM measurement is shown below in Figure 4.35. The duty cycle for the SEPIC was 23%. Switching frequency is about 36 kHz between each cycle.

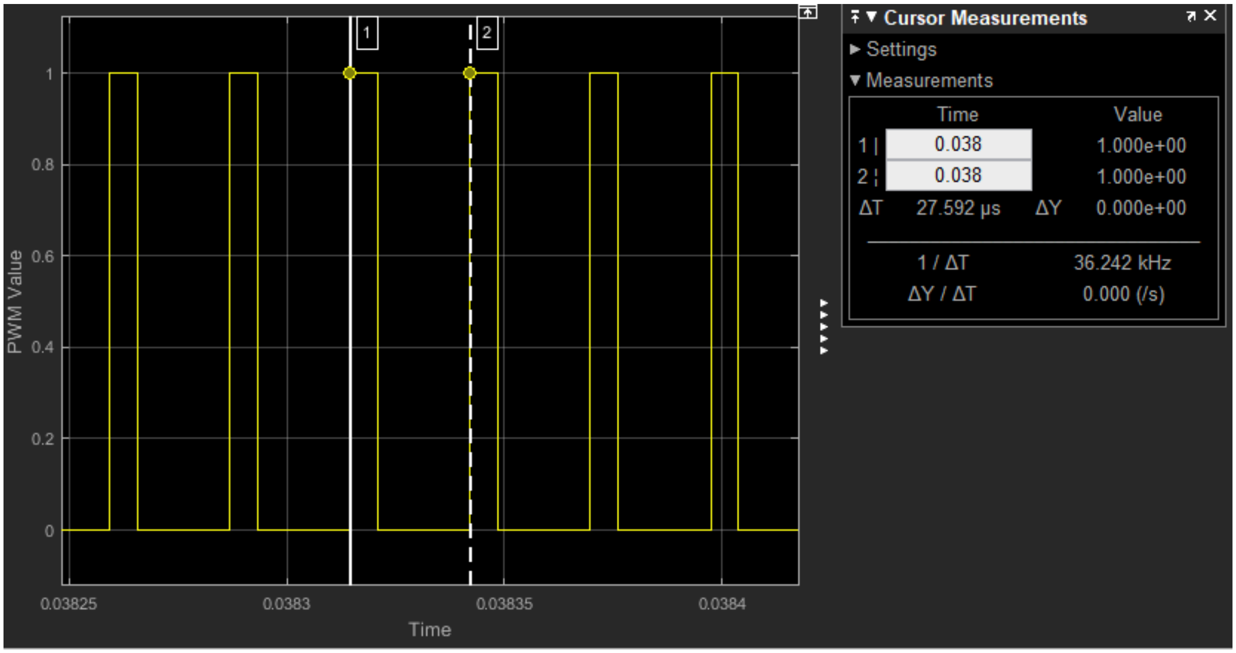

Figure 4.35, SEPIC Simulation, PWM Result with no Randomization, Low Vout

<u>SEPIC Converter, PWM, FFT and Voltage Measurements Low Vout</u>

FFT results of the no PWM randomization is shown below, same 42 cycles were evaluated of the SEPIC converter.

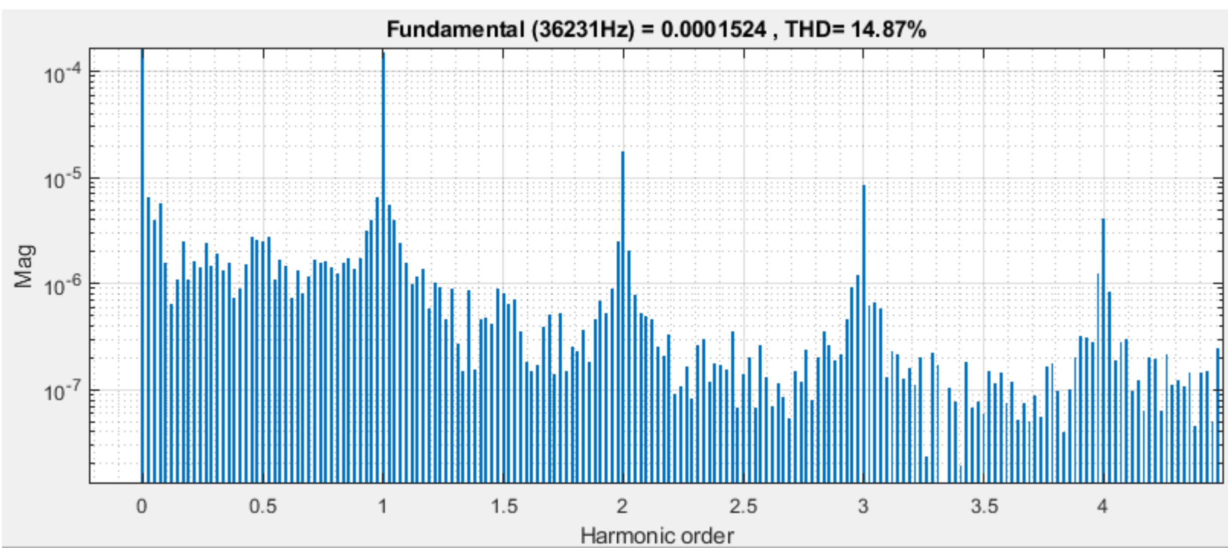

Figure 4.36, SEPIC Simulation, FFT Result, PWM, Low Vout

The input and output voltage results are shown in Figure 4.37. The output voltage of the SEPIC oscillates between about 5 volts and -1 volts, which an average of about 4.15 volts.

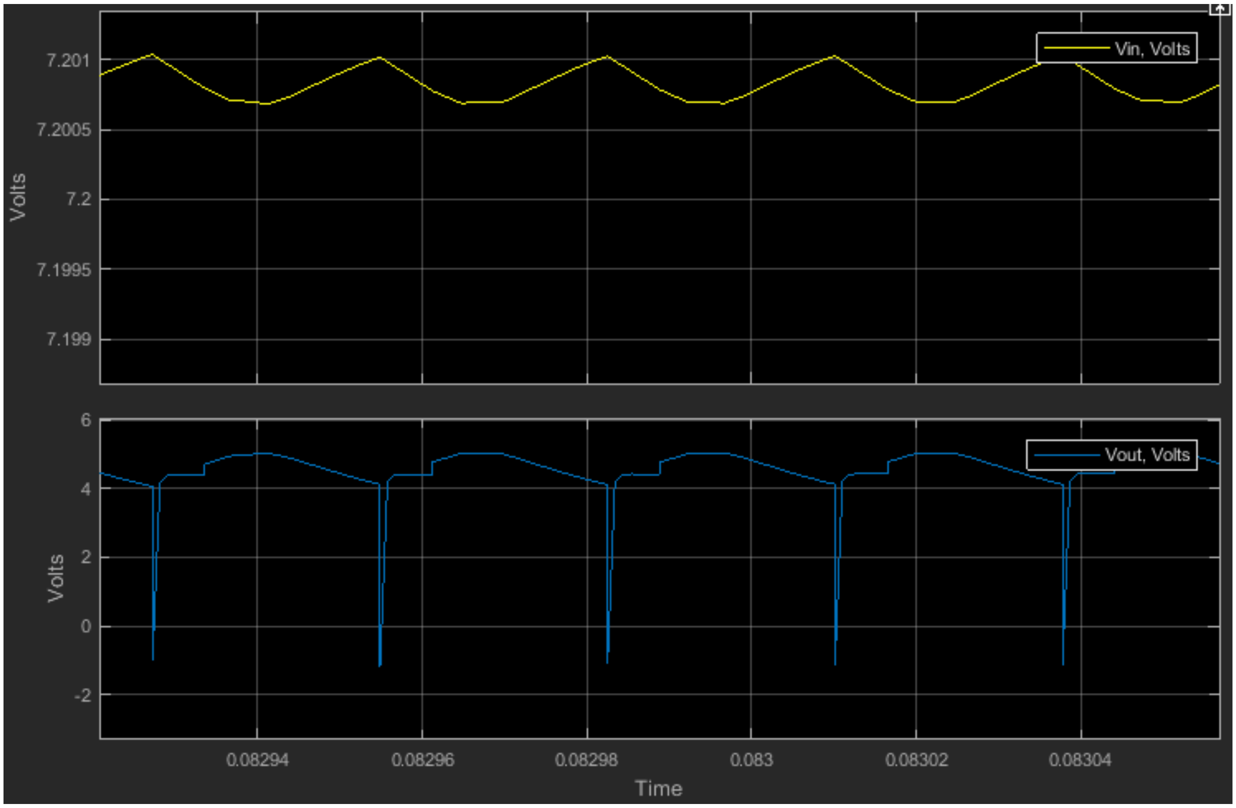

Figure 4.37, SEPIC Simulation, Input and Output Voltage Results, PWM, Low Vout

SEPIC with Additional Inductor Added to the Output

Due to the high output voltage oscillation, if an inductor is added prior to the resistive load the result is a reduction in the output voltage oscillation. Figure 4.38 shows the addition of the inductor prior to output load.

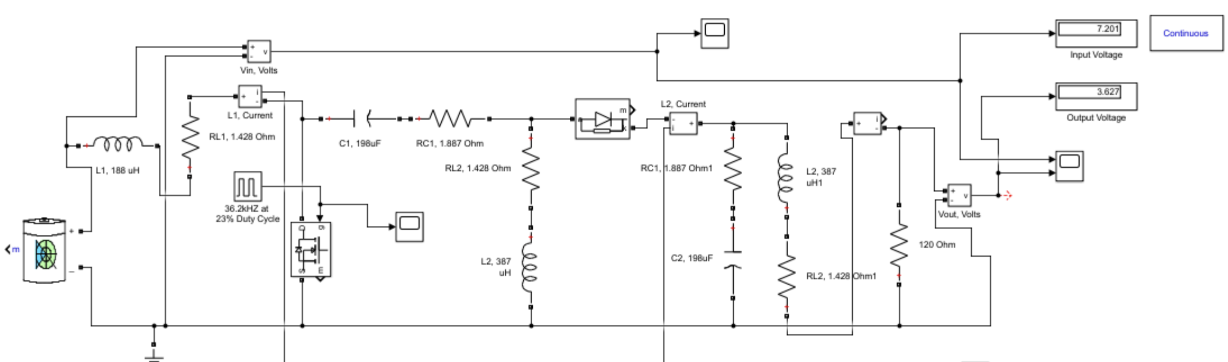

Figure 4.38, SEPIC Converter with Addition of Inductor Prior to Load

SEPIC with Additional Inductor, Input and Output Voltage Results

As a result of the addition of the inductor the output voltage oscillation is greatly improved as shown by Figure 4.39.

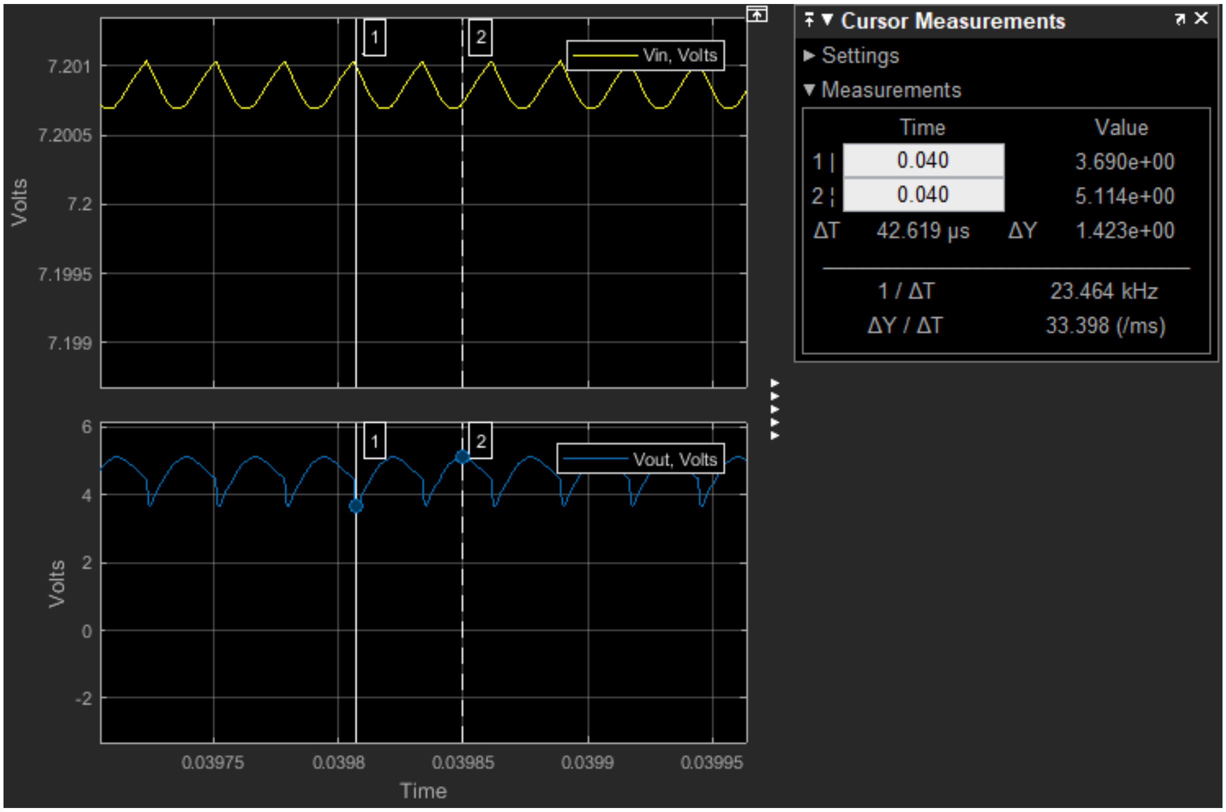

Figure 4.39, SEPIC Converter with Added Inductor, Input and Output Voltage Results

But due to the inclusion of the inductor on the basic SEPIC circuit, this would not meet the basic circuit configuration of the SEPIC converter. So the remaining simulation and experimentation would be matched against the basic SEPIC converter without the inclusion of the extra inductor as shown in Figure 4.34.

SEPIC Simulation, Add RPWM, Low Vout

<u>SEPIC Simulation, Add RPWM, Low Vout, PWM Measurements</u>

PWM measurement for RPWM is shown in Figure 4.40. The PWM results show that the duty cycles would change for the SEPIC converter between 23% and 63%, similar to the Cuk converter. Also similar to the Cuk converter, a random number was assigned to each PWM with a duty cycle between 23% and 63%.

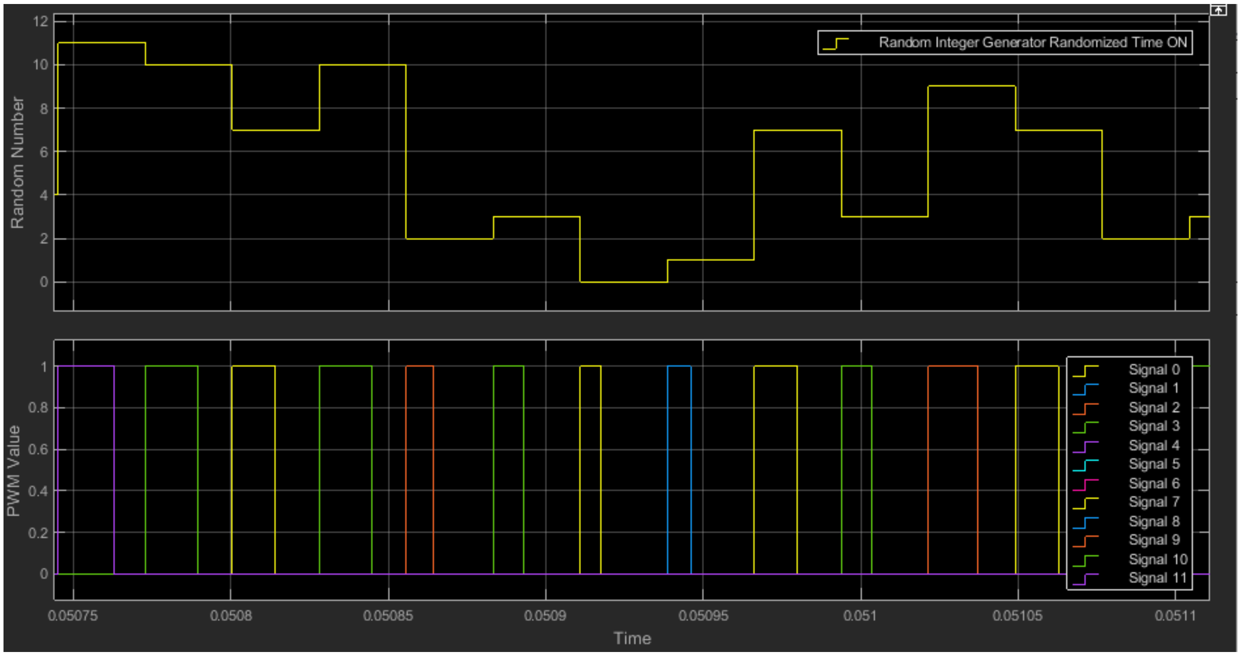

Figure 4.40, SEPIC Simulation, RPWM Result, Low Vout

<u>SEPIC Simulation, RPWM, FFT and Voltage Measurements for Low Vout</u>

The FFT results of the RPWM for the SEPIC converter are shown in Figure 4.41. The results of the FFT show that the discrete voltage harmonics are still present and the THD has also increased when compared to the PWM FFT result in Figure 4.36.

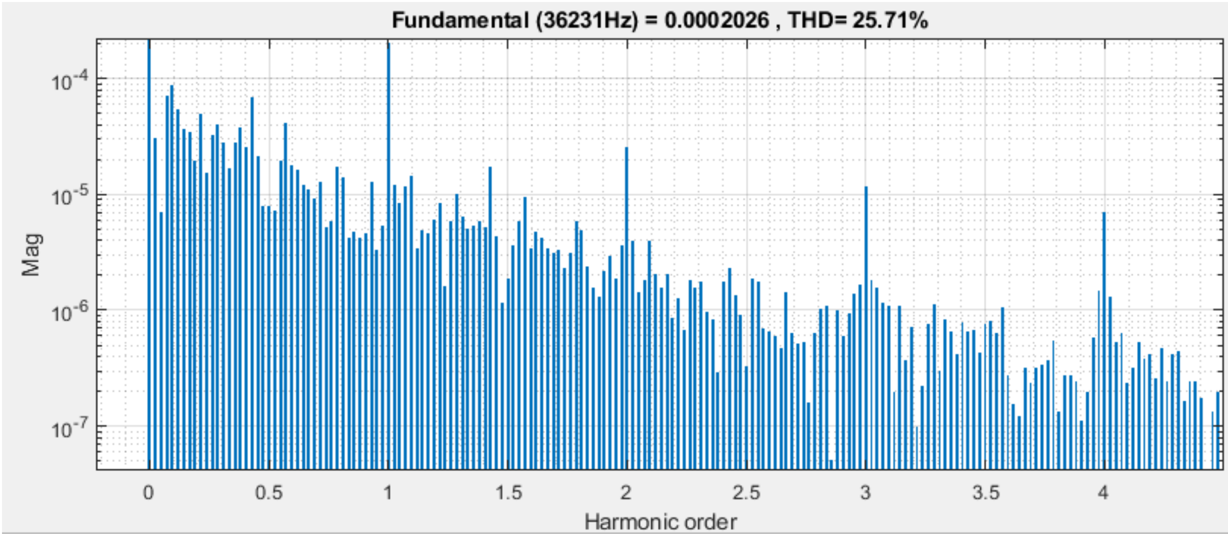

Figure 4.41, SEPIC Simulation, FFT Results, RPWM, Low Vout

Voltage input and output measurement are shown by Figure 4.42. The input voltage is about 7.20 volts and the output voltage is about 8.38 volts and can peak up to 6.92 Volts and drop to 0 volts.

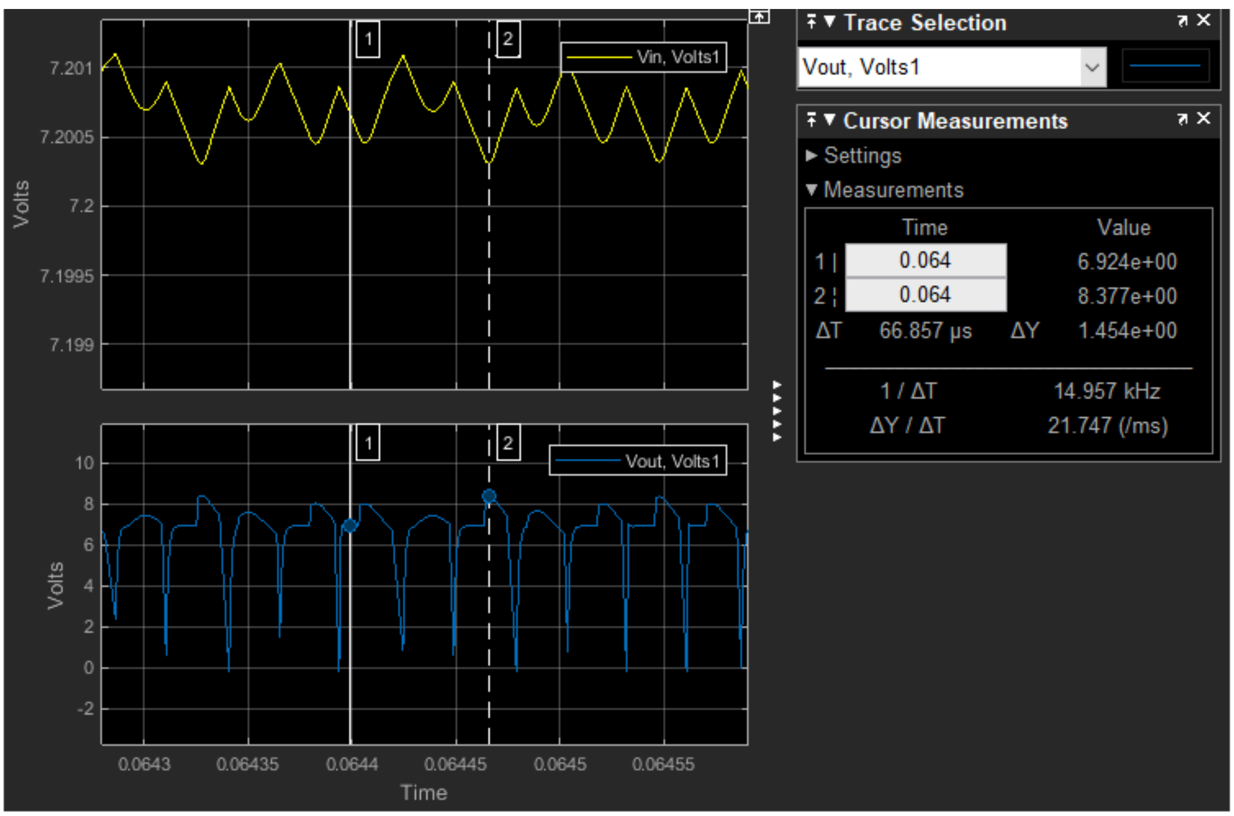

Figure 4.42, SEPIC Simulation, Input and Output Voltage Results, RPWM, Low Vout

SEPIC Simulation, Add RPWM and RPPM, Low Voltage

SEPIC Simulation, Add RPWM and RPPM, Low Voltage, PWM Measurements

The PWM simulation results are shown in Figure 4.43. As shown by the figure, the PWM vary in duty cycle and phase position. This simulation utilized 42 combinations which was similar to the Cuk simulation. For each random number, the circuit would experience a pulse that would have a specific duty cycle and phase position delay.

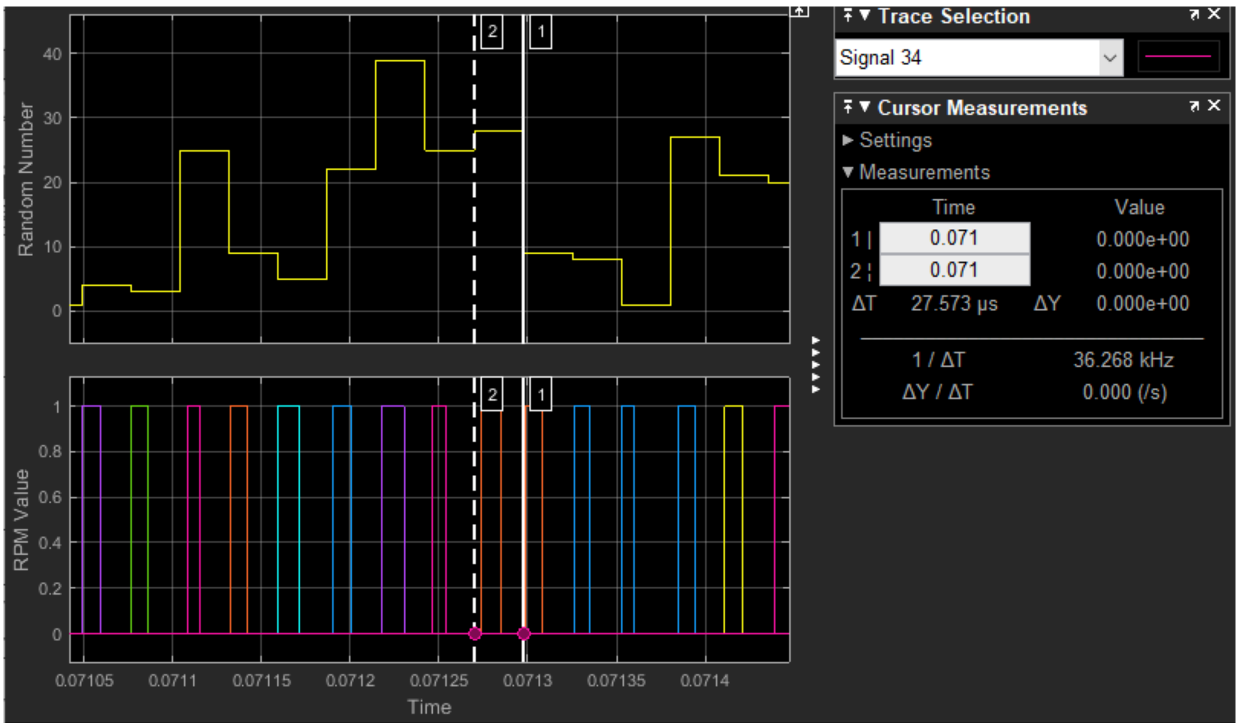

Figure 4.43, SEPIC Simulation, RPWM and RPPM, Low Vout

SEPIC Simulation, RPWM and RPPM, FFT and Voltage Measurements for Low Vout

The FFT results are shown in Figure 4.44 where the discrete harmonic was reduced slightly but the THD were increased when compared to the PWM FFT measurement found in Figure 4.36.

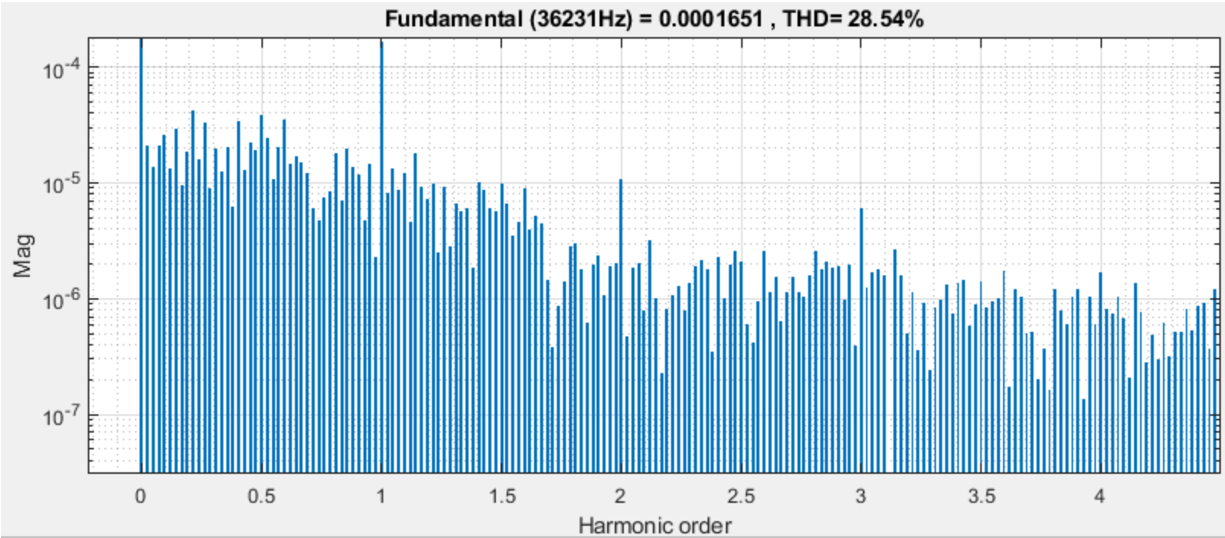

Figure 4.44, SEPIC Simulation, FFT Results, RPWM and RPPM, Low Vout

Voltage measurements are shown Figure 4.45 show the input voltage about 7.20 volts and the output voltage is about 4.91 volts and can oscillate down to about -0.21 volts.

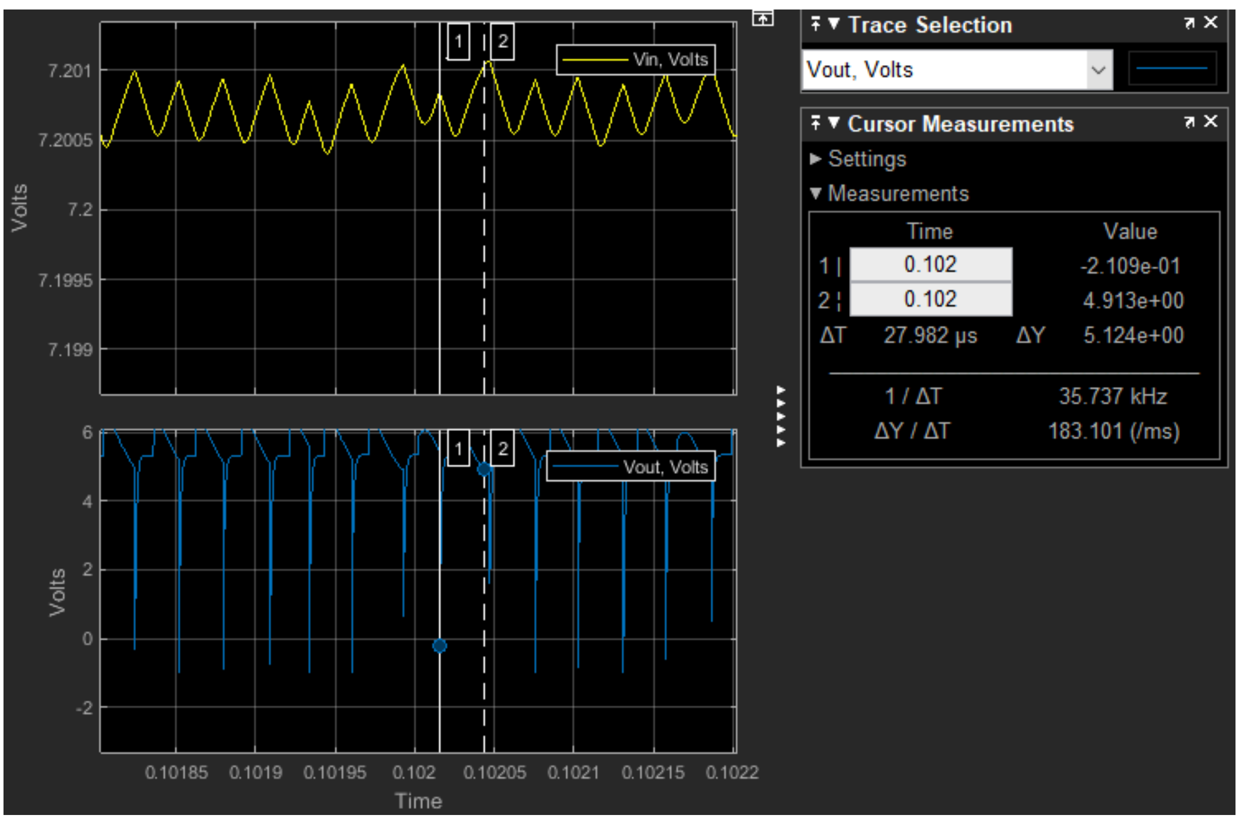

Figure 4.45, SEPIC Simulation, Input and Output Voltage Results, RPWM and RPPM, Low Vout

SEPIC Simulation, Add RPPM, for Low Vout

SEPIC Simulation, Add RPPM for Low Vout, PWM Measurements

PWM simulated measurements are shown in Figure 4.46 which utilize the same RPPM approach as the Cuk circuit. The PWM has a phase position delay that is assigned to a random value from 0 to 11. For each number, a phase position is delayed from a range of 0 to 11 microseconds. The figure below shows that PWM is delayed by a few microseconds.

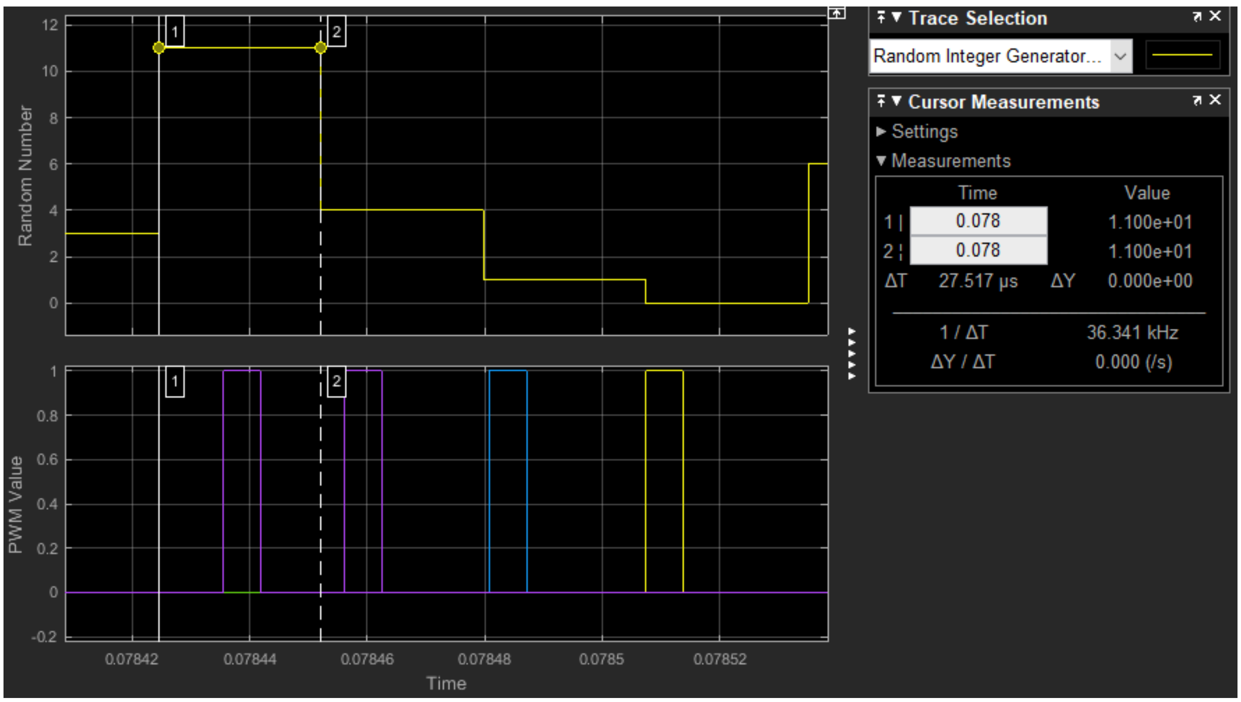

Figure 4.46, SEPIC Simulation, RPPM Results, Low Vout

SEPIC Simulation for RPPM of Low Vout, FFT and Voltage Measurements

The FFT results are shown in Figure 4.47. The results show that the discrete harmonics are adjusted and the smaller frequencies have increased in magnitude when compared to PWM FFT result found in Figure 4.36. The THD value increased as a result of the RPPM.

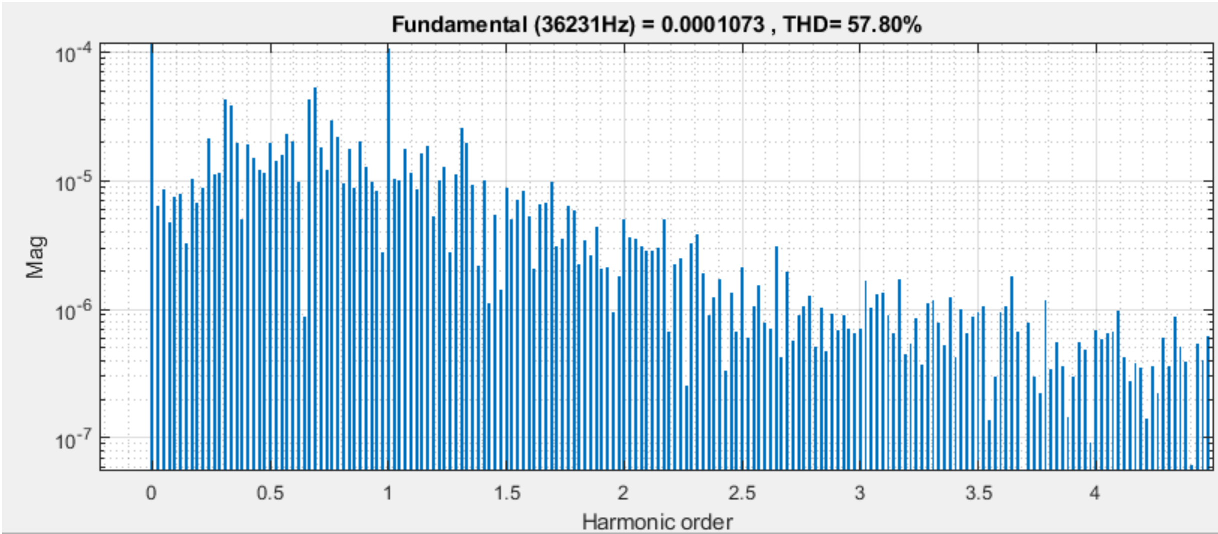

Figure 4.47, SEPIC Simulation, FFT Results, RPPM, Low Vout

The input and output voltages are shown in Figure 4.48. The input voltage is about 7.20 volts while the output voltage is about 3.9 volts with an oscillation of about -1.6 volts.

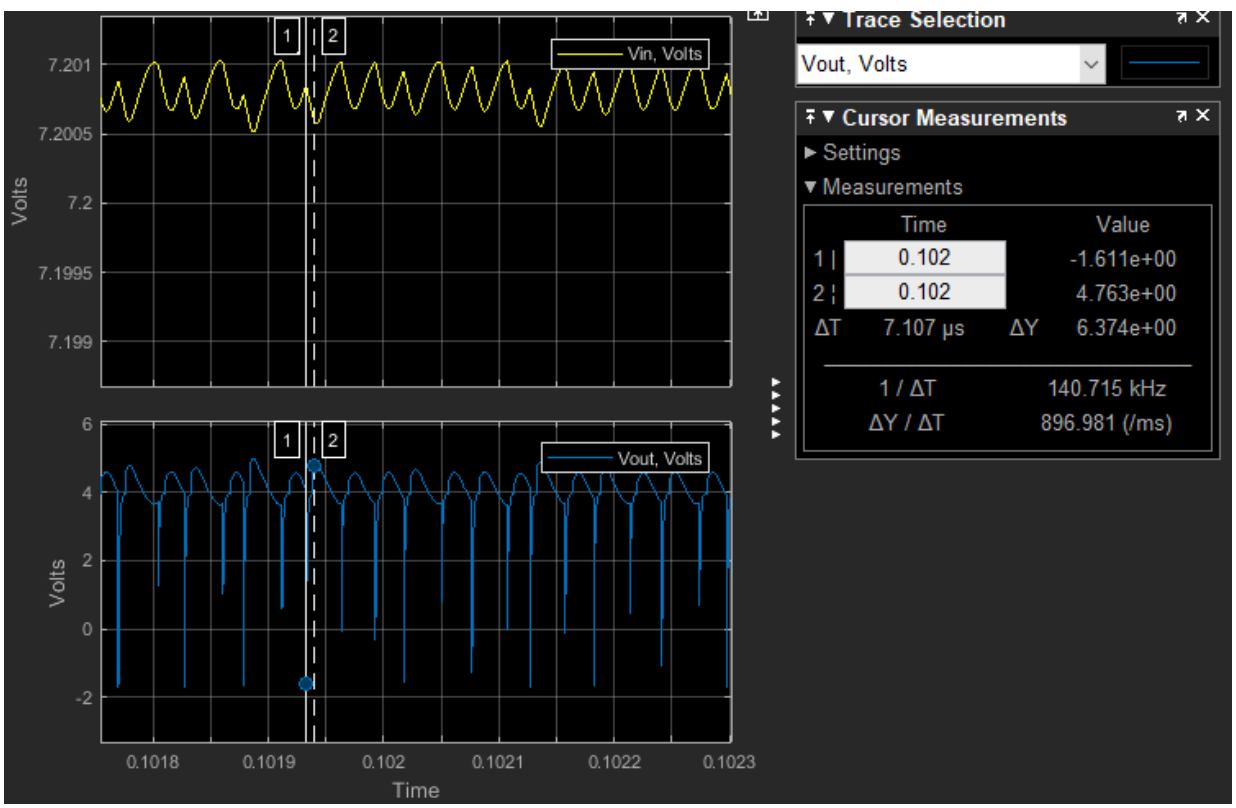

Figure 4.48, SEPIC Simulation, Input and Output Voltage Results, Low Vout

SEPIC Converter Vout Higher than Vin

SEPIC, Simulation, No Randomization, High Vout

<u>SEPIC, Simulation, PWM Measurements</u>

PWM measurement for SEPIC with no randomization is shown Figure 4.49. The duty cycle for the high voltage was about 52% and the switching frequency was 36 kHz.

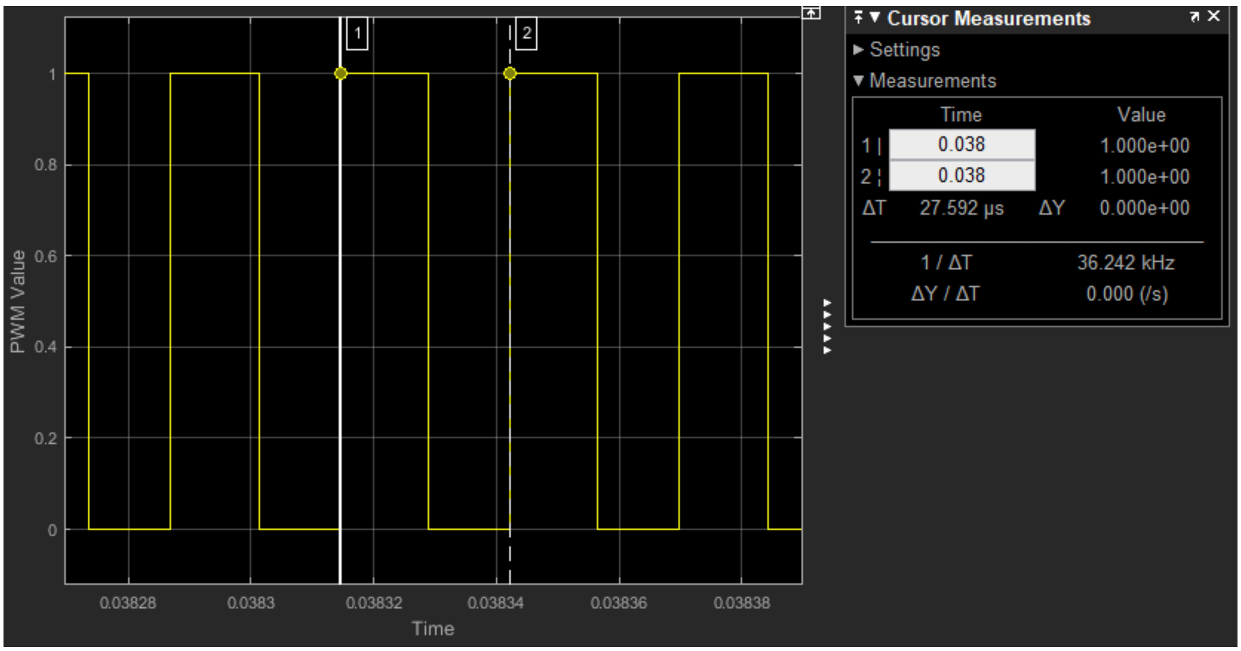

Figure 4.49, SEPIC Simulation, PWM Results, High Vout

<u>SEPIC Simulation, No PWM Randomization, FFT and Voltage Measurements for High Vout</u>

FFT results of the no randomization is shown in Figure 4.50. The discrete harmonics are shown and the THD is also shown below.

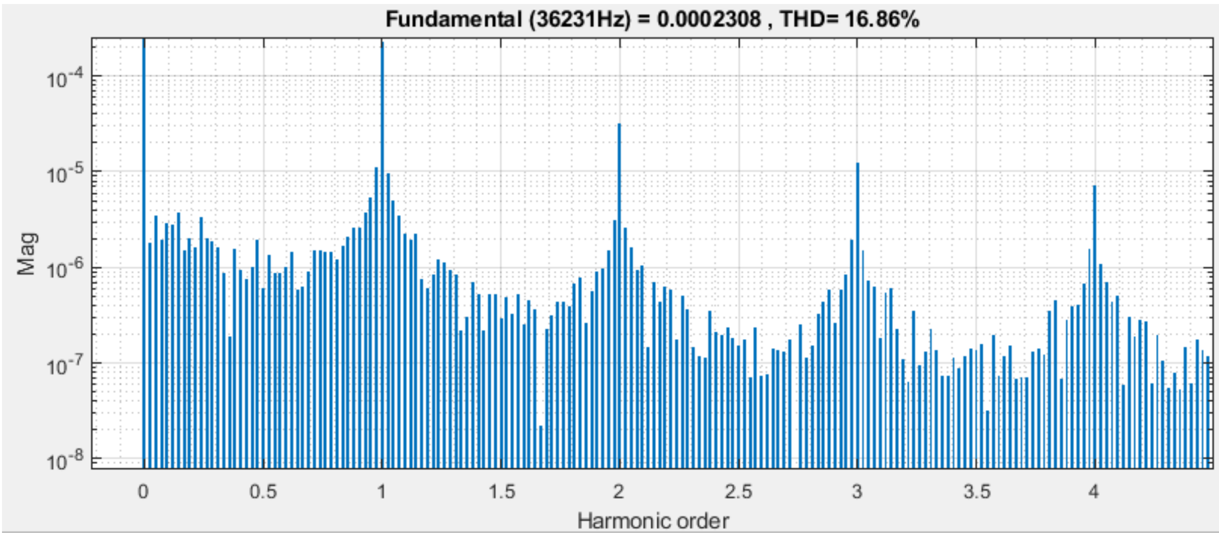

Figure 4.50, SEPIC Simulation, FFT Results, PWM, High Vout

Input and output voltage results are shown below in Figure 4.51. The figure shows that the input voltage is about 7.2 volts and the output voltage is about 8.90 volts and it can oscillate to 3.29 volts. The duty cycle for no randomization PWM is about 52%.

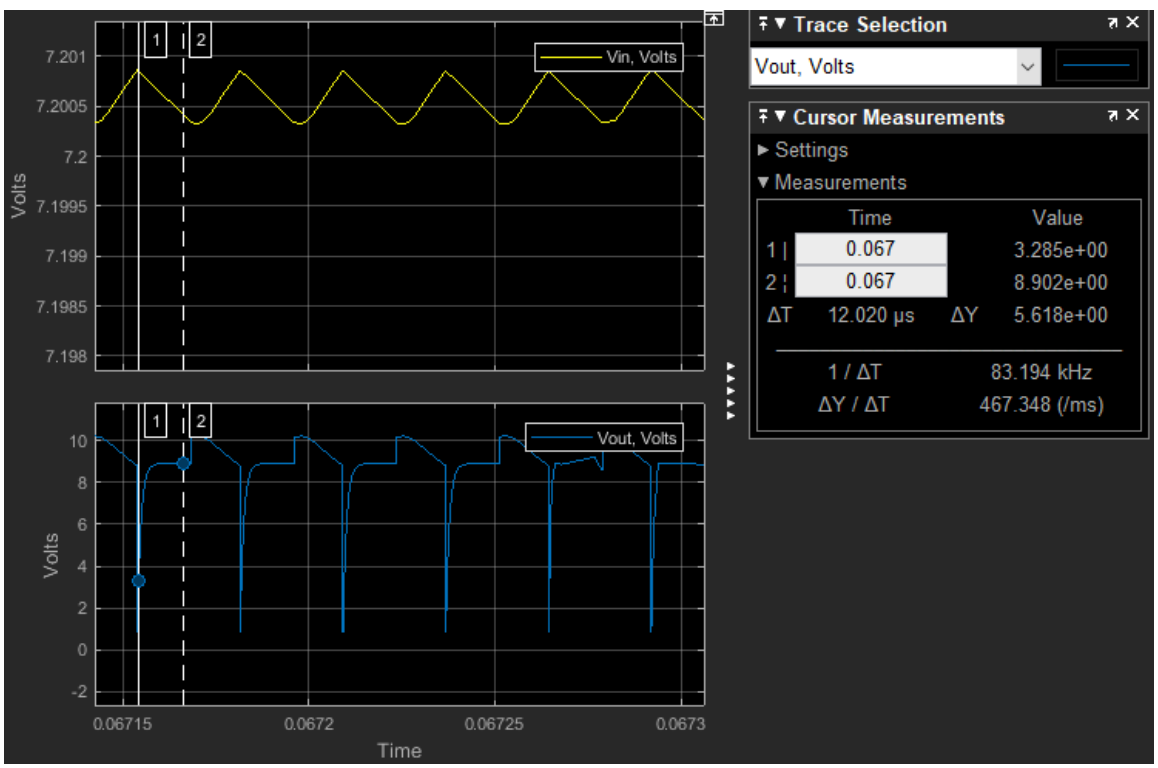

Figure 4.51, SEPIC Simulation, Input and Output Voltage Results, PWM, High Vout

SEPIC Simulation, Add RPWM, High Vout

SEPIC Simulation, Add RPWM High Vout, PWM Measurements

SEPIC PWM measurements during RPWM is shown in Figure 4.52. The PWM shows the various duty cycles that the SEPIC converter would experience through the randomization. The duty cycles which the SEPIC converter experienced is between 52% and 63%.

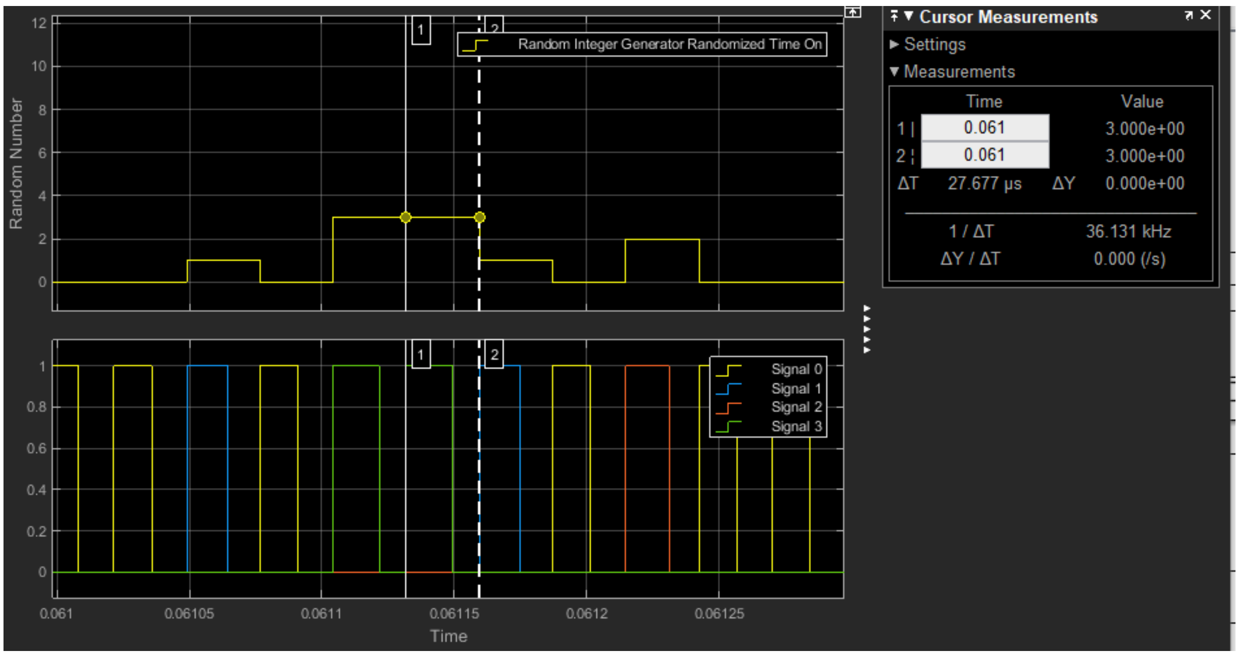

Figure 4.52, SEPIC Simulation, RPWM Result, High Vout

SEPIC Simulation, RPWM, FFT and Voltage Measurements

FFT results of SEPIC's RPWM is shown Figure 4.53. The discrete harmonics are still visible and the THD also increased when compared to the PWM FFT result found in Figure 4.50.

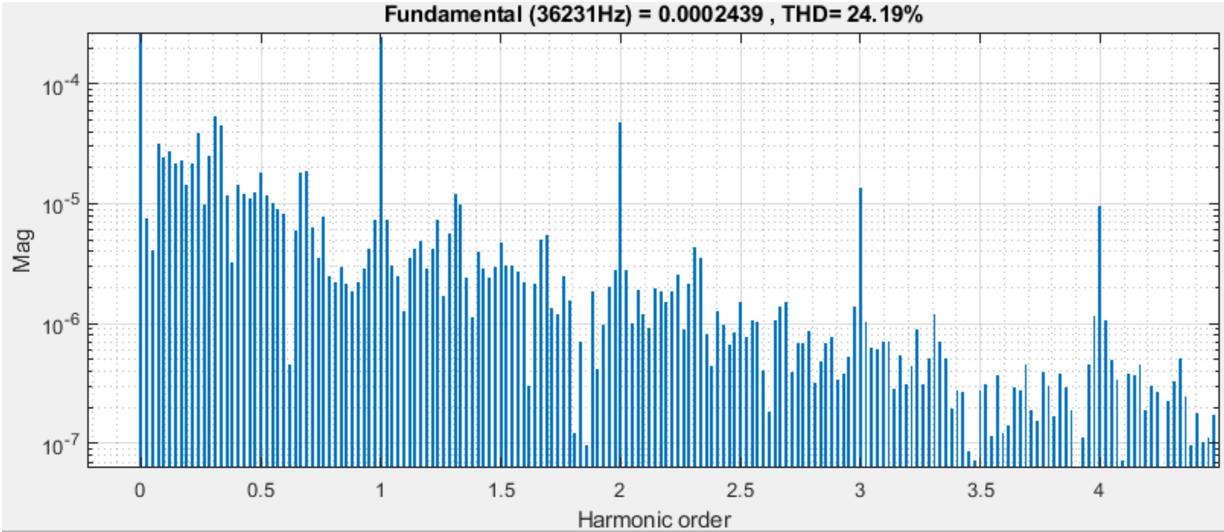

Figure 4.53, SEPIC Simulation, FFT Results, RPWM High Vout

The output voltage for SEPIC during RPWM is about 12.1 volts with a high peak of 13.4 and an oscillation of 2.66 volts. The input voltage is about 7.2 volts as shown by Figure 4.54.

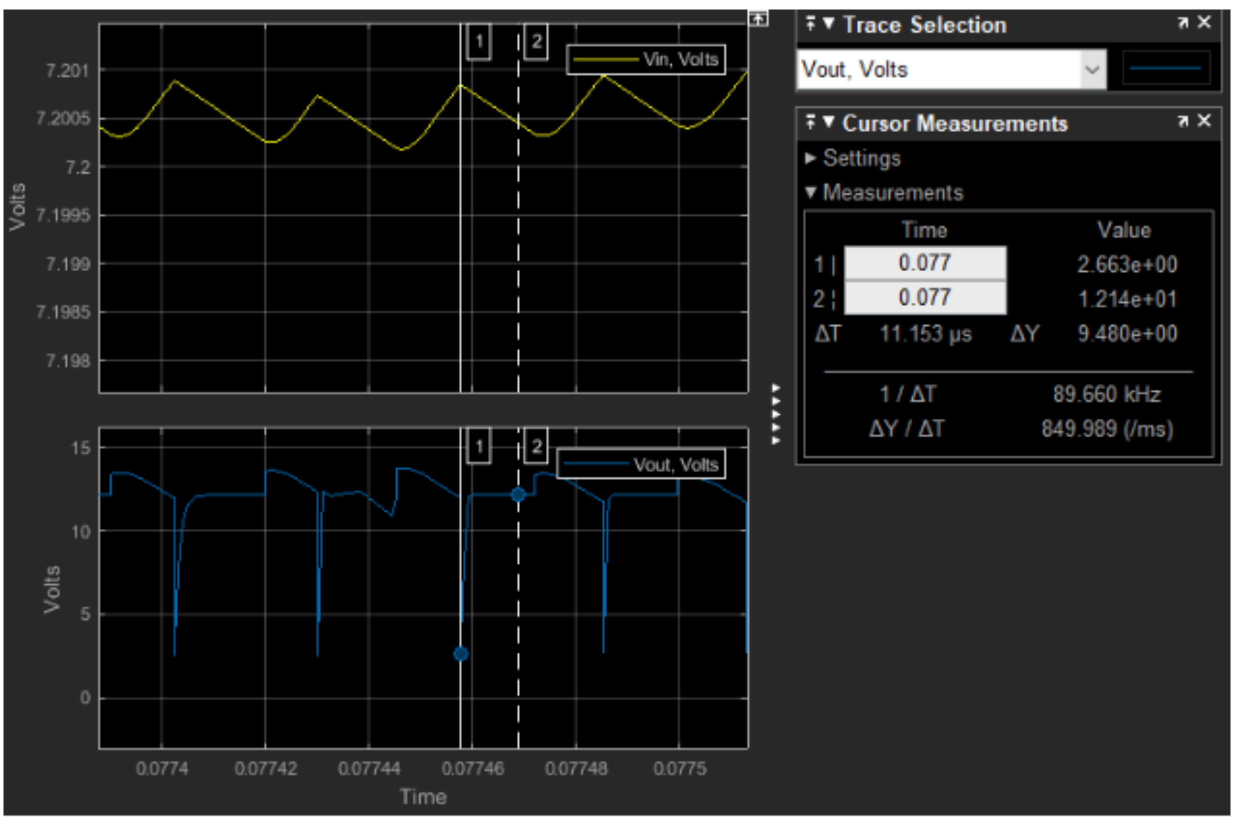

Figure 4.54, SEPIC Simulation, Input and Output Voltage, RPWM, High Vout

SEPIC Simulation, Add RPWM and RPPM for High Vout

SEPIC Simulation, Add RPWM and RPPM for High Vout, PWM Measurement

SEPIC's PWM measurements during the randomization techniques for both the RPWM and RPPM are shown in Figure 4.55. The SEPIC converter experiences both randomization of duty cycle and of the phase position delay. The circuit experienced randomly 52% and 56% duty cycles with phase position delays from 0 to 2 microseconds.

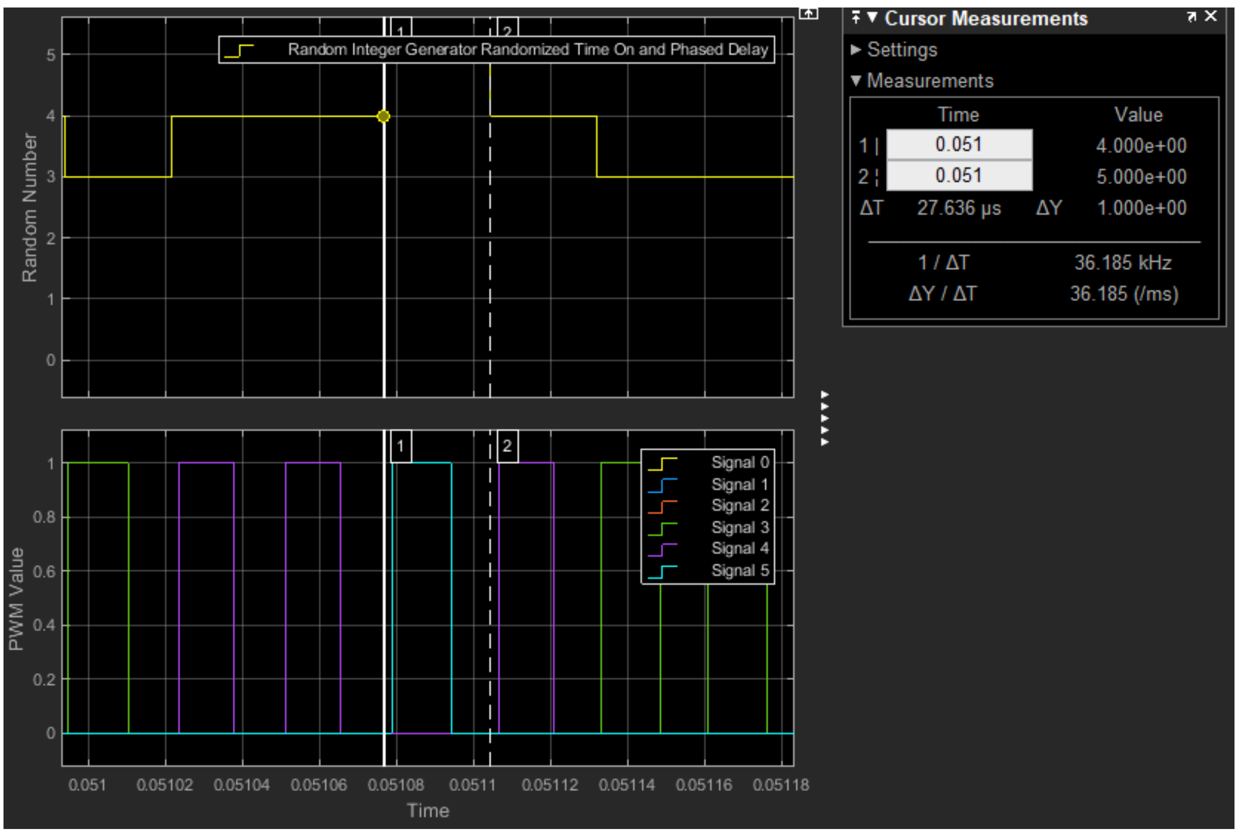

Figure 4.55, SEPIC Simulation, RPWM and RPPM Results, High Vout

SEPIC Simulation, RPWM and RPPM for FFT and Voltage Measurements

The FFT results of the RPWM and RPPM are shown in Figure 4.56. The discrete harmonics appear similar to the no randomization, but the THD is slightly higher when compared to the PWM FFT results found in Figure 4.50.

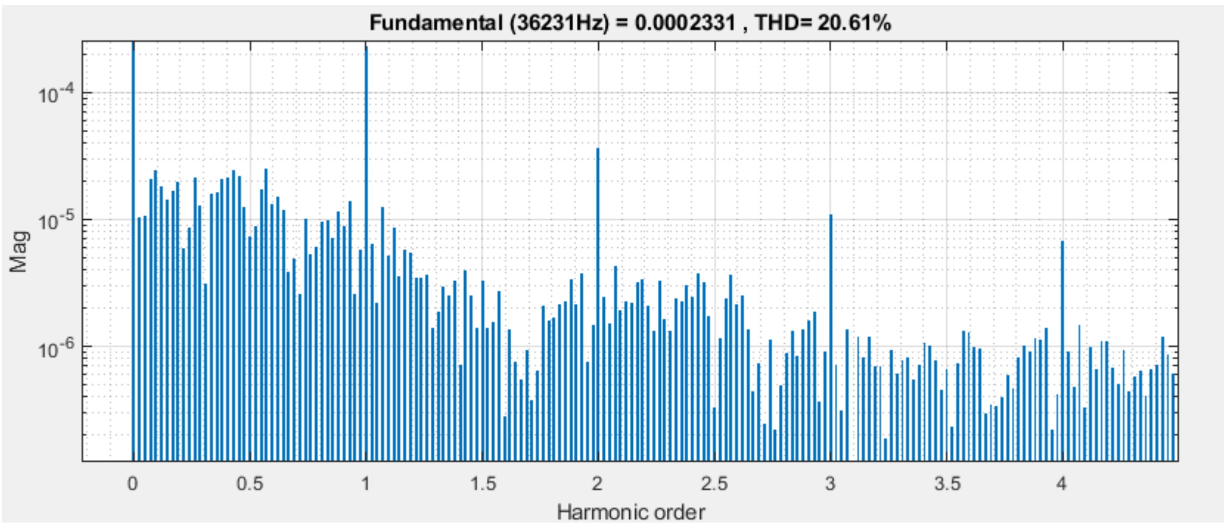

Figure 4.56, SEPIC Simulation, FFT Result of RPWM and RPPM, High Vout

SEPIC's input and output voltage results are shown in Figure 4.57. The input voltage is about 7.20 volts while the output voltage is about 9.77 volts and oscillates down to 1.66 volts.

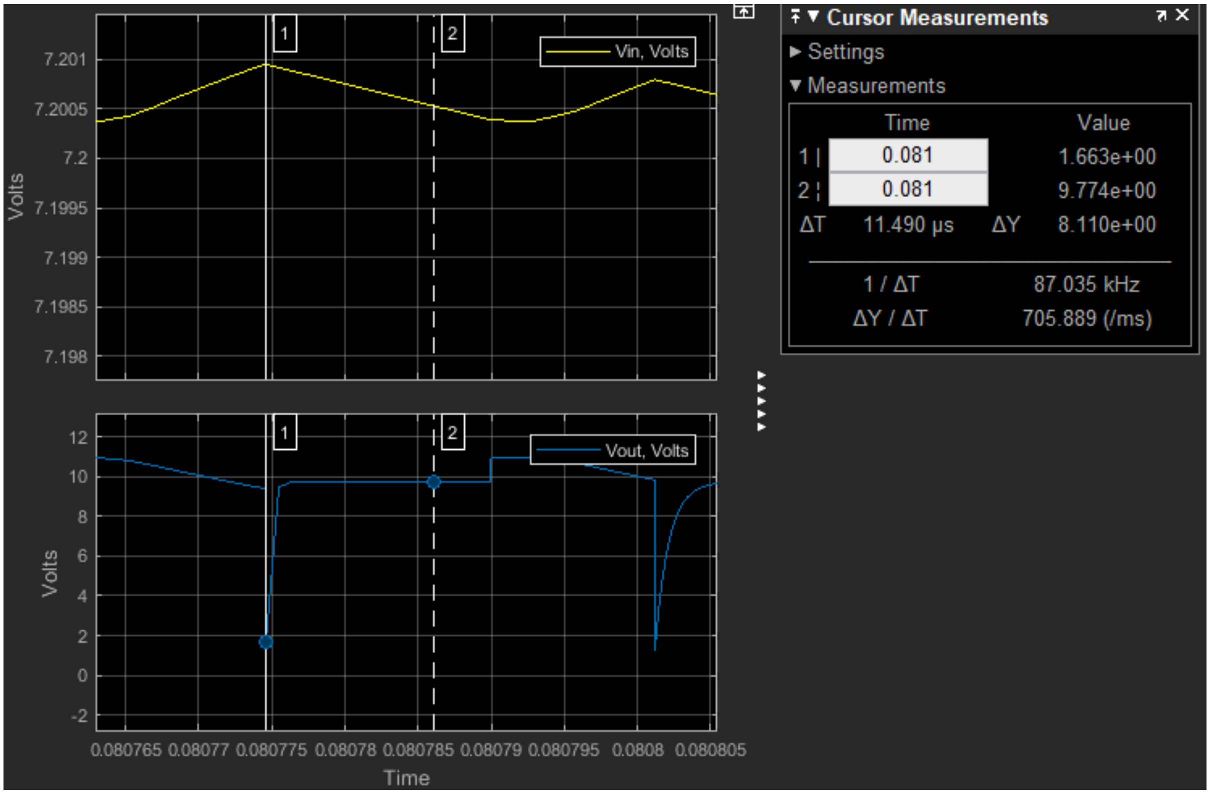

Figure 4.57, SEPIC Simulation Input and Output Voltage Results, RPWM and RPPM, High Vout

SEPIC Simulation, Add RPPM

<u>SEPIC Simulation, RPPM for High Vout, PWM Measurements</u>

SEPIC's PWM measurement during RPPM is shown Figure 4.58. The PWM was able to delay the phase position from 0 to 3 microseconds.

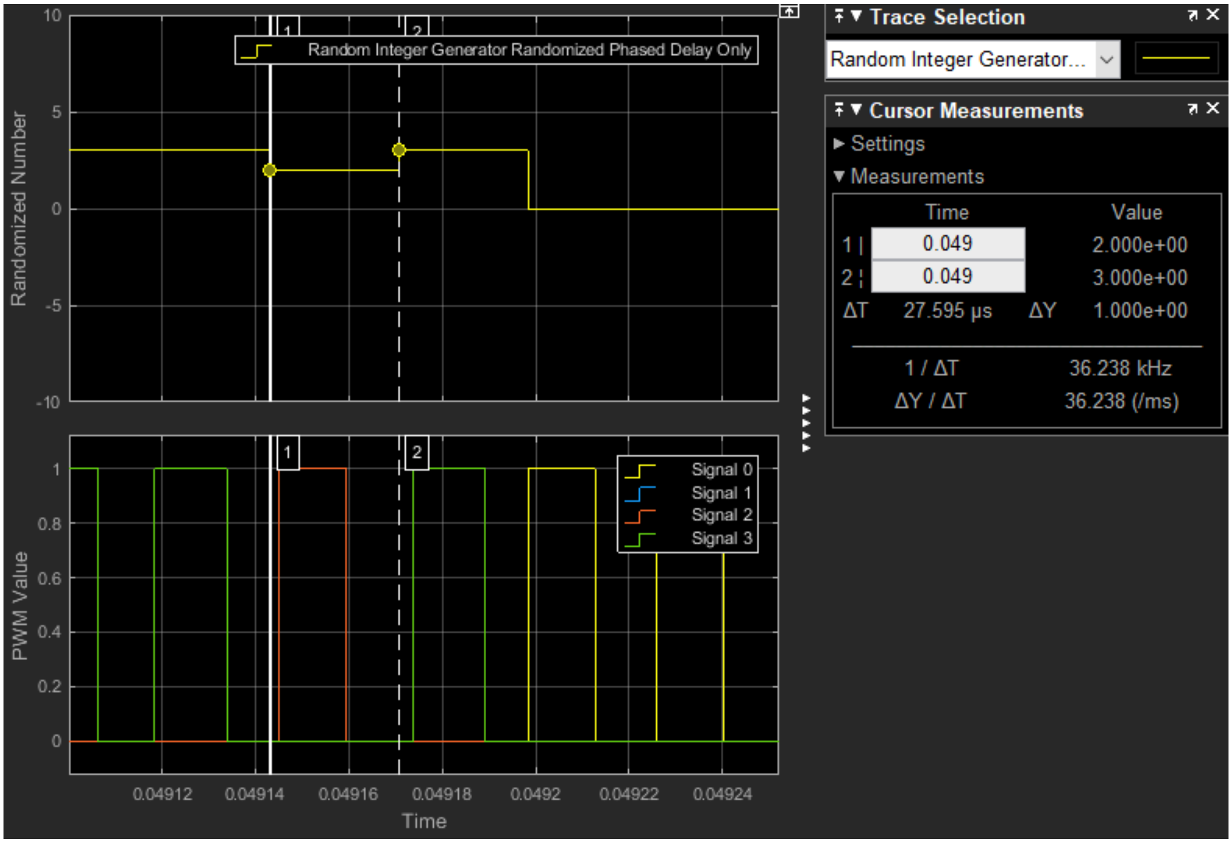

Figure 4.58, SEPIC Simulation, RPPM Result, High Vout

<u>SEPIC Simulation, RPPM and High Vout FFT and Voltage Measurements</u>

SEPIC's FFT results of RPPM is shown in Figure 4.59. FFT results show that the THD have increased slightly than the no randomization PWM FFT result found in Figure 4.50.

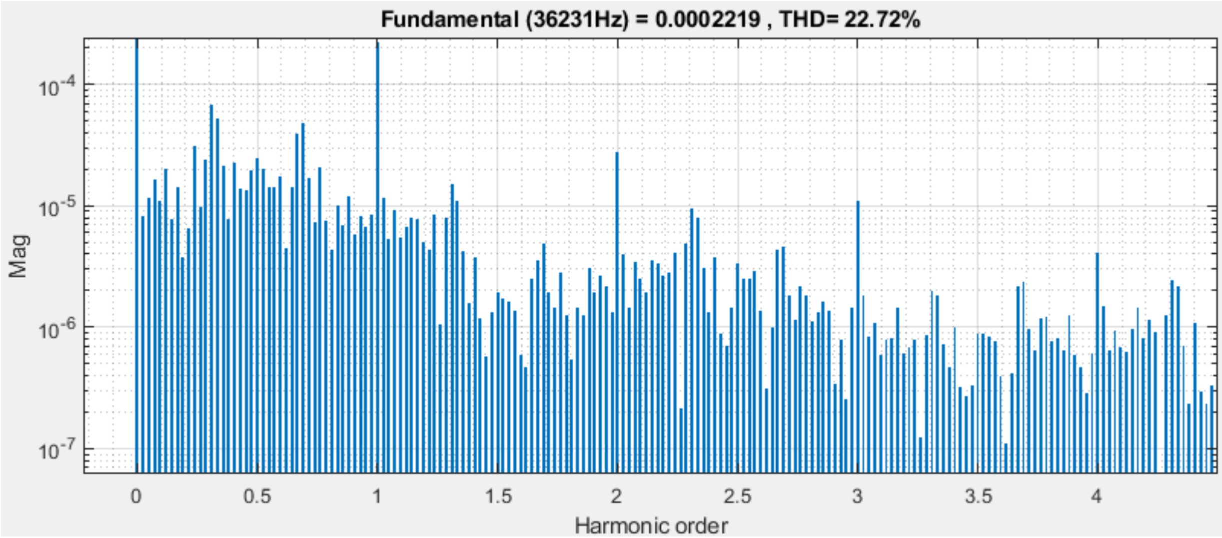

Figure 4.59, SEPIC Simulation, RPPM FFT Results, High Vout

SEPIC's voltage measurement during RPPM is shown Figure 4.60. The input voltage is about 7.2 volts while the output voltage is about 9.37 volts and oscillates down to 1.67 volts. The output voltage can also oscillate as high as 10.76 volts.

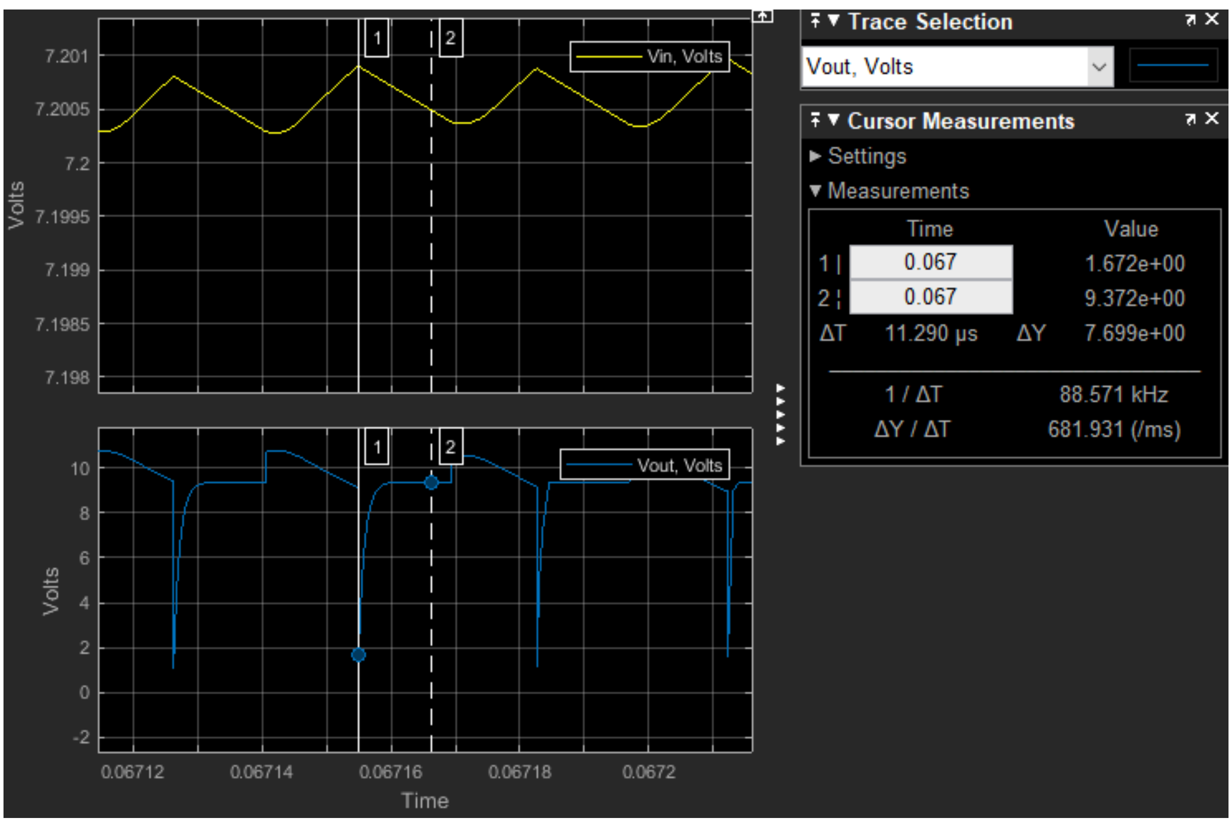

Figure 4.60, SEPIC Simulation, Input and Output Voltage Measurement, RPPM, High Vout

Simulation Summary of Cuk Converter

The Cuk converters accomplished simulations which focused on their input, output voltage during PWM, RPWM, RPPM and both RPWM and RPPM. Additionally, the circuits had two duty cycles of focus where the randomization began at, Low Vout was at 23% duty while High Vout was at 52% duty. Table 4.1 summarizes the results for the Cuk during each duty cycle starting option.

Table 4.1, Cuk Simulation Results during Low and High Vout

Converter Type	Duty Cycle	Phase Delay	PWM Type	Harmonic No.	FFT Value	THD	Vout
Cuk Converter, Low Vout Measurements							
CUK, Low Vout	23%	0 μSec.	PWM	1	2.1mV	16.38%	-6.5 Volts
				2	0.31mV		
				3	0.14mV		
				4	0.067mV		
CUK, Low Vout	23% to 63%	0 μSec.	RPWM	1	2.5mV	26.24%	-9.034 volts
				2	0.33mV		
				3	0.16mV		
				4	0.09mV		
CUK, Low Vout	23% to 45%	0 to 5 μSec.	RPWM and RPPM	1	2.1mV	32.97%	-5.974 volts
				2	0.12mV		
				3	0.055mV		
				4	0.0004mV		
CUK, Low Vout	23%	0 to 11 μSec.	RPPM	1	1.5mV	52.11%	-4.3 volts
				2	0.09mV		
				3	0.003mV		
				4	0.002mV		
Cuk Converter, High Vout Measurements							
CUK, High Vout	52%	0 μSec.	PWM	1	3.0mV	18.75%	-10.0 volts
				2	0.49mV		
				3	0.17mV		
				4	0.09mV		
CUK, High Vout	52% to 63%	0 μSec.	RPWM	1	3.0mV	24.98%	-11.51 volts
				2	0.7mV		
				3	0.14mV		
				4	0.13mV		
CUK, High Vout	52% to 56%	0 to 2 μSec.	RPWM and RPPM	1	3.0 mV	22.40%	-10.48 volts
				2	0.51mV		
				3	0.14mV		
				4	0.09mV		
CUK, High Vout	52%	0 to 3 μSec.	RPPM	1	3.0mV	21.94%	-10.07 volts
				2	0.44mV		
				3	0.15mV		
				4	0.07mV		

As shown from Table 4.1, highest impact to voltage harmonic adjustment was the RPPM technique. But when the duty cycle was higher the margin for randomization decreased and as a result not much impact occurred. The combination of both RPPM and RPWM also reduced the harmonic content but the THD was increased. Output voltage increased the most when duty cycle was randomized.

Simulation Summary of SEPIC

As shown in Table 4.2, the SEPIC went through the same duty cycle parameters of 23% to 52% and the same randomization RPWM, RPPM and both RPWM and RPPM.

Table 4.2, SEPIC Simulation Results during Low and High Vout

Converter Type	Duty Cycle	Phase Delay	PWM Type	Harmonic No.	FFT Value	THD	Vout
SEPIC Converter, Low Vout Measurements							
SEPIC, Low Vout	23%	0 μSec.	PWM	1	140μV	14.87%	8.38 volts
				2	19μV		
				3	8μV		
				4	4μV		
SEPIC, Low Vout	23% to 63%	0 μSec.	RPWM	1	150μV	25.71%	4.15 volts
				2	26μV		
				3	12μV		
				4	7μV		
SEPIC, Low Vout	23% to 45%	0 to 5 μSec.	RPWM and RPPM	1	90μV	28.54%	4.91 volts
				2	10μV		
				3	6μV		
				4	1.8μV		
SEPIC, Low Vout	23%	0 to 11 μSec.	RPPM	1	107μV	57.80%	3.9 volts
				2	4.9μV		
				3	0.7μV		
				4	0.7μV		
SEPIC Converter, High Vout Measurements							
SEPIC, High Vout	52%	0 μSec.	PWM	1	231μV	16.86%	8.9 volts
				2	30μV		
				3	12μV		
				4	7μV		
SEPIC, High Vout	52% to 63%	0 μSec.	RPWM	1	243μV	24.19%	12.1 volts
				2	49μV		
				3	14μV		
				4	9μV		
SEPIC, High Vout	52% to 56%	0 to 2 μSec.	RPWM and RPPM	1	233μV	20.61%	9.77 volts
				2	38μV		
				3	11μV		
				4	6.8μV		
SEPIC, High Vout	52%	0 to 3 μSec.	RPPM	1	222μV	22.72%	9.37 volts
				2	28μV		
				3	11μV		
				4	4μV		

As shown from the table randomization technique RPPM had the biggest impact to voltage adjustment but increased the THD. The combination of RPPM and RPWM utilized an adjustment to the voltage harmonic and a slight increase in the THD.

Chapter 5

EXPERIMENTATION RESULTS OF CUK AND SEPIC RPWM

CUK Experimentation Lower Vout than Vin

Cuk Experimentation, No Randomization, Low Vout, PWM Measurement

During the experimentation, the same approaches were taken with the simulation as different sections, Cuk and SEPIC, randomization techniques and Low and High Vout. The Cuk converter operated in DCM mode, except at high Vout, the Cuk operated in DCM and occasionally CCM as shown by Figure 3.15 and Figure 3.16 when the circuit's duty cycle reached 63%. When the circuit was operating in CCM the Arduino Due didn't have enough time remaining per cycle to perform the randomization. Randomization techniques for Cuk are RPWM, RPPM and a combination of both. Random frequency switching was a technique not utilized into this experiment due to the switching frequency already occurred at about 36 kHz and lower frequencies would require higher inductors to accommodate the lower frequencies. During this configuration operating duty cycle of the switch is shown below and this operation is maintain constantly since there was no randomization from the Arduino Due. The Arduino Due was set to duty cycle of 23%. Figure 5.1 shows the time ON duration of 6.4 microseconds.

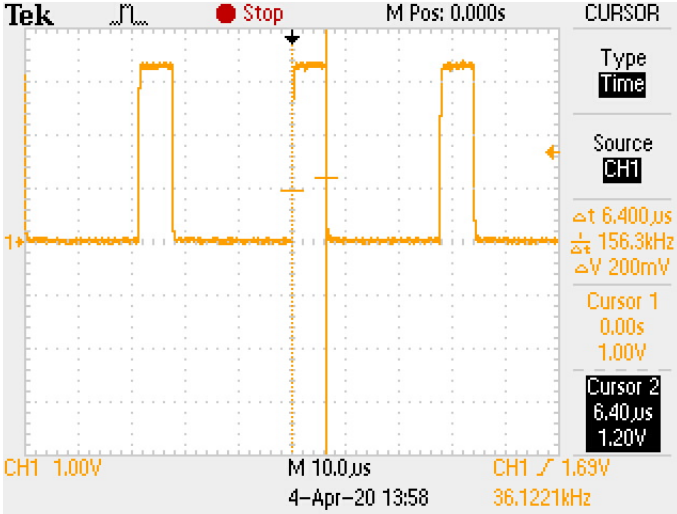

Figure 5.1, Cuk Experimentation, PWM Result 23% Duty Cycle, Low Vout

The constant switching time of 27.6 microseconds is measured between the pulses as shown in Figure 5.2 below:

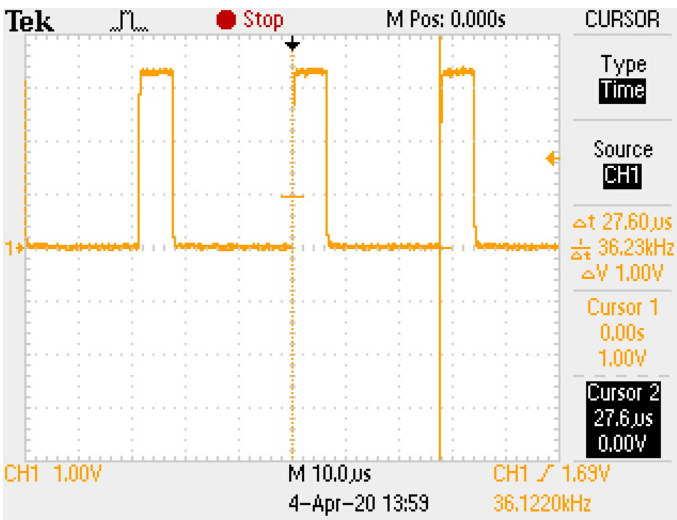

Figure 5.2 Cuk Experimentation, PWM Switching Measurement, Low Vout

Cuk Experimentation, Low Vout, PWM FFT and Voltage Measurements

With a switching time of 27.6 microseconds and time ON of 6.4 microseconds the duty cycle is 23% duty. Measuring the input power's and enabling the FFT function on the Tektronix 2014B Oscilloscope shows Figure 5.3 where the distinct harmonic levels are displayed. These distinct harmonic levels are easily shown of the 1st through the 6th Harmonic Order with a fundamental frequency of 36 kHz. THD measurements are computed in Table 5.1 from the experimentation results. Results are provided in dB which are calculated in mV prior to Table 5.1.

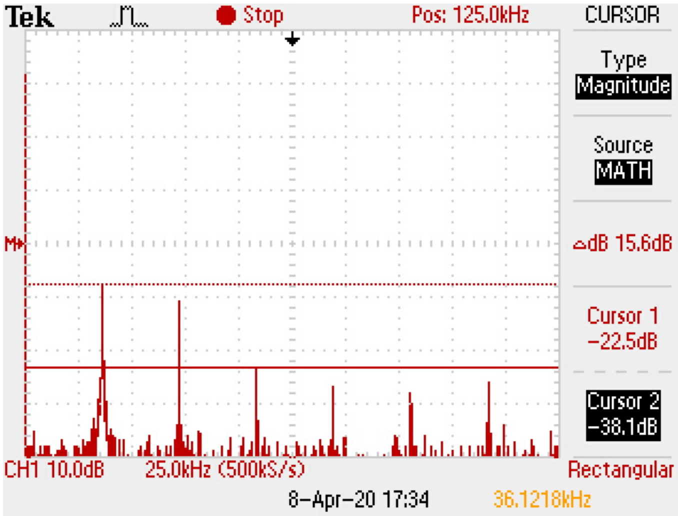

Figure 5.3, Cuk Experimentation, Low Vout, PWM FFT Result

The output voltage of the CUK circuit is -4.8 Volts is shown by Figure 5.4.

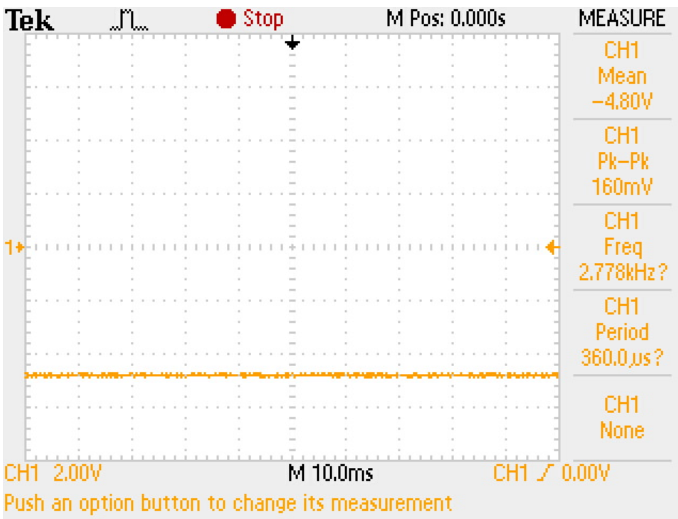

Figure 5.4, Cuk Experimentation, Low Vout, PWM Output Voltage Measurement

Cuk Experimentation, Add RPWM, Low Vout

Cuk Experimentation, Add RPWM, Low Vout, RPWM Measurements

PWM measurements were accomplished with only the time ON duration being randomized. The phase position delay time duration was zero and not randomized. The time ON was measured at three iterations. The first iteration was measured at 6.4 microseconds as shown in Figure 5.5.

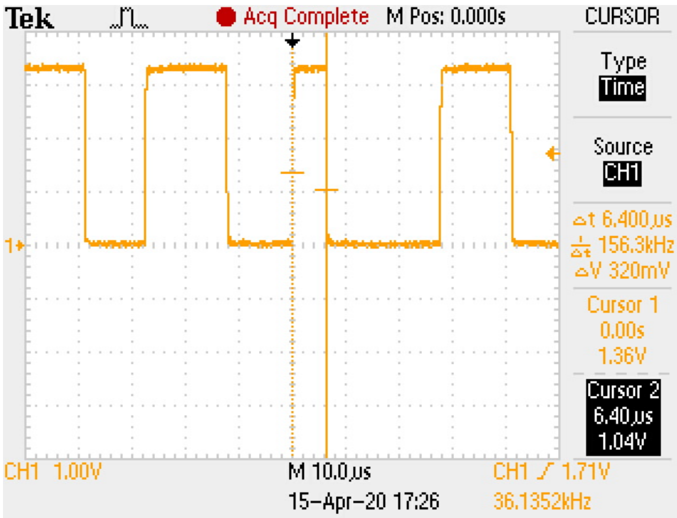

Figure 5.5, Cuk Experimentation, RPWM Result, Low Vout, Measurement 1 of 3

The second iteration was measured at 7.6 microseconds as shown in Figure 5.6.

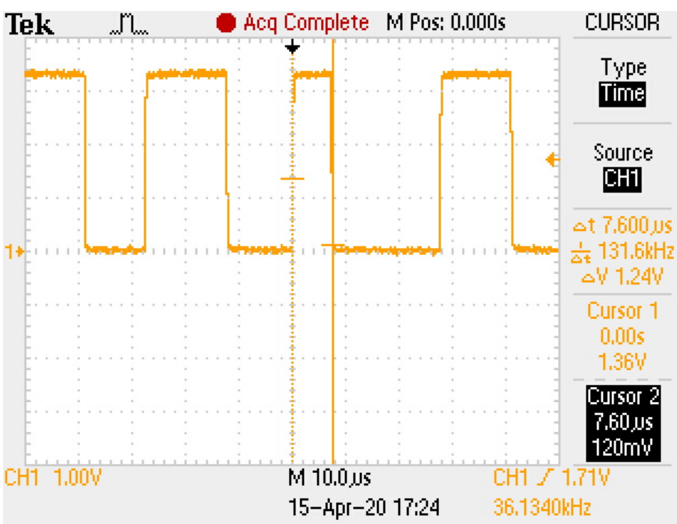

Figure 5.6, Cuk Experimentation, RPWM Result, Low Vout, Measurement 2 of 3

The third iteration was measured at 15.6 microseconds as shown in Figure 5.7.

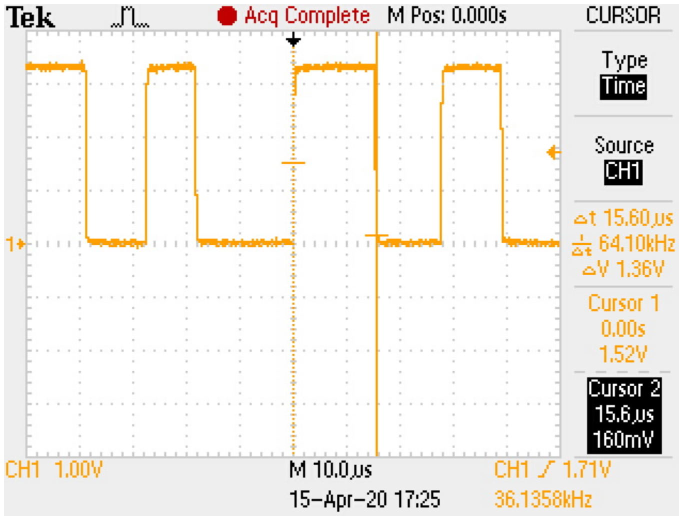

Figure 5.7, Cuk Experimentation, RPWM Result, Low Vout, Measurement 3 of 3

All three iterations resulted in the same switching time since the delay phase position was set to zero. The switching time was 27.6 microseconds as shown in Figure 5.8.

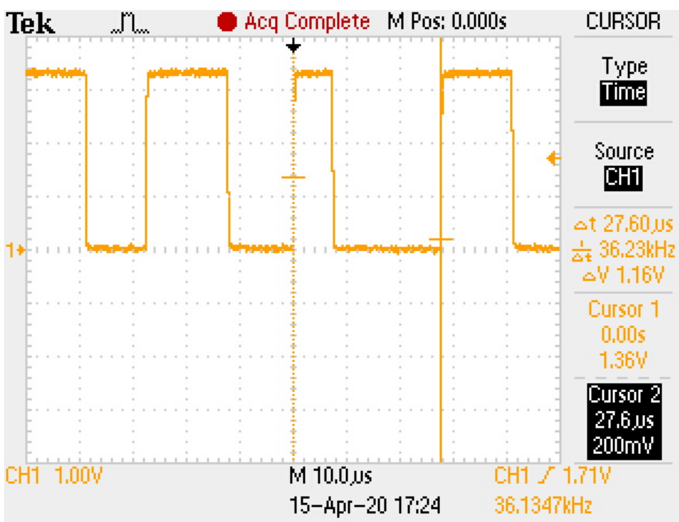

Figure 5.8, Cuk Experimentation, RPWM, Low Vout, PWM Switching time

<u>Cuk Experimenation, RPWM, Low Vout, FFT and Voltage Measurements</u>

The RPWM FFT measurements are shown in Figure 5.9. when compared to PWM FFT results in Figure 5.3, the higher order harmonics are reduced and the lower frequencies increase in magnitude.

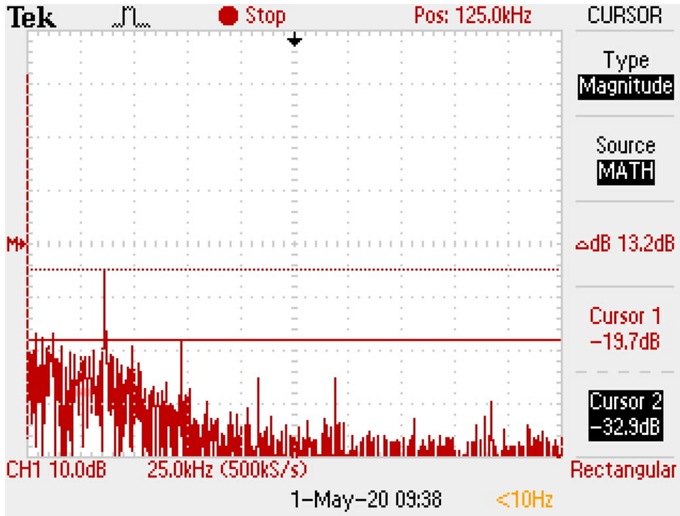

Figure 5.9, Cuk Experimentation, FFT Results, RPWM, Low Vout

The Output voltage measured with the time On randomization was -8.29 Volts as shown in Figure 5.10.

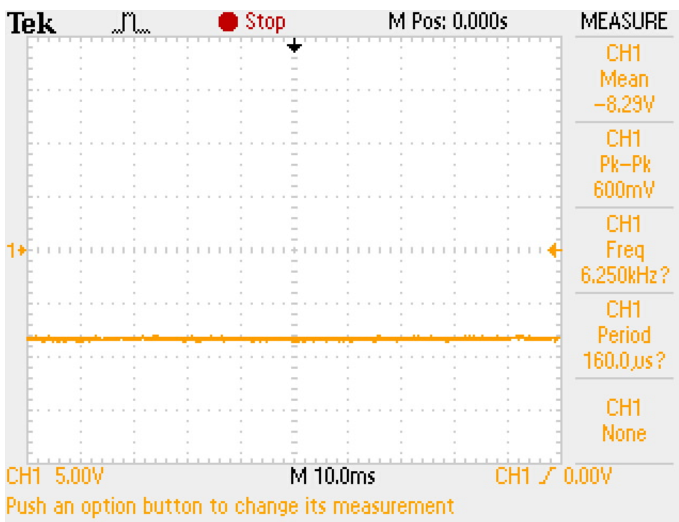

Figure 5.10, Cuk Experimentation, RPWM, Output Voltage Measurement, Low Vout

Cuk Experimentation, Add RPWM and RPPM, Low Vout

Cuk Experimentation, RPWM and RPPM, Low Vout, PWM Measurements

The PWM measurements for this scenario utilized randomized switching which occurred on both time ON and phase position delay. The Arduino Due duty cycle during this mode was 23% to 41%. While the phase position delay received a randomized time delay of 0 to 5 microseconds.

Three iterations were measured of the RPWM and RPPM during the randomization of both scenarios. The first iteration resulted in time on 9.6 microseconds and the switching time resulted in 24.8 microseconds as shown in Figure 5.11 and Figure 5.12, respectively.

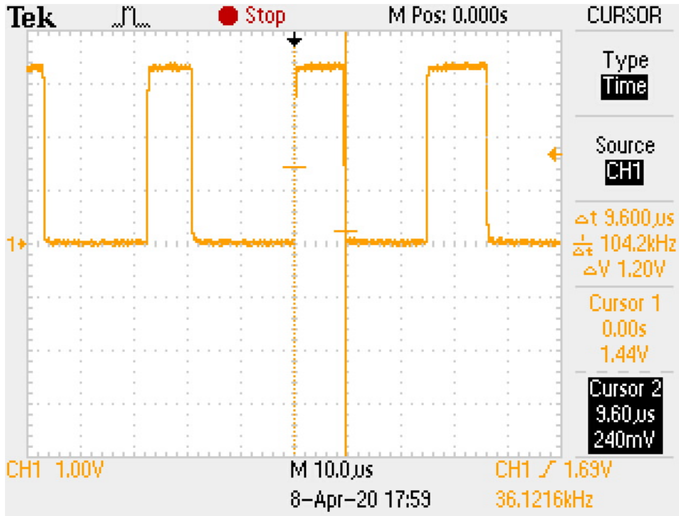

Figure 5.11, Cuk Experimentation, RPWM and RPPM Result, Low Vout, Iteration 1 of 3

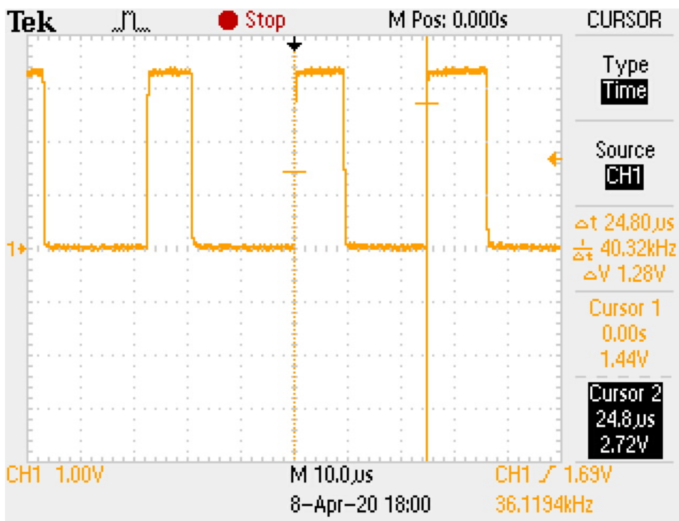

Figure 5.12, Cuk Experimentation, RPWM and RPPM Result, Low Vout, Switching Time Iteration 1 of 3

The second iteration of the time ON and phase position delay resulted in 11.6 microseconds for time on and 27.6 microseconds as shown in Figure 5.13 and Figure 5.14, respectively.

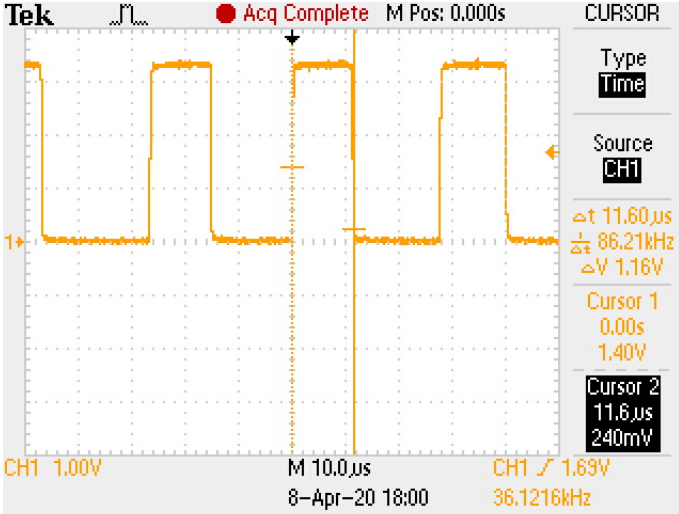

Figure 5.13, Cuk Experimentation, RPWM and RPPM Result, Low Vout, Iteration 2 of 3

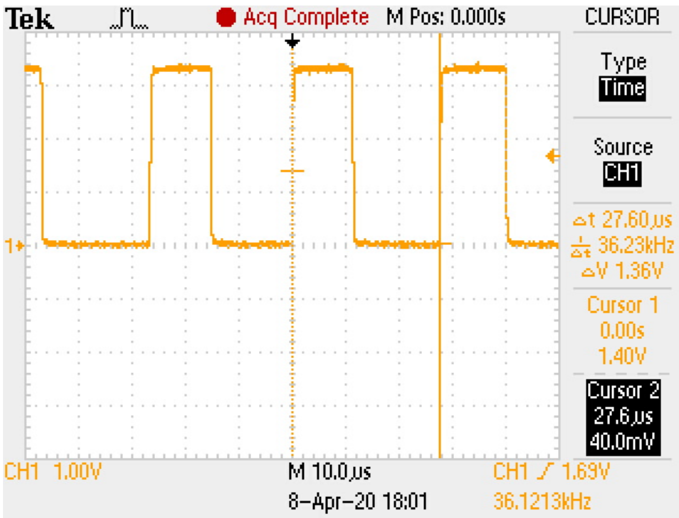

Figure 5.14, Cuk Experimentation, RPWM and RPPM, Low Vout, Switching Time Iteration 2 of 3

For the third iteration, the time ON and phase position delay resulted in 8.4 microseconds while the switching time was 28.8 microseconds as shown by Figure 5.15 and Figure 5.16, respectively.

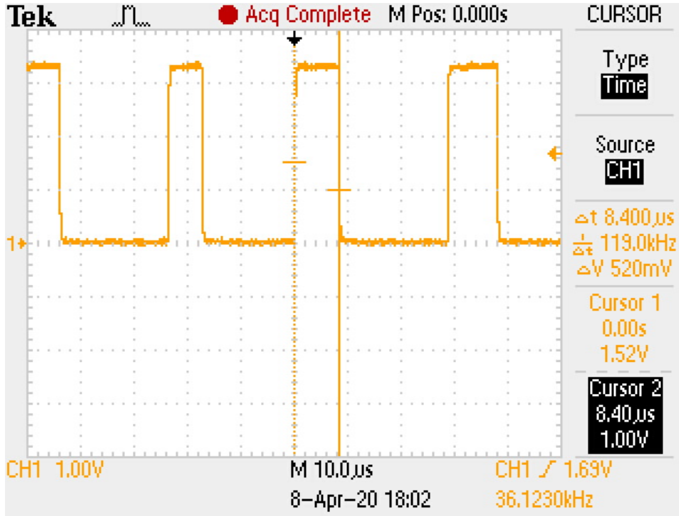

Figure 5.15, Cuk Experimentation, RPWM and RPPM Result, Low Vout, Iteration 3 of 3

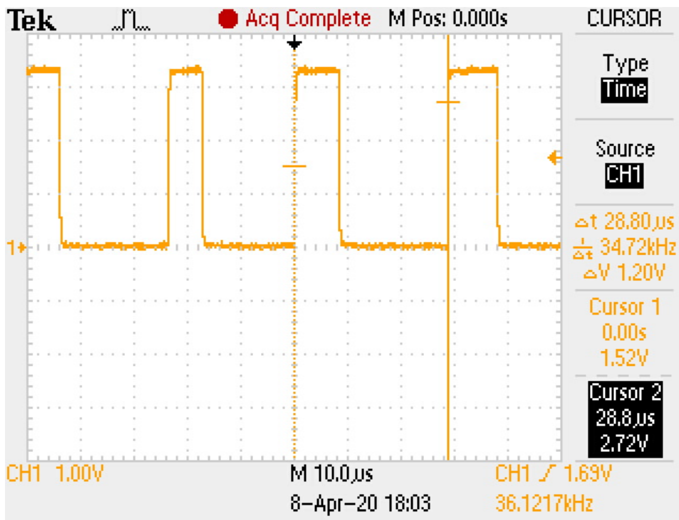

Figure 5.16, Cuk Experimentation, RPWM and RPPM, Low Vout, Switching Time Iteration 3 of 3

This results on randomizing the switching time. As a result, the duty cycle for which the circuit experiences would be varied.

<u>Cuk Experimentation, Low Vout, RPWM and RPPM, FFT and Voltage Measurements</u>

The measurements of the RPWM and RPPM FFT function are shown in Figure 5.17. when compared to Figure 5.3, the discrete harmonics starting at the 2nd harmonic and higher are decreased in magnitude. The lower frequencies have increased in magnitude.

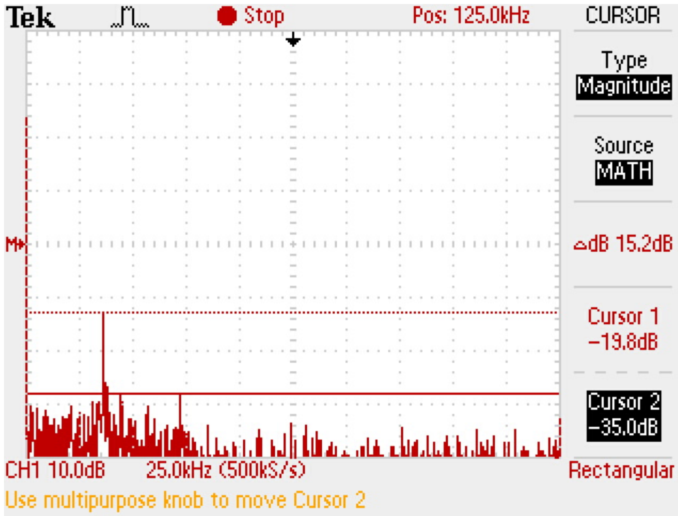

Figure 5.17, Cuk Experimentation, Low Vout, RPWM and RPPM, FFT Result

The output voltage from the circuit is -6.77 volts with the inclusion of the RPWM and RPPM are included Figure 5.18.

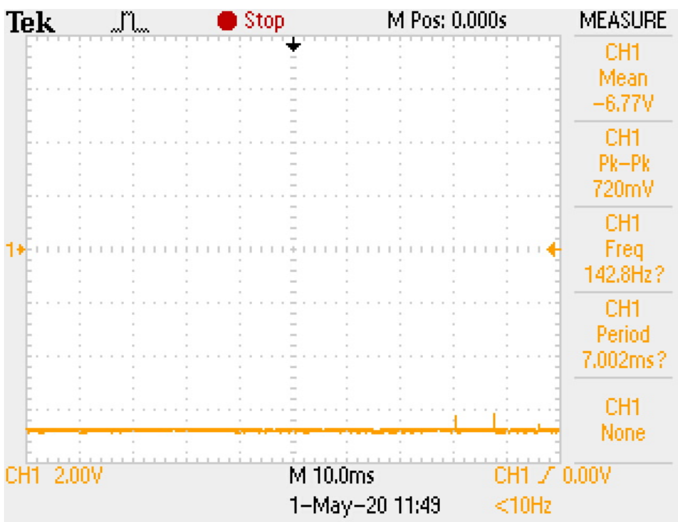

Figure 5.18, Cuk Experimentation, Low Vout, RPWM and RPPM, Output Voltage Measurement

Cuk Experimentation, Low Vout, Added RPPM

<u>Cuk Experimentation, Low Vout, RPPM, PWM Measurements</u>

With the same time ON duration of 6.4 microseconds but the phase position delay can change randomly between 0 microseconds to 11 microseconds, this results in the converter experiencing a different duty cycle. This occurs since the converter would experience a different switching time. Figure 5.19, Figure 5.20, Figure 5.21 and Figure 5.22 show the same time ON of 6.4 microseconds. So the parameter that is changing is the time between pulses due to the randomized phase position. Figure 5.19 shows the time ON being 6.4 microseconds.

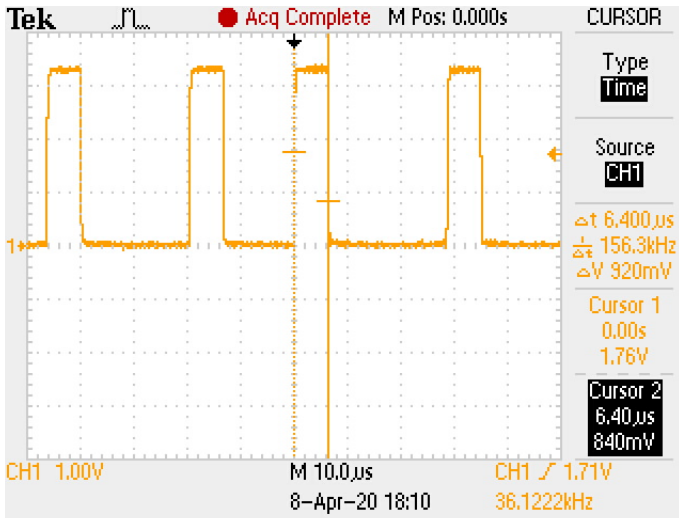

Figure 5.19, Cuk Experimentation, Low Vout, RPPM Result

Figure 5.20 shows the switching time, T_S, of being 28.8 microseconds which is one of three switching times measured for this scenario. The duty cycle which the circuit experiences during this iteration is 22%.

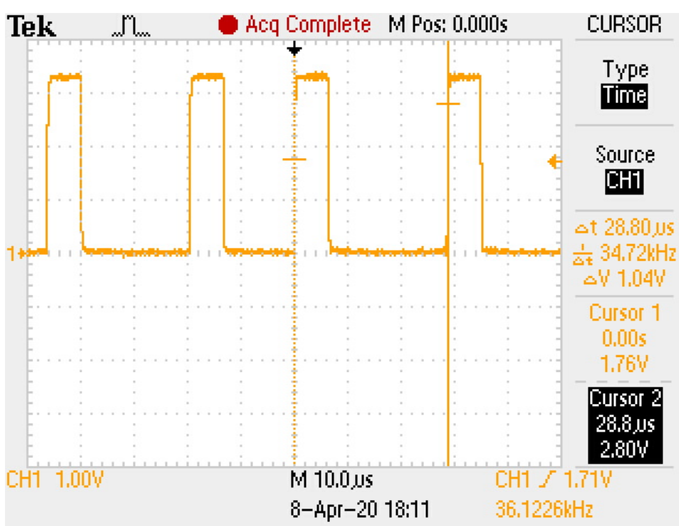

Figure 5.20, Cuk Experimentation, Low Vout, RPPM, Switching Time Result 1 of 3 Iterations

The next iteration shows the switching time is 22.8 microseconds as shown in Figure 5.21. With a constant time ON and T_S is now 22.8 microseconds the duty cycle which the Cuk circuit experiences is 28%.

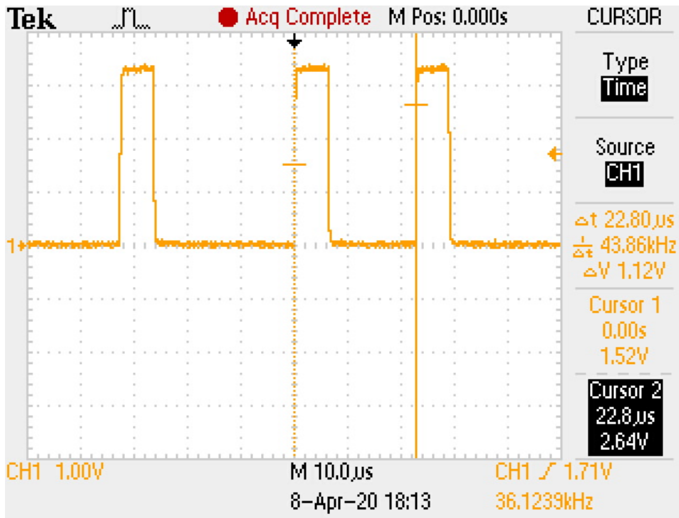

Figure 5.21, Cuk Experimentation, Low Vout, RPPM, Switching Time Result 2 of 3

The next iteration shows the switching time is 30.8 microseconds as shown in Figure 5.22. With T_S now being 30.8 microseconds the duty cycle which the Cuk circuit experiences in this iteration is about 21%.

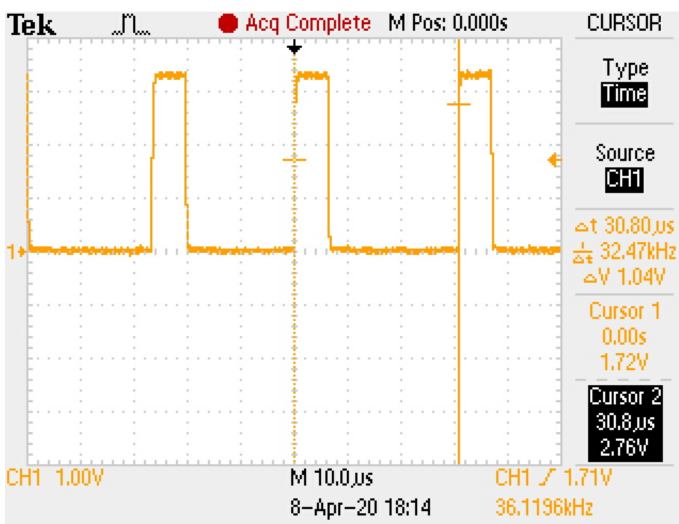

Figure 5.22, Cuk Experimentation, Low Vout, RPPM, Switching Time Result 3 of 3

Cuk Experimentation, Low Vout, RPPM FFT and Voltage Measurements

When RPPM is applied to the circuit the following FFT shows that the discrete voltage harmonics have moved to lower frequencies. The result of RPPM is shown in Figure 5.23 this is the result of the Cuk circuit experiencing delayed duty cycles which range from 21% to 28% as shown previously above. When compared to the PWM FFT result found in Figure 5.3 the discrete harmonics have adjusted in magnitude.

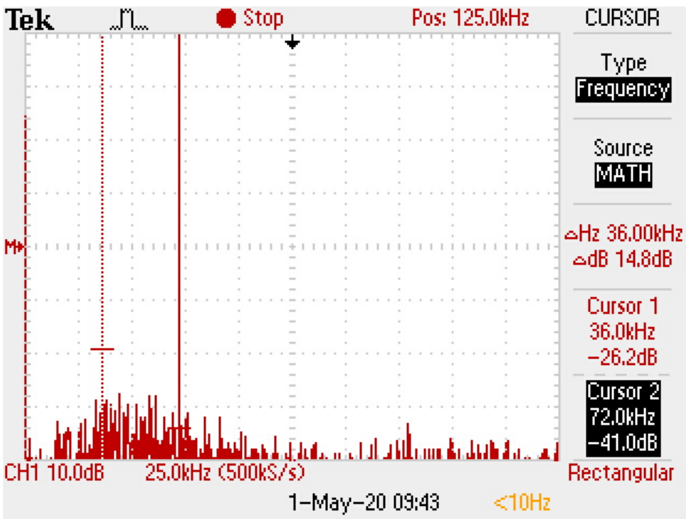

Figure 5.23, Cuk Experimentation, FFT Result, RPPM, Low Vout

This shows that when RPPM is incorporated into a circuit the results show a decrease in harmonic order magnitude but an increase towards the smaller frequencies.

The voltage measurement output is about -4.64 volts as shown by Figure 5.24. The peak to peak is about 160 mV.

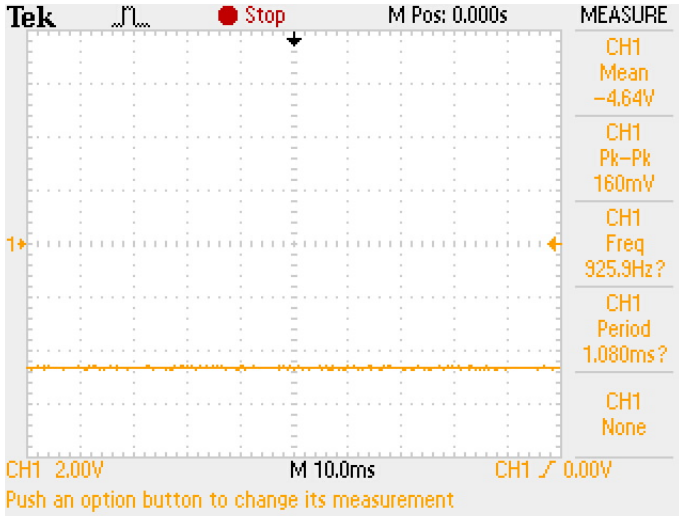

Figure 5.24, Cuk Experimentation, Low Vout, RPPM, Output Voltage Measurement

CUK Experimentation, Higher Vout than Vin

Cuk Experimentation, High Vout, No Randomization of PWM

Cuk Experimentation, High Vout, No Randomization of PWM, PWM Measurement

At higher duty cycles the circuit starts to operate into its boost configuration. The PWM measurements are constant in this section to provide a baseline measurement. Figure 5.25 shows the time on duration of 14.4 microseconds as shown below.

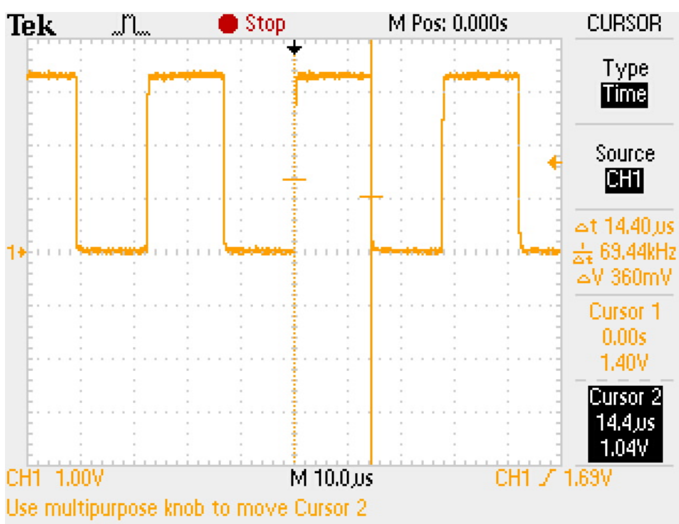

Figure 5.25, Cuk Experimentation, PWM Result, High Vout

The switching time measured with no randomization applied is 27.6 microseconds are shown in Figure 5.26 below. This results in the circuit experience 52.1% duty cycle.

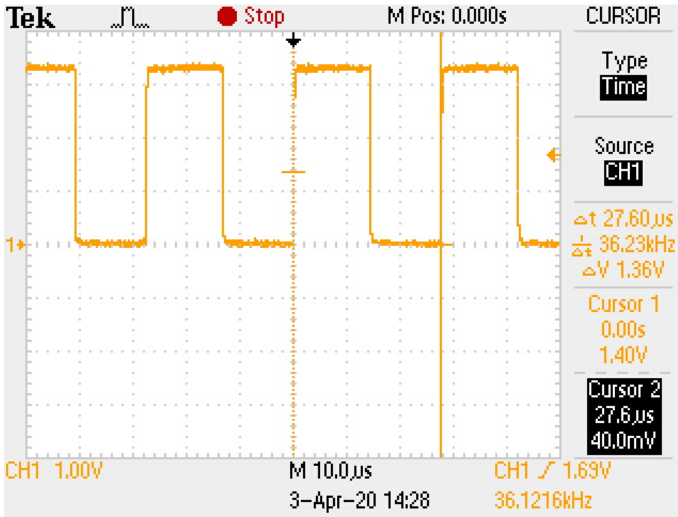

Figure 5.26, Cuk Experimentation, PWM, Switching Time Result, High Vout

<u>Cuk Experimentation, High Vout, PWM, FFT and Voltage Measurement</u>

The resulting PWM FFT measurement with no randomization is shown by Figure 5.27 as shown below.

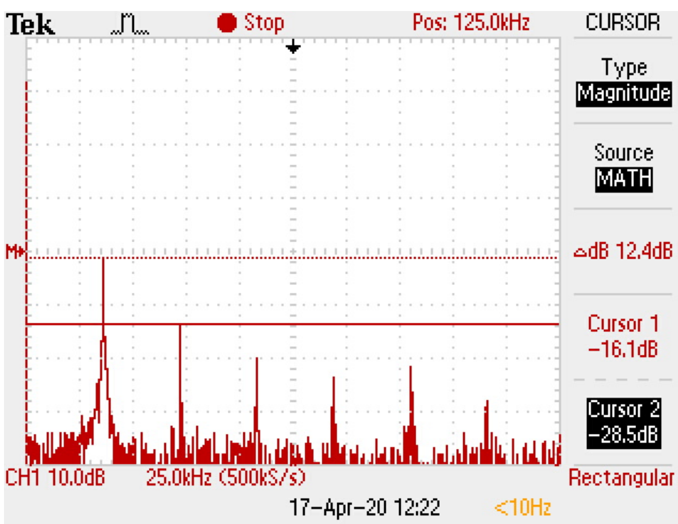

Figure 5.27, Cuk Experimentation, FFT Result, PWM, High Vout

The resulting output voltage is -9.87 volts as shown by Figure 5.28.

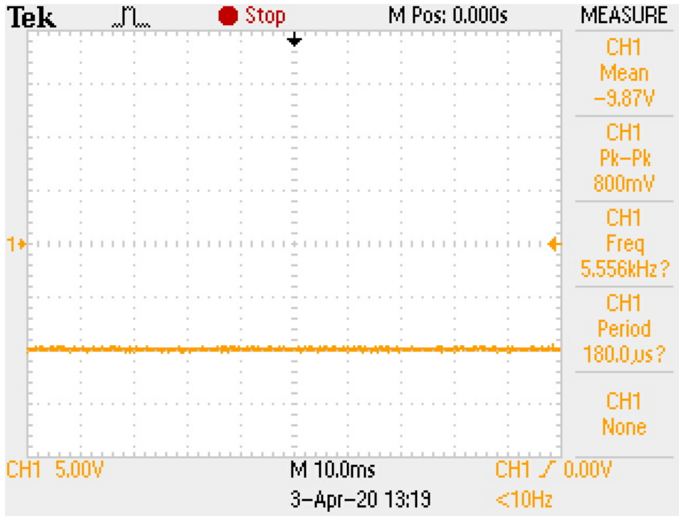

Figure 5.28, Cuk Experimentation, PWM Output Voltage Result, High Vout

Cuk Experimentation, High Vout, Add RPWM

<u>Cuk Experimentation, High Vout, RPWM, RPWM Measurements</u>

PWM measurements during RPWM randomization occurred at 14.4 microseconds for time ON as shown by Figure 5.29 below:

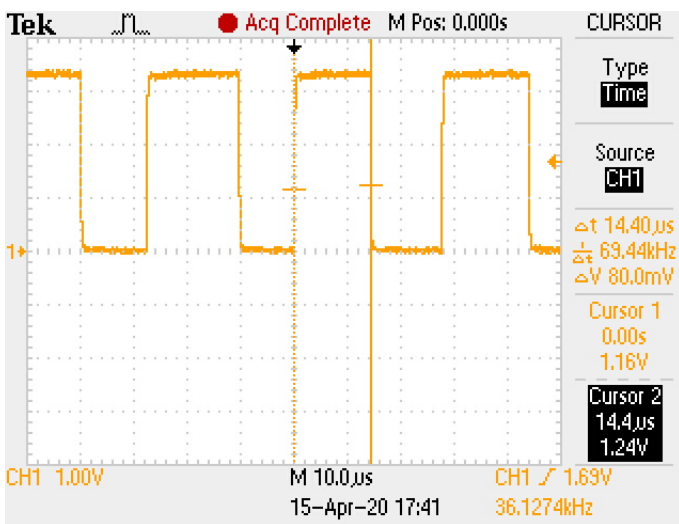

Figure 5.29, Cuk Experimentation, RPWM Result, Iteration 1 of 2, High Vout

The second iteration of time ON occurred at 17.6 microseconds as shown by Figure 5.30.

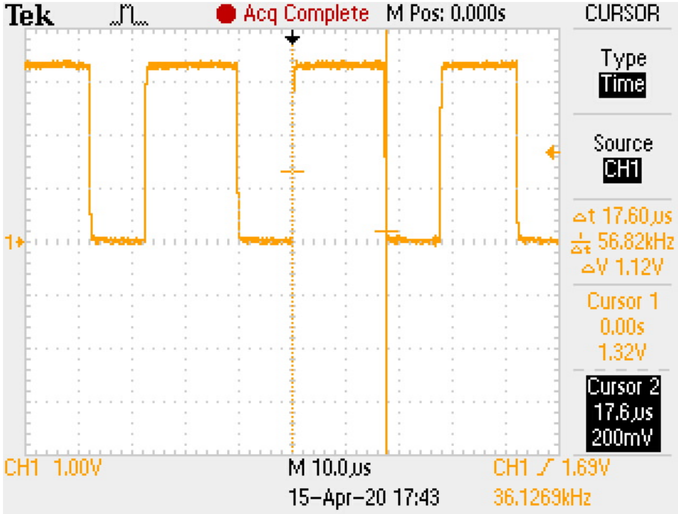

Figure 5.30, Cuk Experimentation, RPWM Result, Iteration 2 of 2, High Vout

Both durations have a constant switching frequency of 27.6 microseconds since the phase position delay is constant as shown by Figure 5.31.

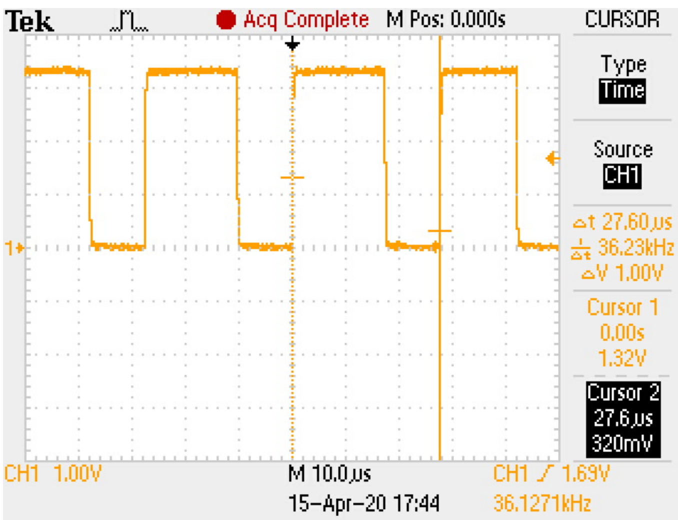

Figure 5.31, Cuk Experimentation, RPWM, Switching Time Result, High Vout

<u>Cuk Experimentation, High Vout, RPWM, FFT and Voltage Measurement</u>

The FFT measurements of RPWM is shown in Figure 5.32. When compared to PWM FFT found in Figure 5.27, the RPWM discrete harmonics appear the same except for harmonic 5 and 6. Those harmonics are adjust and do not have high magnitudes on the RPWM FFT results. The smaller frequencies have also increased in magnitude of the RPWM FFT result.

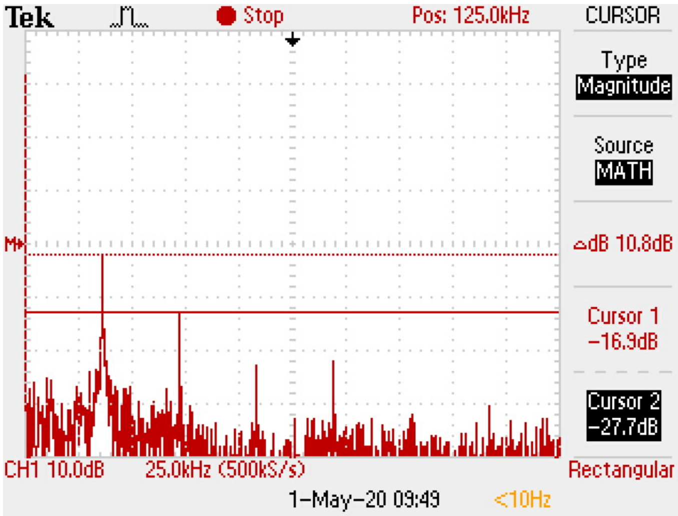

Figure 5.32, Cuk Experimentation, FFT Result, RPWM, High Vout

The output voltage of the Cuk converter is -10.1 Volts as shown by Figure 5.33 below:

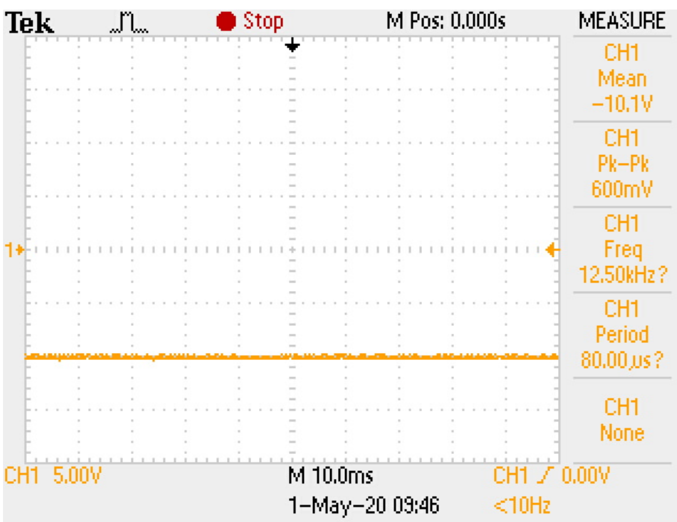

Figure 5.33, Cuk Experimentation, Output Voltage Measurement, RPWM, High Vout

Cuk Experimentation, High Vout, Add RPWM and RPPM

<u>Cuk Experimentation, High Vout, RPWM and RPPM, PWM Measurements</u>

The PWM measured for the RPWM and RPPM randomization shows time ON and switching frequencies seen by the circuit as a result of RPWM and RPPM. Time ON for the first of two iterations is shown by Figure 5.34 and Figure 5.35.

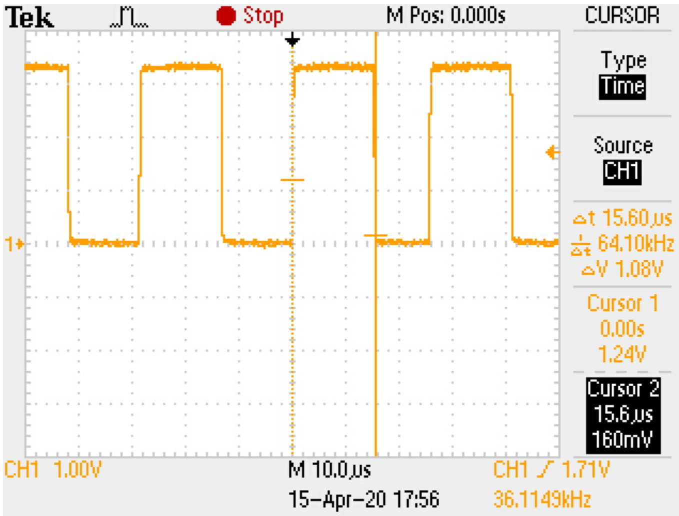

Figure 5.34, Cuk Experimentation, RPWM and RPPM Result, Iteration 1 of 2, High Vout

The second iteration of time On is shown by Figure 5.35 below.

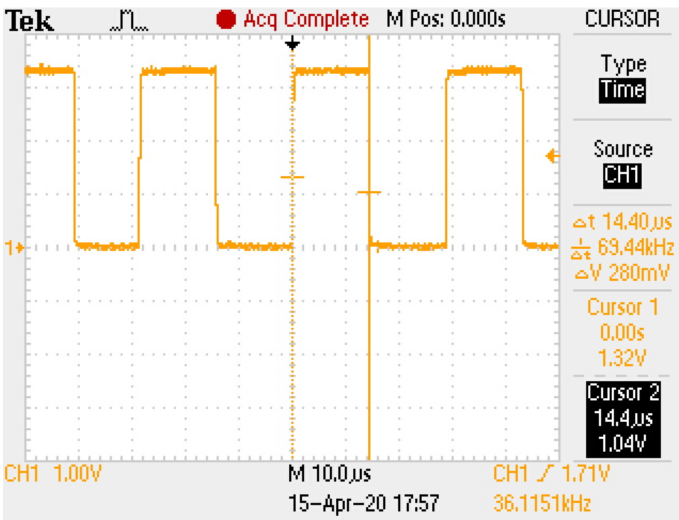

Figure 5.35, Cuk, Experimentation, RPWM and RPPM Result, Iteration 2 of 2, High Vout,

The switching time as a result of the phase position delay occurs at 25.6 microseconds as shown by Figure 5.36.

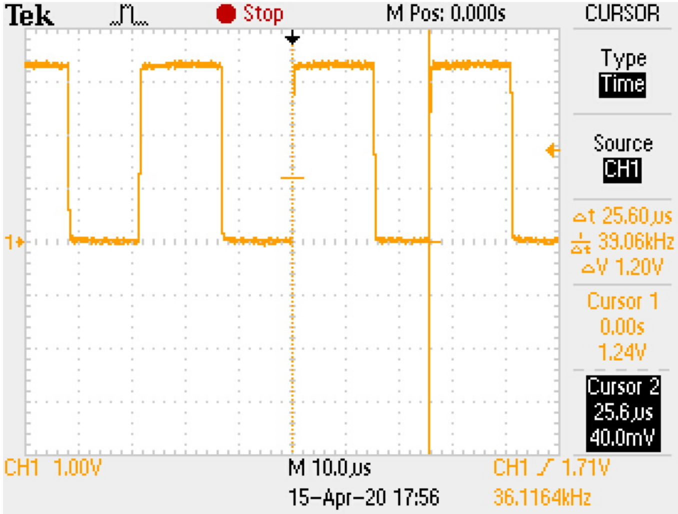

Figure 5.36, Cuk Experimentation, RPWM and RPPM Switching Time Result, Iteration 1 of 2, High Vout

The switching time as a result of the phase position delay occurs at 28.8 microseconds as shown by Figure 5.37 below.

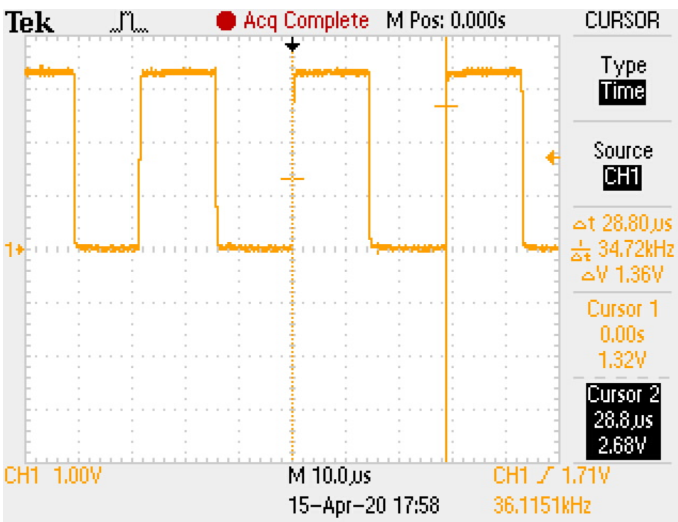

Figure 5.37, Cuk Experimentation, RPWM and RPPM Switching Time for Iteration 2, High Vout,

<u>Cuk Experimentation, High Vout, RPWM and RPPM, FFT and Voltage Measurements</u>

The RPWM and RPPM FFT measurements for this configuration is shown by Figure 5.38. When compared to the PWM FFT result found in Figure 5.27, the higher harmonics at 4 and above are reduced in magnitude. Additionally the small frequencies have increased in magnitude.

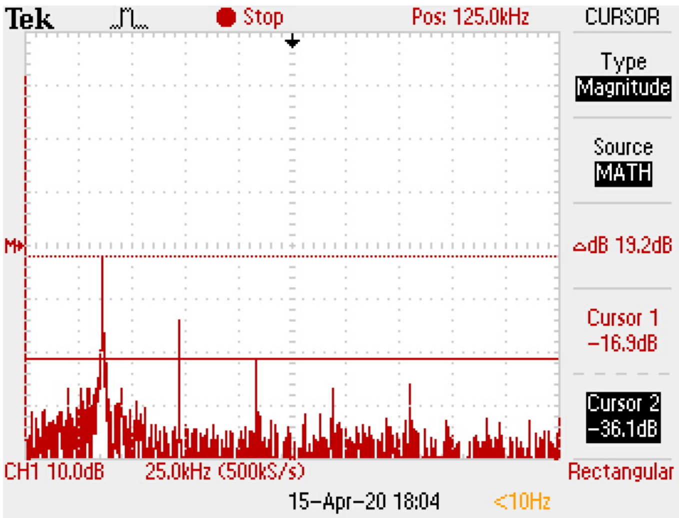

Figure 5.38, Cuk Experimentation, FFT Results, RPWM and RPPM, High Vout

The output voltage measurements were -10.2 Volts as shown by Figure 5.39.

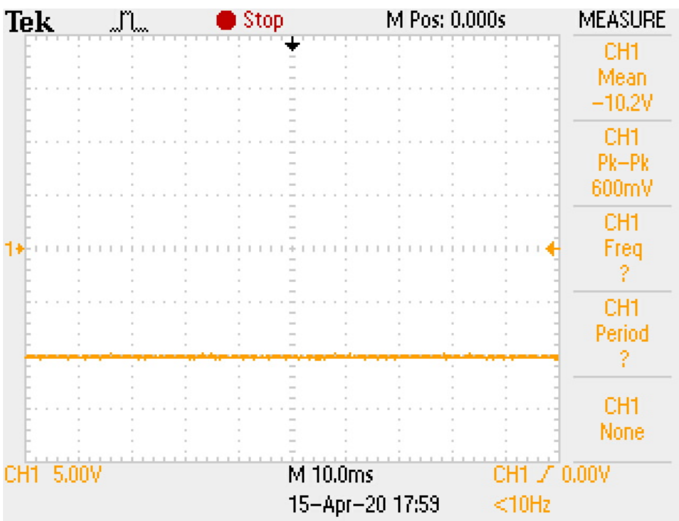

Figure 5.39, Cuk Experimentation, Output Voltage, RPWM and RPPM, High Vout

Cuk Experimentation, High Vout, Added RPPM

Cuk Experimentation, High Vout, RPPM, PWM Measurements

The time ON measurements will be constant during the RPPM randomization. The time On measurement was 14.4 microseconds as shown by Figure 5.40 below.

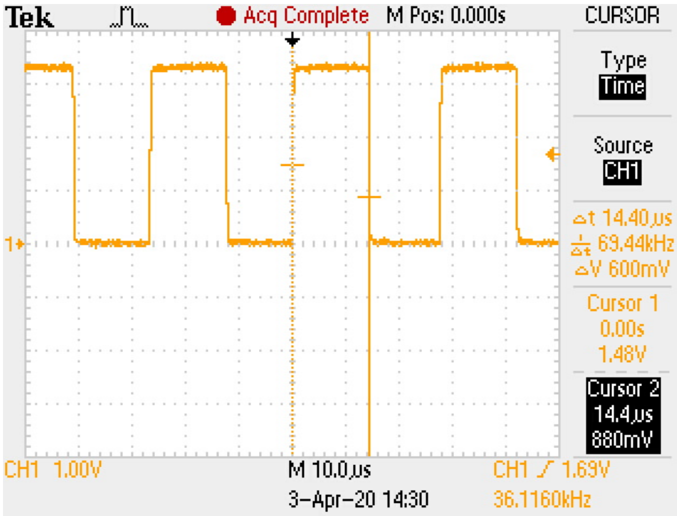

Figure 5.40, Cuk Experimentation, RPPM Time On Measurement, High Vout

The switching time witnessed by the circuit would vary due to the phase position delay. The values measured were three iterations of this ranged from 24.8 microseconds to 30.8 microseconds as shown by Figure 5.41, Figure 5.42 and Figure 5.43 below:

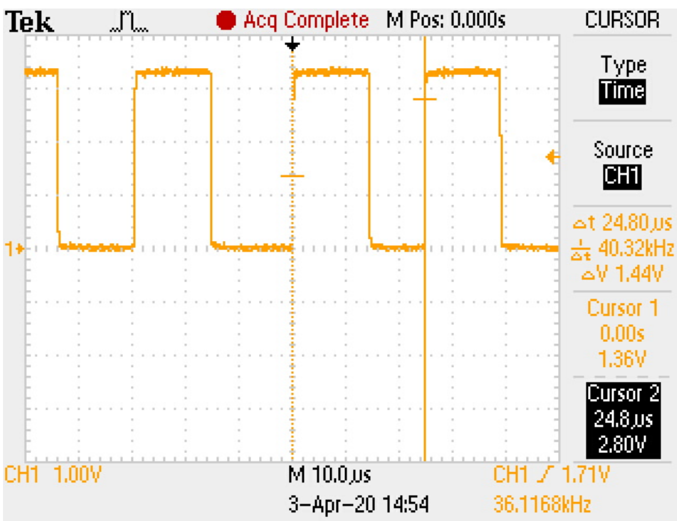

Figure 5.41, Cuk Experimentation, RPPM Switching Time of Iteration 1 of 3, High Vout

The second iteration shows a switching time of 27.6 microseconds as shown by Figure 5.42 below.

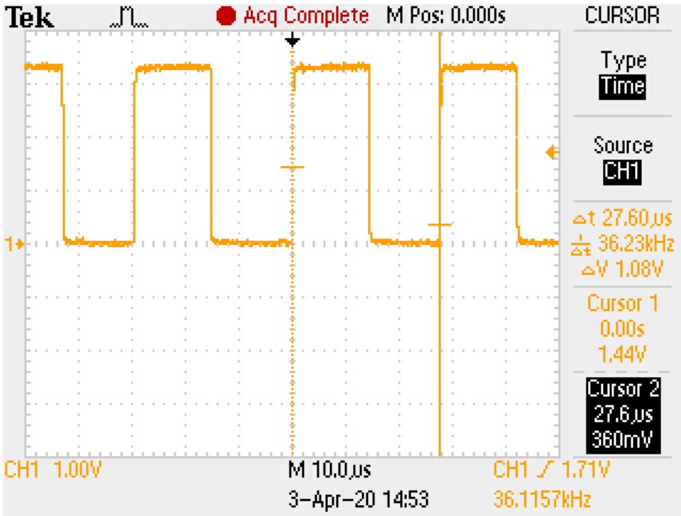

Figure 5.42, Cuk Experimentation, RPPM Switching Time of Iteration 2 of 3, High Vout

The third iteration shows a switching time of 30.8 microseconds as shown by Figure 5.43 below:

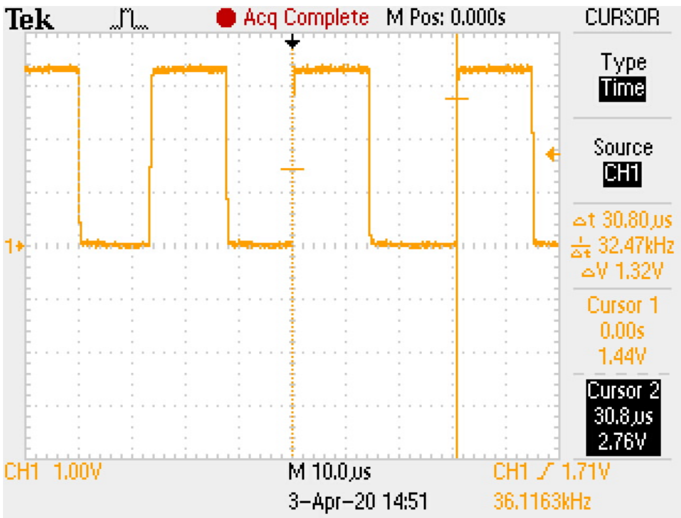

Figure 5.43, Cuk Experimentation, RPPM Switching Time of Iteration 3 of 3, High Vout

<u>Cuk Experimentation, High Vout, RPPM, FFT and Voltage Measurements</u>

The FFT measurements of this randomization is shown by Figure 5.44. When compared to the PWM FFT measurement found in Figure 5.27, the third and above harmonics are reduced in magnitude. Additionally the smaller frequencies around the fundamental frequency have increased in magnitude.

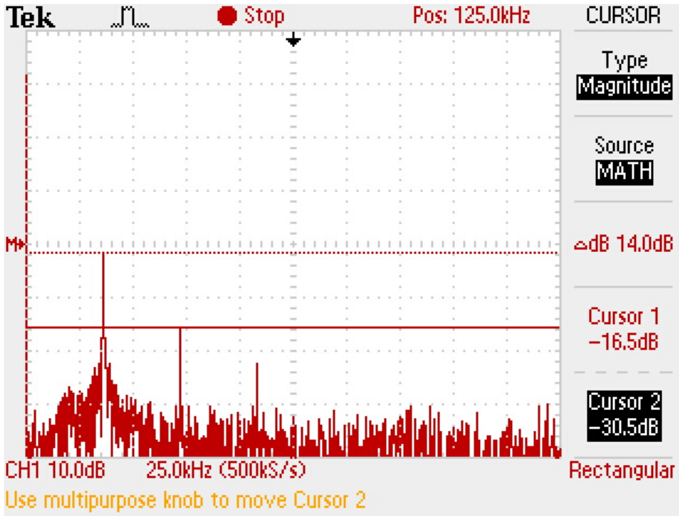

Figure 5.44, Cuk Experimentation, FFT Results, RPPM, High Vout

The output voltage measured with the randomization phase delay is -9.47 Volts as shown by Figure 5.45.

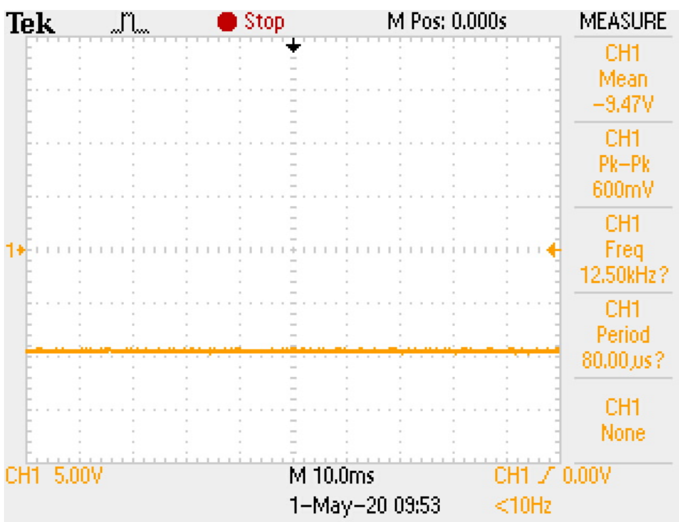

Figure 5.45, Cuk Experimentation, Output Voltage Result, RPPM, High Vout

SEPIC Converter Vout Lower than Vin

SEPIC Experimentation, Low Vout, PWM

<u>SEPIC Experimentation, Low Vout, PWM Measurements</u>

Similar to the Cuk converter, the SEPIC converter was operated in DCM mode. Figure 5.46 shows the time ON duration for the PWM measurement of 6.4 microseconds.

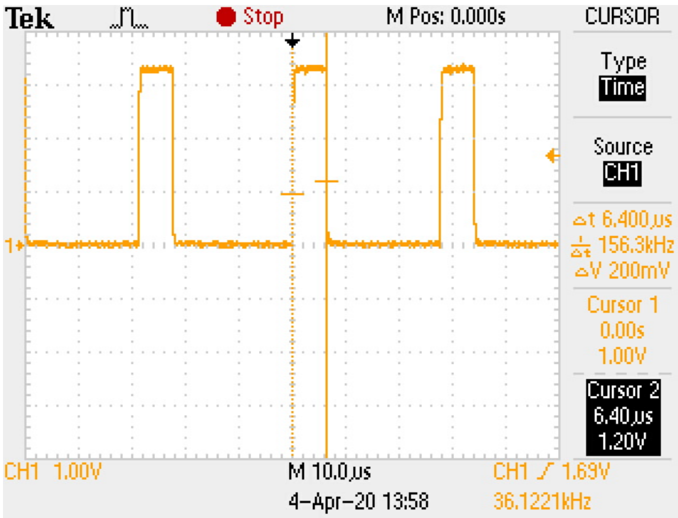

Figure 5.46, SEPIC Experimentation, PWM Results, Low Vout

The constant time switching is measured between the pulses as shown in Figure 5.47 and is measured to 27.6 microseconds. This provides the SEPIC circuit a duty cycle of 23%.

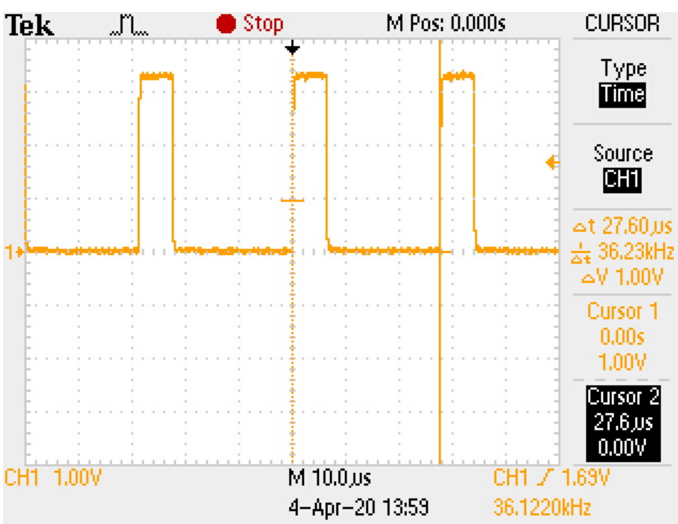

Figure 5.47, SEPIC Experimentation, PWM Switching Time Results, Low Vout

SEPIC Experimentation, Low Vout, PWM, FFT and Voltage Measurements

The PWM FFT measurements of the SEPIC converter are shown in Figure 5.48. This is with no randomization of the PWM. The randomization of the PWM occurs later in this section.

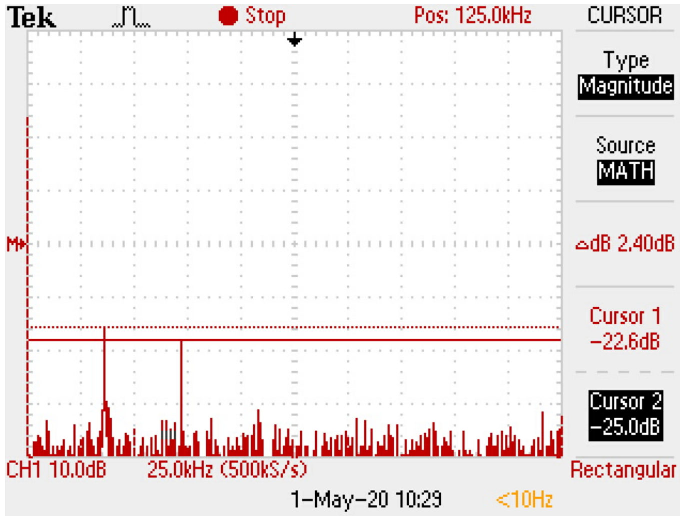

Figure 5.48, SEPIC Experimentation, FFT Results, PWM, Low Vout

The output voltage of the SEPIC converter is 4.78 Volts as shown by Figure 5.49 below.

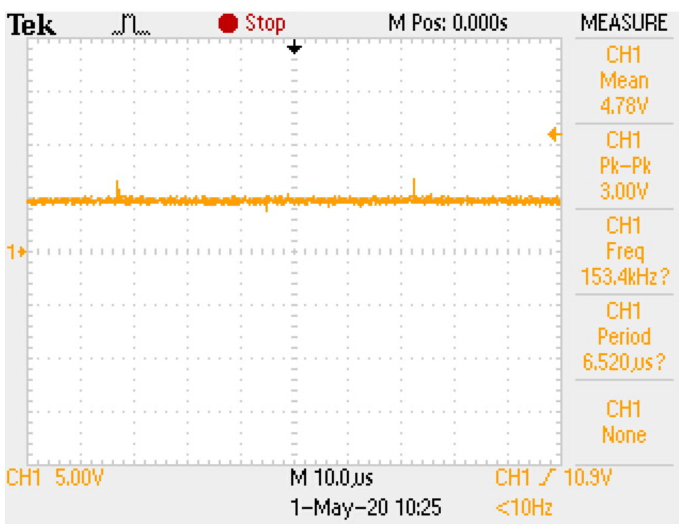

Figure 5.49, SEPIC Experimentation, Output Voltage Result, PWM, Low Vout

SEPIC Converter, Low Vout, Add RPWM

<u>SEPIC Converter, Low Vout, RPWM Measurements</u>

RPWM measurements for randomization of time ON occurred with a constant switching time of 27.6 microseconds as shown in Figure 5.50.

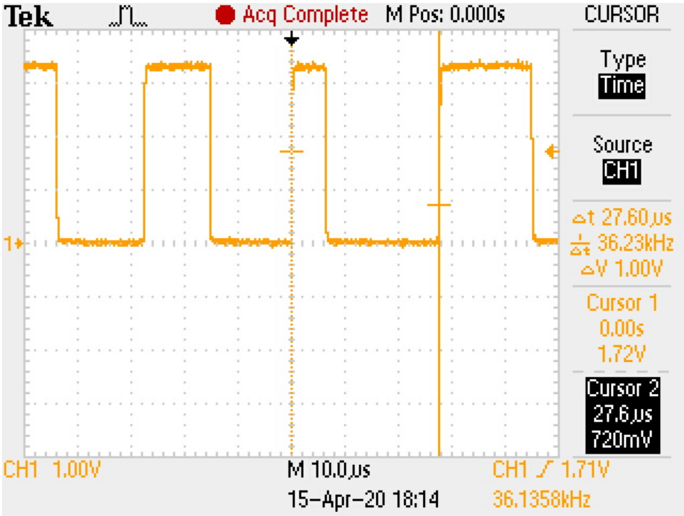

Figure 5.50, SEPIC Experimentation, RPWM, Switching Time Results, Low Vout

The time ON durations were measured at two different iterations. The first iteration showed a time ON duration of 6.4 microseconds as shown by Figure 5.51.

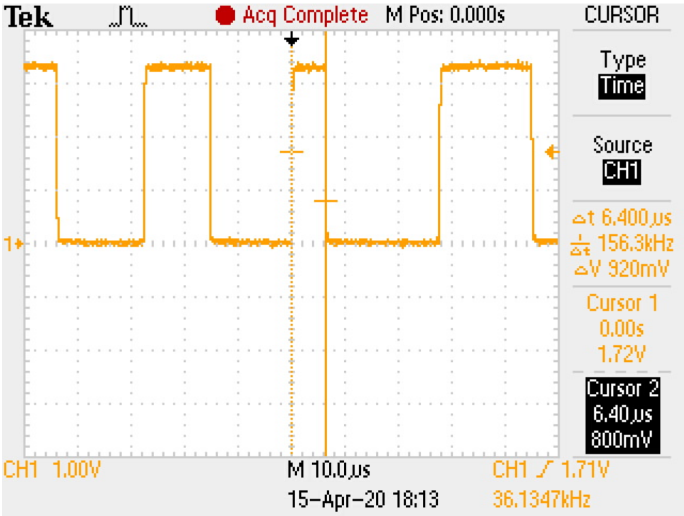

Figure 5.51, SEPIC Experimentation, RPWM Result first Iteration, Low Vout

The second iteration shows the time On duration of 17.6 microseconds as shown in Figure 5.52.

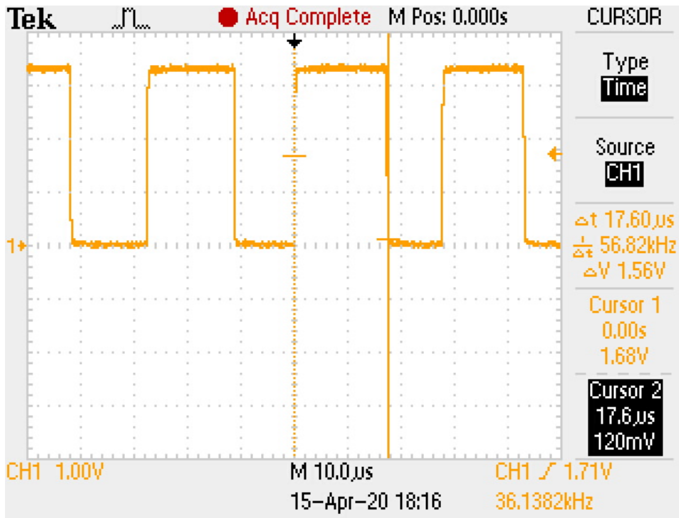

Figure 5.52, SEPIC Experimentation, RPWM Result for Second Iteration, Low Vout

<u>SEPIC Experimentation, Low Vout, RPWM, FFT and Voltage Measurements</u>

The FFT measurements of the RPWM randomization is shown by Figure 5.53. When compared to the PWM FFT measurement of Figure 5.48, the RPWM FFT second harmonic was reduced and the smaller frequencies increased in magnitude.

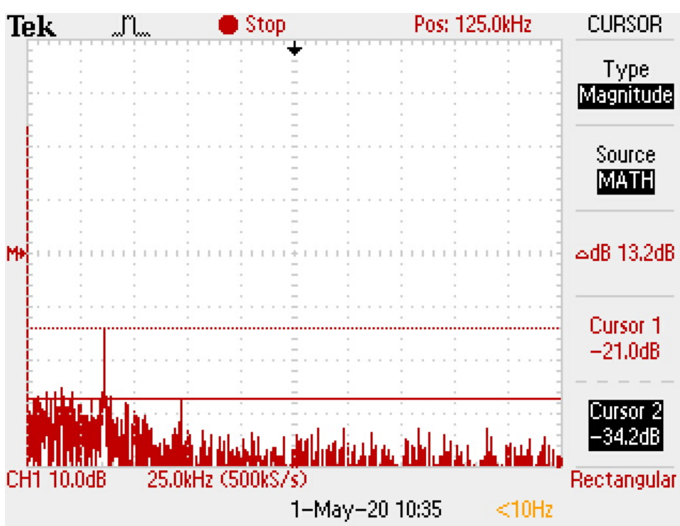

Figure 5.53, SEPIC Experimentation, FFT Result, RPWM, Low Vout

The measured output voltage was 8.80 Volts as shown by Figure 5.54.

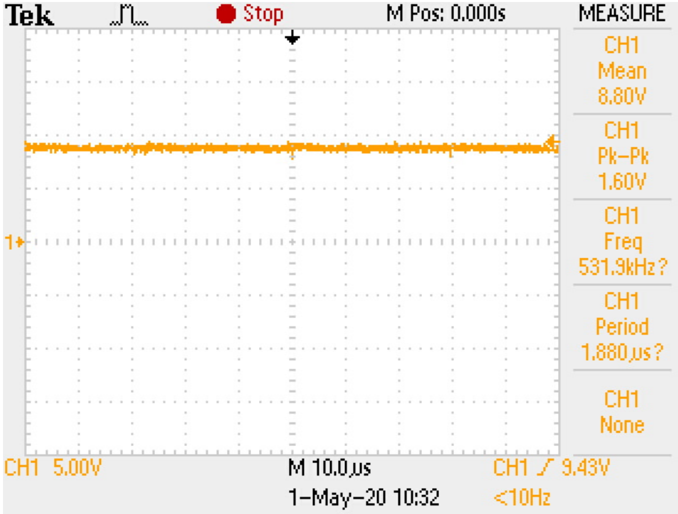

Figure 5.54, SEPIC Experimentation, Output Voltage Result, RPWM, Low Vout

SEPIC, Low Vout, Added RPWM and RPPM

<u>SEPIC, Low Vout, Added RPWM and RPPM Measurements</u>

The PWM signals had RPWM and RPPM randomization applied to both the time ON duration and the phase position delay. So, there were two iterations for the time ON with the first iteration is 8.4 microseconds as shown by Figure 5.55.

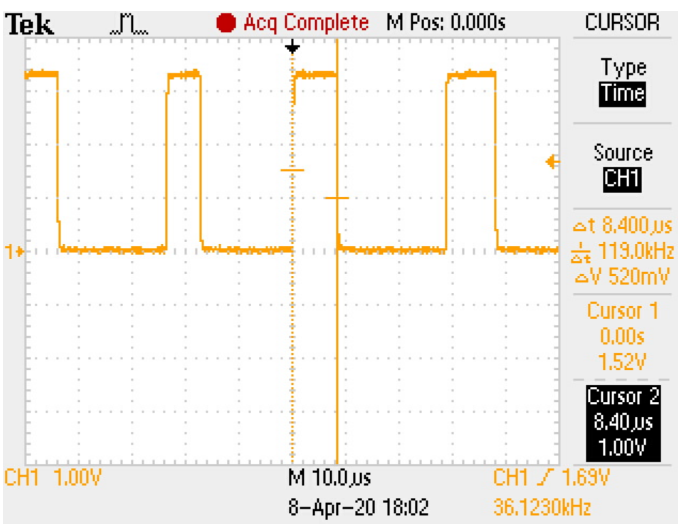

Figure 5.55, SEPIC Experimentation, RPWM and RPPM Result Iteration 1 of 2, Low Vout

The second iteration of the time on was measured to be 11.6 microseconds as shown by Figure 5.56.

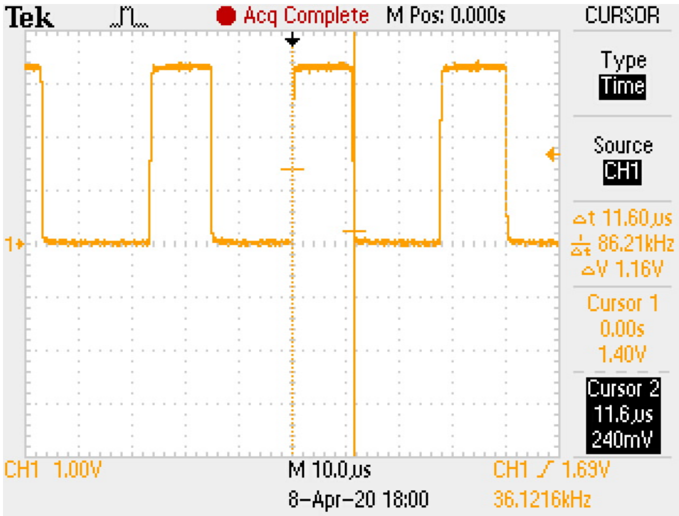

Figure 5.56, SEPIC Experimentation, RPWM and RPPM Result Iteration 2 of 2, Low Vout

The switching time was also measured with two iterations. The first iteration was 28.8 microseconds as shown in Figure 5.57.

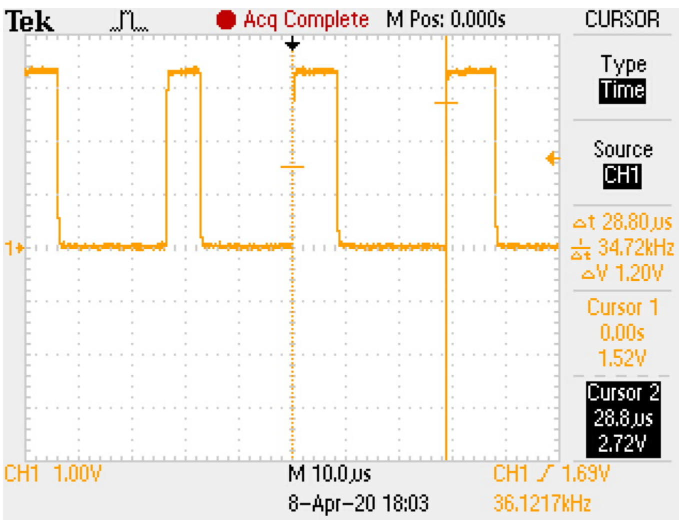

Figure 5.57, SEPIC Experimentation, RPWM and RPPM Switching Time Resul Iteration 1 of 2, Low Vout

The second iteration of the switching time was measured at 27.6 microseconds as shown by Figure 5.58.

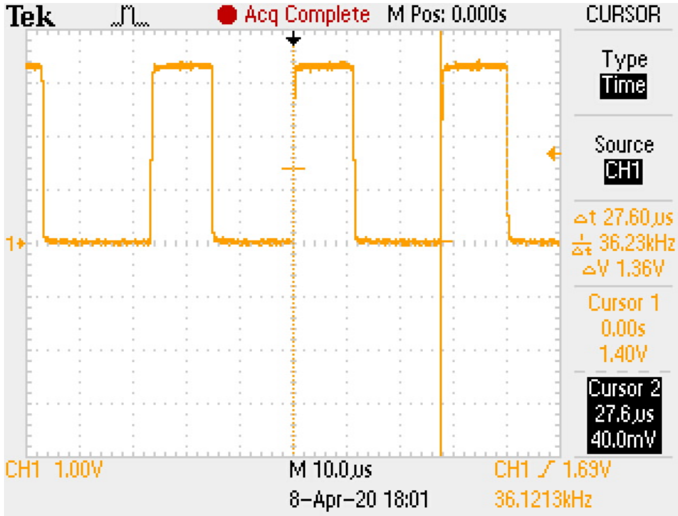

Figure 5.58, SEPIC Experimentation, RPWM and RPPM, Switching Time Result Iteration 2 of 2, Low Vout

<u>SEPIC Experimentation, Low Vout, RPWM and RPPM, FFT and Voltage Measurements</u>

RPWM and RPPM FFT measurements are shown by Figure 5.59 as shown below. When compared to the PWM FFT result found in Figure 5.48, the RPWM and RPPM FFT reduced the second harmonic and the smaller frequencies increased in magnitude.

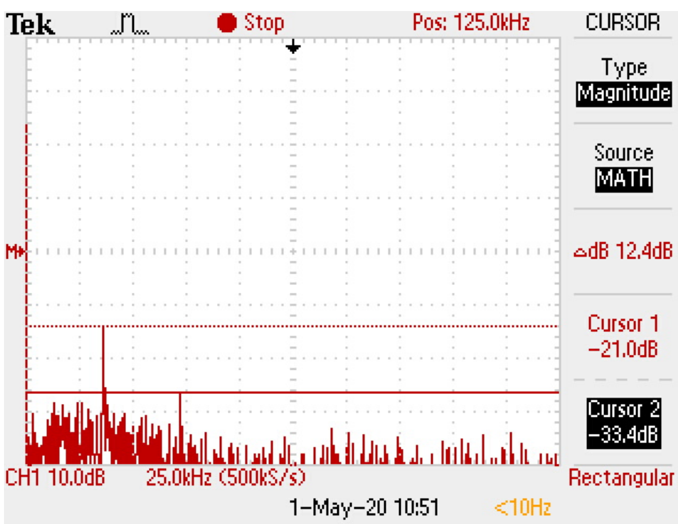

Figure 5.59, SEPIC Experimentation, FFT Result, RPWM and RPPM, Low Vout

Output voltage measurement was 6.92 Volts as shown by Figure 5.60.

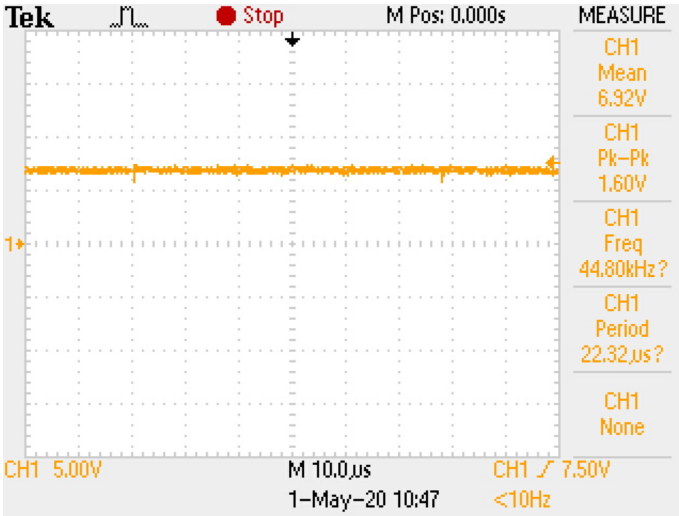

Figure 5.60, SEPIC Experimentation, Output Voltage Result, RPWM and RPPM, Low Vout

SEPIC Experimentation, Low Vout, Add RPPM

<u>SEPIC Experimentation, Low Vout, RPPM, PWM Measurement</u>

The PWM measurements with the RPPM randomization showed that the time ON duration was constant while the circuit would see different switching frequencies as a result of RPPM. The measurement for the time ON was 6.4 microseconds as shown by Figure 5.61.

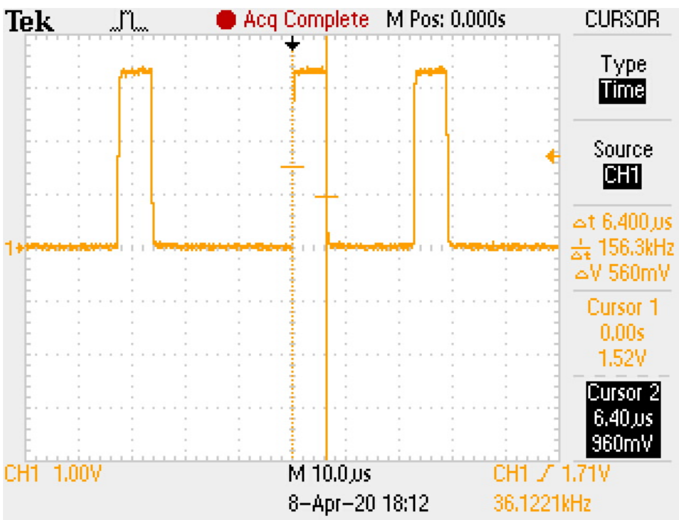

Figure 5.61, SEPIC Experimentation, RPPM Result, Low Vout

The switching times measured by the circuit occurred at two iterations. The first iteration was 22.8 microseconds as shown by Figure 5.62.

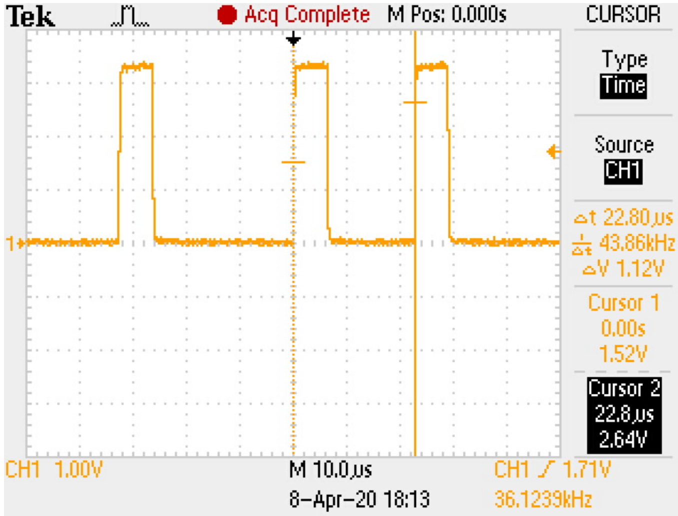

Figure 5.62, SEPIC Experimentation, RPPM Switching Time Result Iteration 1 of 2, Low Vout

The second iteration measured shows a measurement of 30.8 microseconds as shown by Figure 5.63.

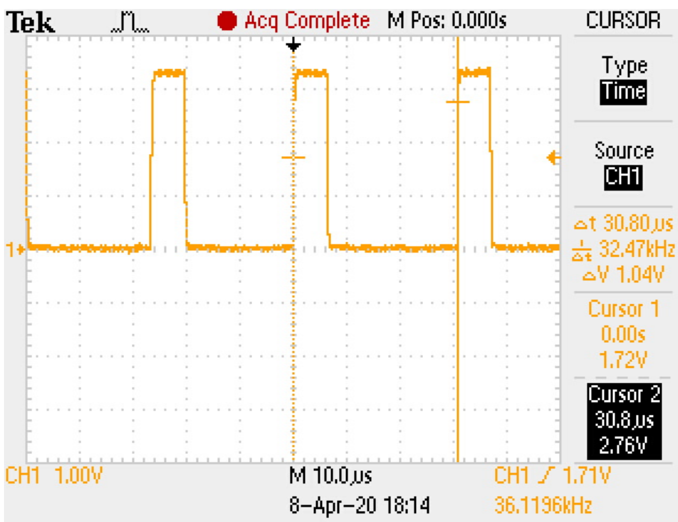

Figure 5.63, SEPIC Experimentation, RPPM Switching Time Result Iteration 2 of 2, Low Vout

<u>SEPIC Experimentation, Low Vout, RPPM, FFT and Voltage Measurements</u>

The FFT measurements is shown by Figure 5.64 below. When compared to the PWM FFT result found in Figure 5.48, the second harmonic is reduced drastically. Additionally the smaller frequencies increased in magnitude.

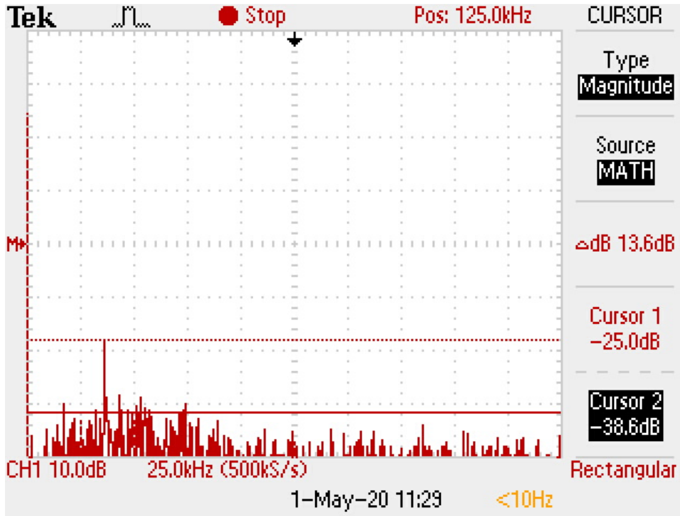

Figure 5.64, SEPIC Experimentation, FFT Result, RPPM, Low Vout

The output voltage of the RPPM is 4.79 Volts as shown by Figure 5.65.

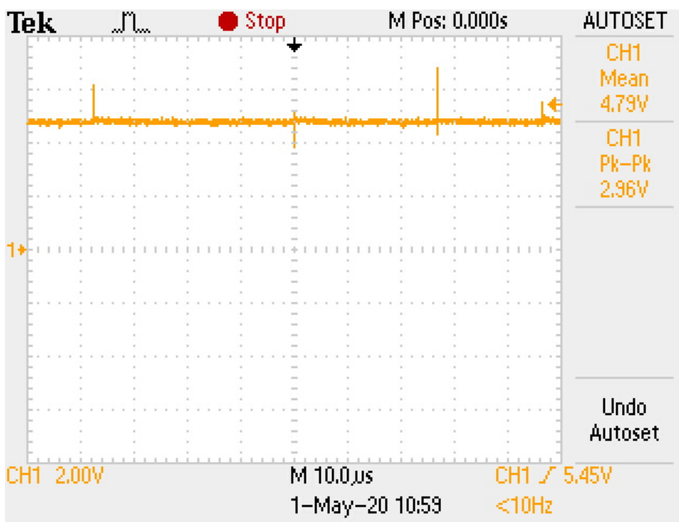

Figure 5.65, SEPIC Experimentation, Output Voltage Result, RPPM, Low Vout

SEPIC Experimentation, Higher Vout than Vin

SEPIC Experimentation, High Vout, No Randomized PWM

<u>SEPIC Experimentation, High Vout, PWM Measurements</u>

The PWM measurements is held constant in this section since there is no randomization applied to either the time ON duration or the phase position delay. Figure 5.66 shows the time ON duration of 14.4 microseconds as shown below.

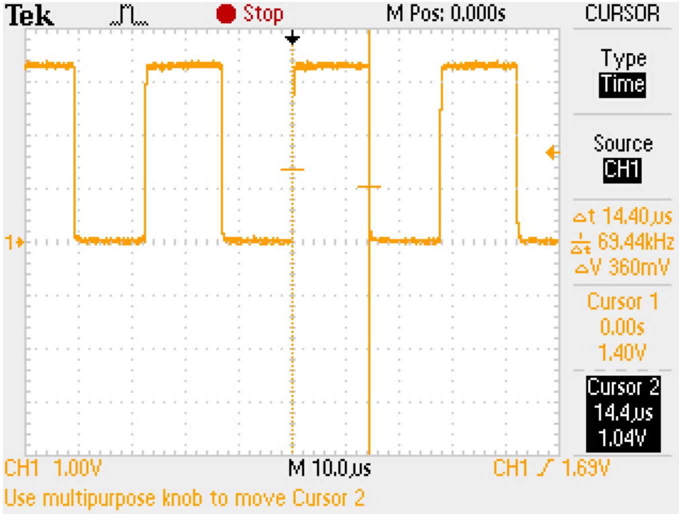

Figure 5.66, SEPIC Experimentation, PWM Result, High Vout

The switching time measured with no randomization applied is 27.6 microseconds are shown in Figure 5.67 below.

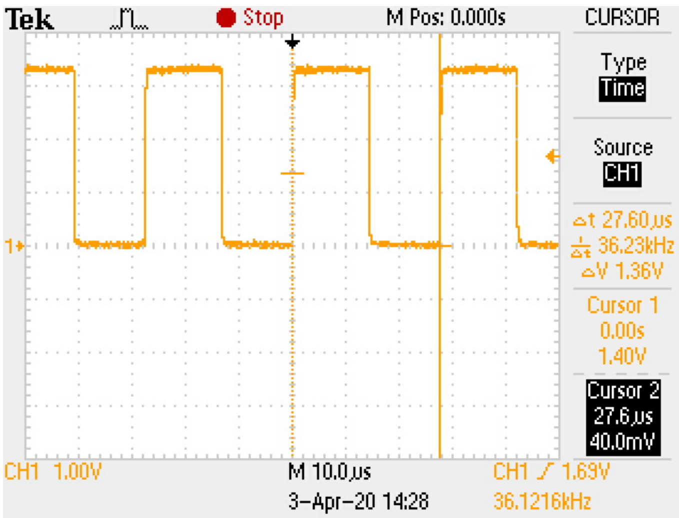

Figure 5.67, SEPIC Experimentation, PWM Switching Time, High Vout

<u>SEPIC Experimentation, High Vout, PWM FFT and Voltage Measurements</u>

The PWM FFT measurements as a result of constant PWM applied to the circuit is shown in Figure 5.68.

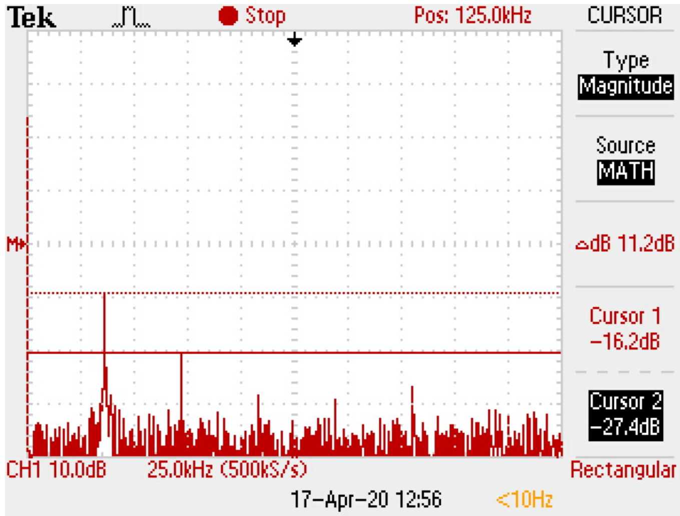

Figure 5.68, SEPIC Experimentation, PWM, FFT Result, High Vout

The output voltage with a constant PWM applied to the circuit is 9.92 Volts as shown by Figure 5.69.

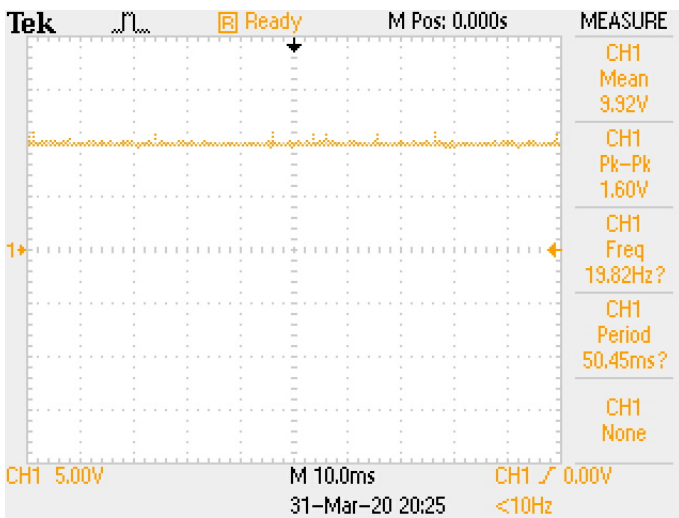

Figure 5.69, SEPIC Experimentation, PWM, Output Voltage Result, High Vout

SEPIC Experimentation, High Vout, Add RPWM

<u>SEPIC Experimentation, High Vout, RPWM Measurements</u>

RPWM measurements during time ON occurred at 14.4 microseconds as shown by Figure 5.70 below.

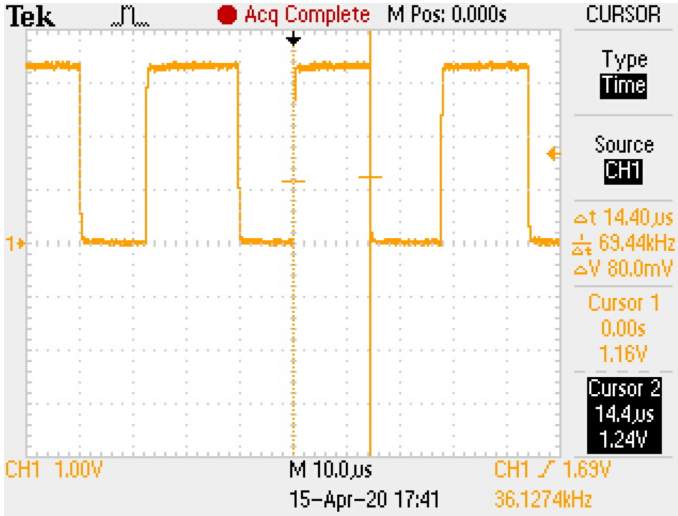

Figure 5.70, SEPIC Experimentation, RPWM Result, High Vout, Iteration 1 of 2

The second iteration of time ON measurements occurred at 17.6 microseconds as shown by Figure 5.71 below.

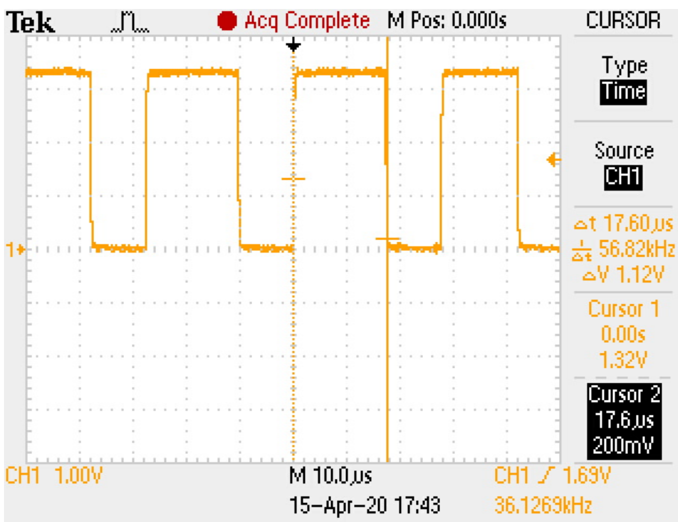

Figure 5.71, SEPIC Experimentation, RPWM Result, High Vout, Iteration 2 of 2

Both durations have a constant switching frequency of 27.6 microseconds since the phase position delay is constant as shown by Figure 5.72.

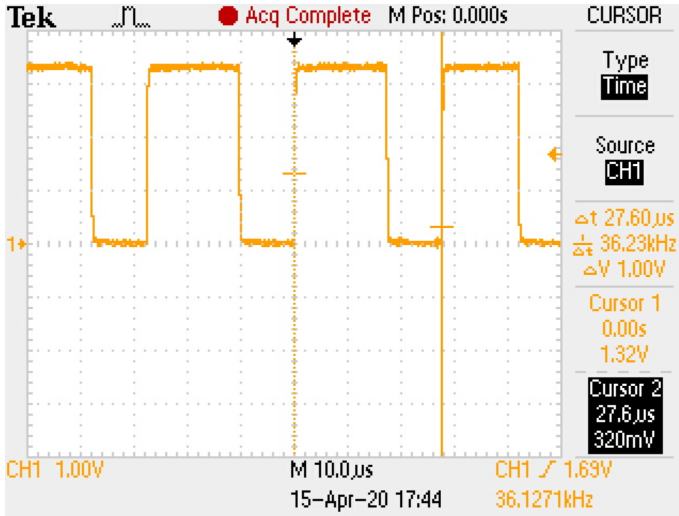

Figure 5.72, SEPIC Experimentation, RPWM Result Switching Time, High Vout

<u>SEPIC Experimentation, High Vout, RPWM FFT and Voltage Measurements</u>

The FFT results of the measurements is shown in Figure 5.73. When compared to PWM FFT results in Figure 5.68, the RPWM FFT shows an increase of the fourth harmonic while the 5th harmonic is reduced. The smaller frequencies have slight increase in magnitude.

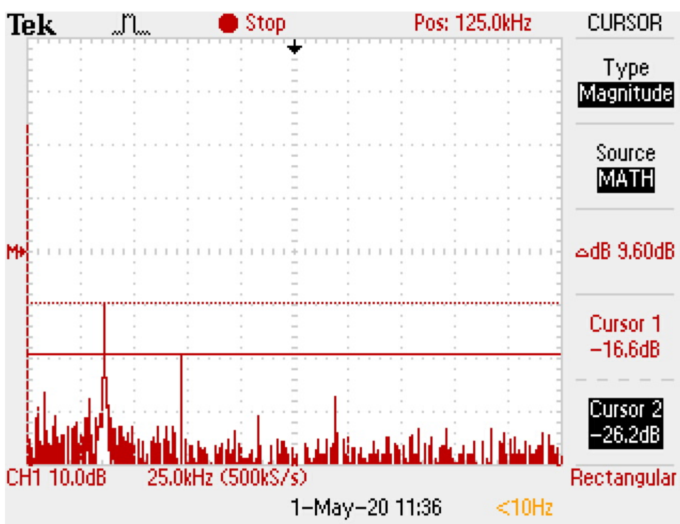

Figure 5.73, SEPIC Experimentation, RPWM, FFT Result, High Vout

The output voltage of the RPWM is 10.9 Volts as shown by Figure 5.74.

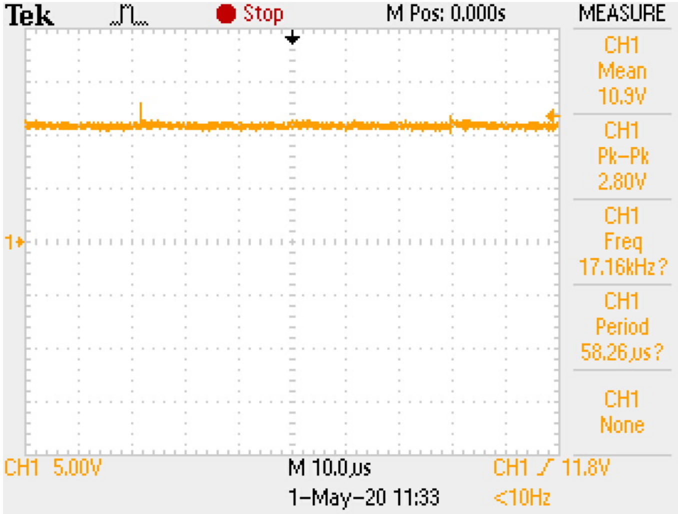

Figure 5.74, SEPIC Experimentation, RPWM, Output Voltage Result, High Vout

SEPIC Experimentation, High Vout, Add RPWM and RPPM

<u>SEPIC Experimentation, High Vout, RPWM and RPPM Measurements</u>

The RPWM and RPPM measurement shows time ON and switching frequencies seen by the SEPIC circuit as a result of the time ON and phase position delay randomization. The time ON for the first of two iterations is shown by Figure 5.75 which is at 15.6 microseconds.

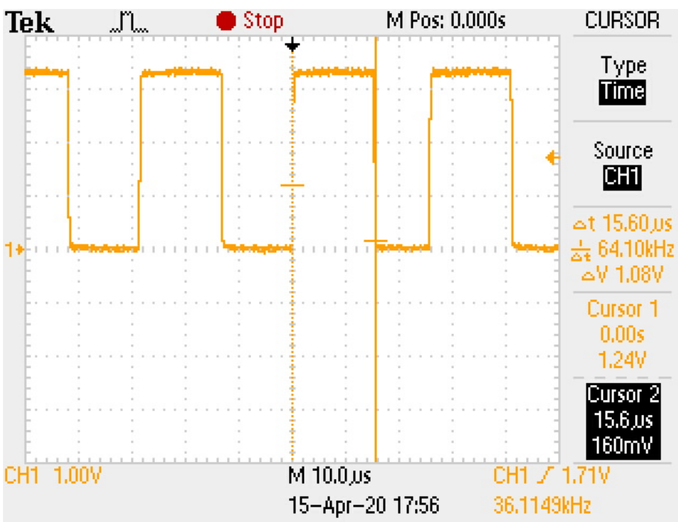

Figure 5.75, SEPIC Experimentation, RPWM and RPPM Result, High Vout, Iteration 1 of 2

The second iteration time ON is shown by Figure 5.76 below, which is at 14.4 microseconds.

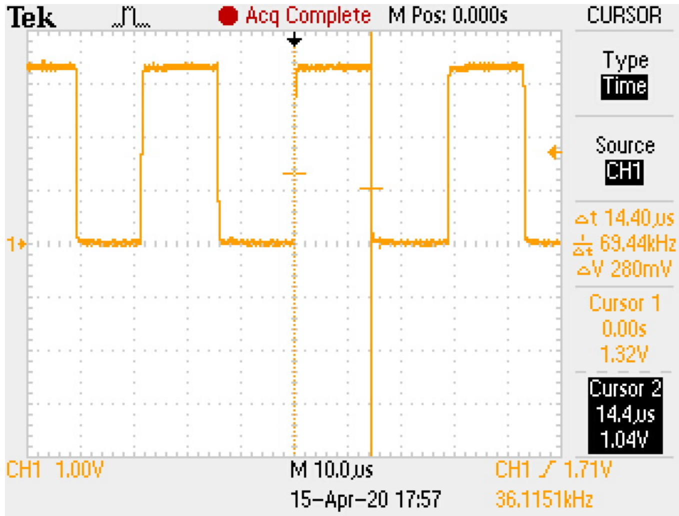

Figure 5.76, SEPIC Experimentation, RPWM and RPPM Result, High Vout, Iteration 2 of 2

The switching time as a result of the phase position delays occur as 29.6 microseconds as shown by Figure 5.77.

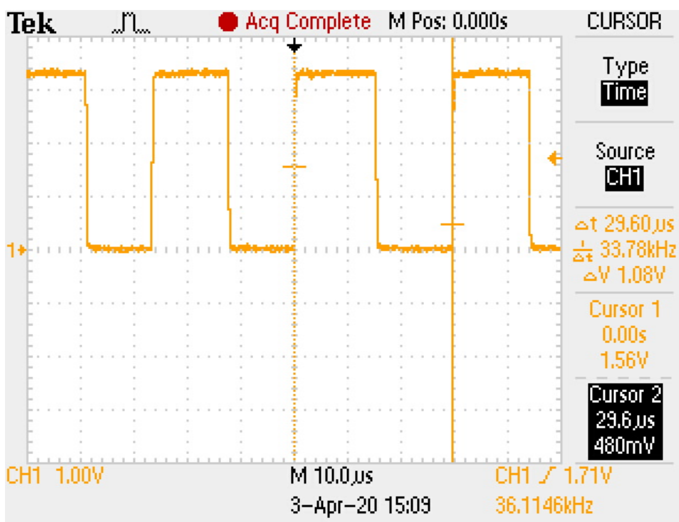

Figure 5.77, SEPIC Experimentation, RPWM and RPPM Switching Time Result, High Vout, Iteration 1 of 2

The switching time as a result of the phase delays occur at 26.8 microseconds as shown by Figure 5.78 below.

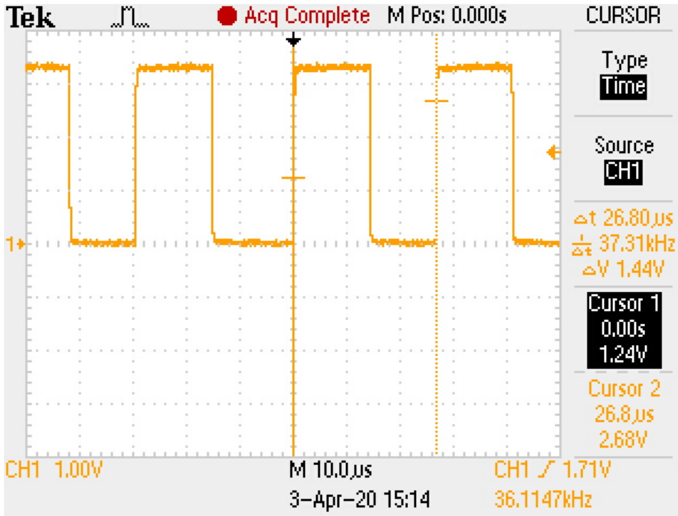

Figure 5.78, SEPIC Experimentation, RPWM and RPPM Switching Time Result, High Vout, Iteration 2 of 2

<u>SEPIC Experimentation, High Vout, RPWM and RPPM FFT and Voltage Measurements</u>

The FFT measurements of both time ON and phase position delay randomizations results as shown in Figure 5.79. When compared to PWM FFT in Figure 5.68, the RPWM and RPPM fourth harmonic increased and the fifth harmonic decreased.

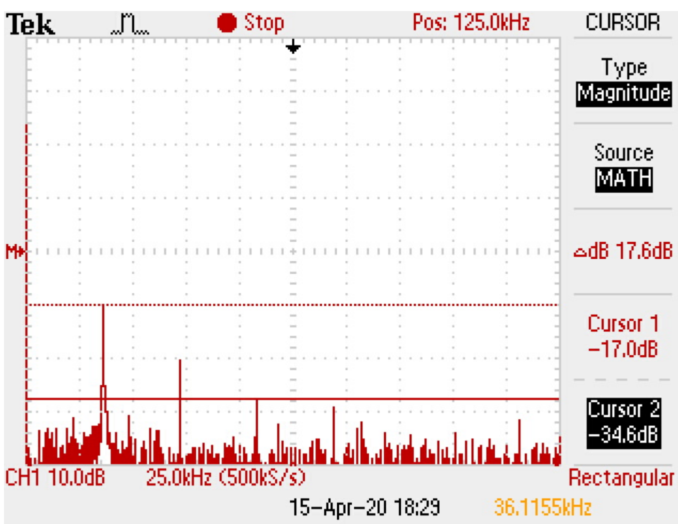

Figure 5.79, SEPIC Experimentation, RPWM and RPPM FFT Results, High Vout

The output voltage measured is 10.2 Volts as shown by Figure 5.80.

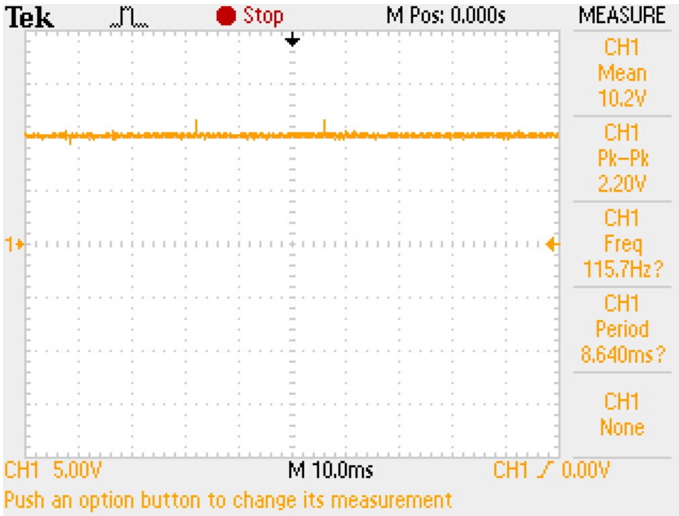

Figure 5.80, SEPIC Experimentation, RPWM and RPPM Output Voltage Result, High Vout

SEPIC Experimentation, High Vout, Add RPPM

<u>SEPIC Experimentation, High Vout, RPPM Measurement</u>

The time ON measurement for RPPM randomization will be constant. The time ON was measured at 14.4 microseconds as shown by Figure 5.81 below.

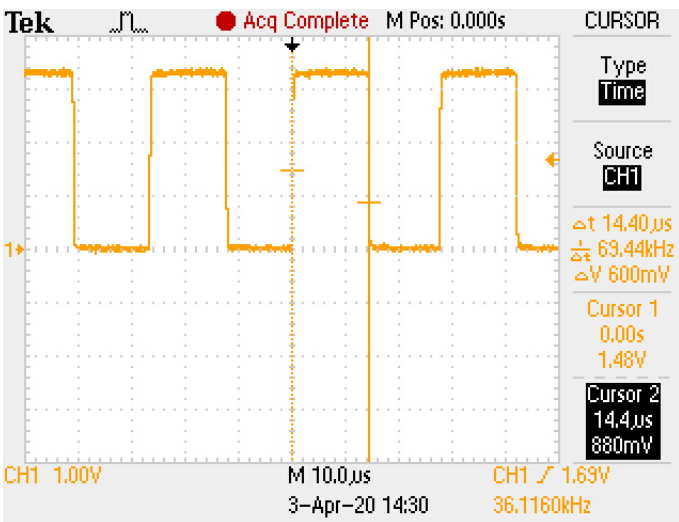

Figure 5.81, SEPIC Experimentation, RPPM Result, High Vout

The switching time witnessed by the circuit would vary due to the phase delay. The values measured were three iterations of this ranged from 24.8 microseconds to 30.8 microseconds as shown by Figure 5.82, Figure 5.83 and Figure 5.84 below. The first iteration shows the switching time of 24.8 microseconds as shown by Figure 5.82.

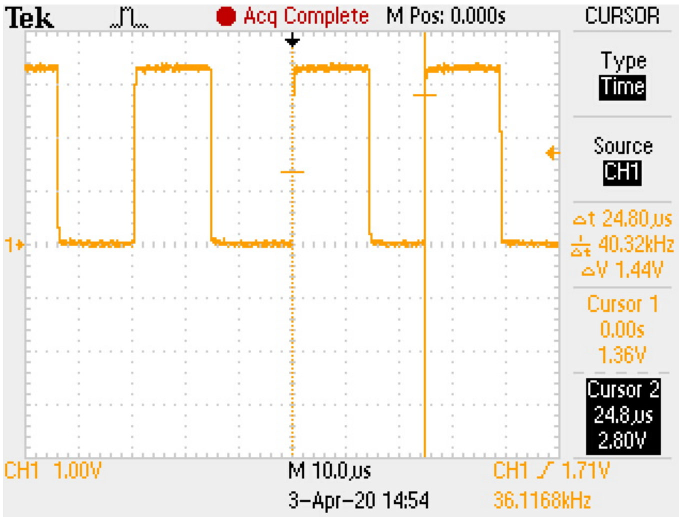

Figure 5.82, SEPIC Experimentation, RPPM Switching Time Result, High Vout, Iteration 1 of 3

The second iteration shows a switching time of 27.6 microseconds as shown by Figure 5.83 below.

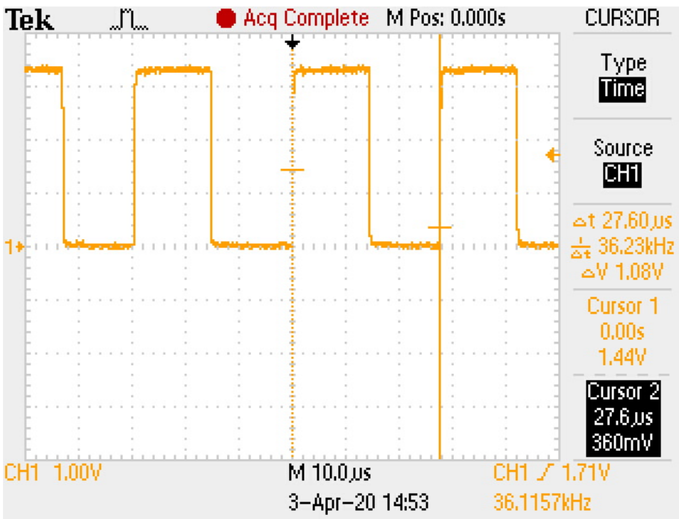

Figure 5.83, SEPIC Experimentation, RPPM Switching Time Result, High Vout, Iteration 2 of 3

The third iteration shows a switching time of 30.8 microseconds as shown by Figure 5.84 below:

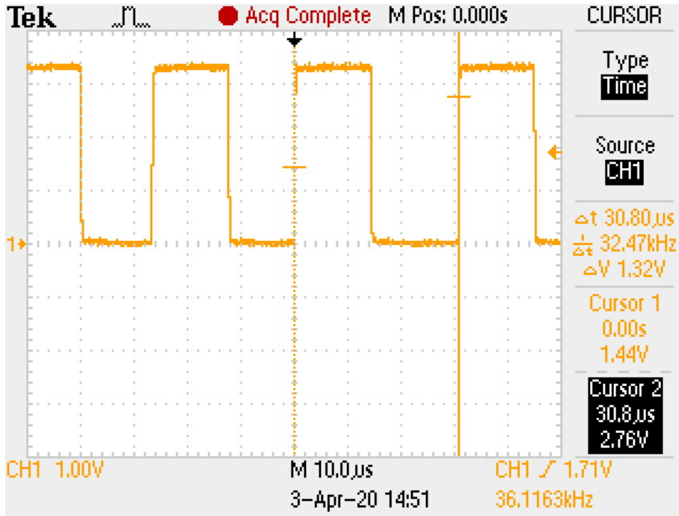

Figure 5.84, SEPIC Experimentation, RPPM Switching Time Result, High Vout, Iteration 3 of 3

<u>SECIC Converter, High Vout, RPPM FFT and Voltage Measurements</u>

The RPPM FFT measurements are shown in Figure 5.85. When compared to the PWM FFT results, the RPPM FFT shows a decrease in the fourth, fifth and sixth harmonics.

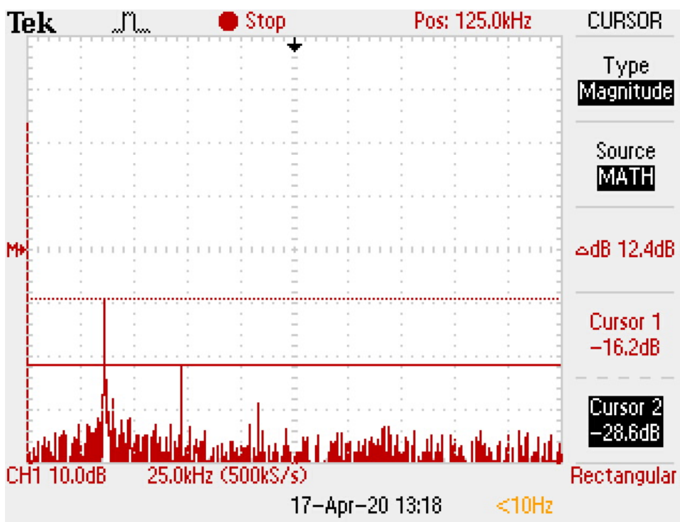

Figure 5.85, SEPIC Experimentation, RPPM FFT Results, High Vout

The output voltage of Phase Delay Randomization is 9.96 Volts as shown by Figure 5.86.

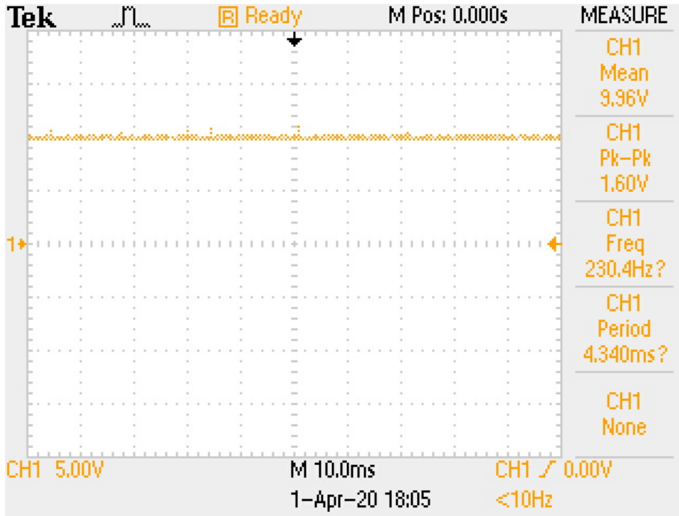

Figure 5.86, SEPIC Experimentation, RPPM Output Voltage Result, High Vout

Experimentation Summary of Cuk Converter

The Cuk experimentation utilized focused on four modes of PWM operation. The four modes are PWM (no randomization), RPWM, RPPM and combined both RPWM and RPPM. The duty cycles experienced are the same as the simulation between 23% up to 56% duty cycle. The phase position delay occurred from 0 and up to 11 microseconds. Results of the experimentation are in dB which need to be converted to Vrms for comparison to the simulation.

To convert from Vrms to dB, the understanding of voltage gain is shown as the following equation [Tektronix]

$$VoltageGain = \frac{output\ amplitude}{input\ amplitude}. \tag{5-1}$$

Tektronix TDS 2014B user manual shows that the Voltage Gain's input amplitude is 1 Vrms. So the dB measurements are compared to 1 Vrms [Tektronix].

To compute from the voltage ratio to dB is shown below:

$$VoltageGain\ (dB) = 20\ X\ log_{10}(VoltageGain). \tag{5-2}$$

To converter, for example, 75mV or 0.075 Vrms to dB scale, the following is calculated:

$$VoltageGain\ (dB) = 20\ \times\ log_{10}(0.075). \tag{5-3}$$

Which the equations becomes:

$$VoltageGain\ (dB) = 20\ \times -1.1249 \tag{5-4}$$

and then the final result is

$$VoltageGain\ (dB) = -22.5\ dB. \tag{5-5}$$

This value of -22.5 dB is shown in Figure 5.1 for the experimentation result of Cuk converter during Low Vout and no randomization applied.

With the Vrms known from dB values, the resulting THD can be calculated from the equation shown below:

$$THD_V = \frac{V_{rms,h}}{V_{rms,1}} = \frac{\sqrt{\sum_{n=2}^{h_{max}} V_{rms,h}^2}}{V_{rms,1}}. \tag{5-6}$$

For example, for the PWM baseline measurement for Cuk, Low Vout, h_{max}= 4 shows the results as shown below.

$$THD_V = \frac{V_{rms,h}}{V_{rms,1}} = \frac{\sqrt{\sum_{n=2}^{h_{max}} V_{rms,h}^2}}{V_{rms,1}} = \frac{\sqrt{12.4^2 + 12.4^2 + 8.61^2}}{75.0} = \frac{19.5}{75.0} = 26.0\%. \tag{5-7}$$

The summary of the Cuk converter's results are shown in Table 5.1 below.

Table 5.1, Cuk Experimentation Results Summary

Converter Type	Duty Cycle	Phase Delay	PWM Type	Harmonic No.	FFT Value (dB)	FFT Value (mV)	THD	Vout
CUK Converter, Low Vout Measurements								
CUK, Low Vout	23%	0 μSec.	PWM Baseline	1	-22.5 dB	75.0mV	26.0%	-6.5 Volts
				2	-24.9 dB	12.4mV		
				3	-38.1 dB	12.4mV		
				4	-41.3 dB	8.61mV		
CUK, Low Vout	23% to 56%	0 μSec.	RPWM	1	-19.7 dB	104mV	25.9%	-8.29 volts
				2	-32.9 dB	22.6mV		
				3	-39.7 dB	10.4mV		
				4	-39.7 dB	10.4mV		
CUK, Low Vout	23% to 41%	0 to 5 μSec.	RPWM and RPPM	1	-19.8 dB	102mV	19.6%	-6.77 volts
				2	-35.0 dB	17.8mV		
				3	-43.0 dB	7.08mV		
				4	-45.0 dB	5.62mV		
CUK, Low Vout	23%	0 to 11 μSec.	RPPM	1	-26.2 dB	49.0mV	22.3%	-4.64 volts
				2	-41.0 dB	8.91mV		
				3	-47.0 dB	4.47mV		
				4	-47.0 dB	4.47mV		
CUK Converter, High Vout Measurements								
CUK, High Vout	52%	0 μSec.	PWM Baseline	1	-16.1	157mV	27.8%	-9.87 volts
				2	-28.5	37.6mV		
				3	-34.5	18.8mV		
				4	-38.5	11.9mV		
CUK, High Vout	52% to 63%	0 μSec.	RPWM	1	-16.9	143mV	32.1%	-10.1 volts
				2	-27.7	41.2mV		
				3	-37.3	13.6mV		
				4	-36.5	15.0mV		
CUK, High Vout	52% to 56%	0 to 2 μSec.	RPWM and RPPM	1	-16.9	143mV	28.0%	-10.2 volts
				2	-28.9	35.9mV		
				3	-36.1	15.7mV		
				4	-41.7	8.22mV		
CUK, High Vout	52%	0 to 3 μSec.	RPPM	1	-16.5	150mV	22.2%	-9.47 volts
				2	-30.5	29.9mV		
				3	-36.9	14.3mV		
				4	-48.9	3.59mV		

SEPIC Experimentation Summary

Table 5.2 shows, SEPIC FFT results under the same PWM randomization techniques and calculation from dB to Vrms. RPPM had the highest voltage adjustment but also had the highest THD, as a result.

Table 5.2, SEPIC Experimentation Result Summary

Converter Type	Duty Cycle	Phase Delay	PWM Type	Harmonic No.	FFT Value (dB)	FFT Value (mV)	THD	Vout
SEPIC Converter, Low Vout Measurements								
SEPIC, Low Vout	23%	0 μSec.	PWM, Baseline	1	-22.6	74.1mV	78.5%	4.78 volts
				2	-25.0	56.2mV		
				3	-37.8	12.9mV		
				4	-42.6	7.41mV		
SEPIC, Low Vout	23% to 56%	0 μSec.	RPWM	1	-21.0	89.1mV	25.4%	8.80 volts
				2	-34.2	19.5mV		
				3	-41.4	8.51mV		
				4	-42.2	7.76mV		
SEPIC, Low Vout	23% to 41%	0 to 5 μSec.	RPWM and RPPM	1	-21.0	89.1mV	26.0%	6.92 volts
				2	-33.4	21.4mV		
				3	-44.6	5.89mV		
				4	-43.4	6.76mV		
SEPIC, Low Vout	23%	0 to 11 μSec.	RPPM	1	-25	25.2mV	56.5%	4.79 volts
				2	-38.6	11.7mV		
				3	-43.4	6.76mV		
				4	-47.0	4.46mV		
SEPIC Converter, High Vout Measurements								
SEPIC, High Vout	52%	0 μSec.	PWM, Baseline	1	-16.2	155mV	31.6%	10.0 volts
				2	-27.4	42.7mV		
				3	-35.0	17.8mV		
				4	-35.8	16.2mV		
SEPIC, High Vout	52% to 63%	0 μSec.	RPWM	1	-16.6	148mV	36.7%	10.9 volts
				2	-26.2	49.0mV		
				3	-37.8	12.9mV		
				4	-34.2	19.5mV		
SEPIC, High Vout	52% to 56%	0 to 2 μSec.	RPWM and RPPM	1	-17.0	141mV	35.0%	10.48 volts
				2	-27.4	42.7mV		
				3	-34.6	18.6mV		
				4	-35.8	16.2mV		
SEPIC, High Vout	52%	0 to 3 μSec.	RPPM	1	-16.2	155mV	27.0%	10.07 volts
				2	-28.6	37.2mV		
				3	-35.4	17.0mV		
				4	-41.0	8.91mV		

Chapter 6

CONCLUSION, THESIS RESULT COMPARISON AND FUTURE WORK

Conclusion of Simulation and Experimentation Results of Cuk and SEPIC

The results of both the simulation and experimentation FFTs and output voltages for PWM and the different randomization techniques (RPWM, RPPM, and both RPWM & RPPM) applied shows are shown by Table 6.1. The randomization technique that contributed the most to the voltage harmonic adjustment was RPPM. But when RPPM was applied to both converters, it was expected to see an increase in THD. Simulation and experimentation were abbreviated to “Sim.” and “Exp.” to conserve space in the table. Sometimes the result for both RPWM and RPPM had a decrease of harmonic content but a slight increase of THD. So RPPM had the most adjustment of discrete voltage harmonics but the THD increased. But, when both RPWM and RPPM had the combination of both decrease in discrete harmonic and slight increase in THD. The THD in the experimentation didn’t increase THD when RPPM was utilized due to THD only focusing on discrete harmonics. If subharmonics were utilized the THD would expect to increase [Langella].

Table 6.1, Cuk Simulation and Experimentation Comparison Result

Converter Type	Duty Cycle	Phase Delay	PWM Type	Harmon. No.	FFT Value Sim.	FFT Value Exp.	THD Sim.	THD Exp.	Vout, Sim.	Vout, Exp.
Cuk Converter, Low Vout Measurements										
CUK, Low Vout	23%	0 μSec.	PWM	1	2.1mV	75.0mV	16.38%	26.0%	-6.5 volts	-6.5 volts
				2	0.31mV	12.4mV				
				3	0.14mV	12.4mV				
				4	0.067mV	8.61mV				
CUK, Low Vout	23% to 56%	0 μSec.	RPWM	1	2.5mV	104mV	26.24%	25.9%	-9.034 volts	-8.29 volts
				2	0.33mV	22.6mV				
				3	0.16mV	10.4mV				
				4	0.09mV	10.4mV				
CUK, Low Vout	23% to 41%	0 to 5 μSec.	RPWM and RPPM	1	2.1mV	102mV	32.97%	19.6%	-5.974 volts	-6.77 volts
				2	0.12mV	17.8mV				
				3	0.055mV	7.08mV				
				4	0.0004mV	5.62mV				
CUK, Low Vout	23%	0 to 11 μSec.	RPPM	1	1.5mV	49.0mV	52.11%	22.3%	-4.3 volts	-4.64 volts
				2	0.09mV	8.91mV				
				3	0.003mV	4.47mV				
				4	0.002mV	4.47mV				
Cuk Converter, High Vout Measurements										
CUK, High Vout	52%	0 μSec.	PWM	1	3.0mV	157mV	18.75%	27.8%	-10.0 volts	-9.87 volts
				2	0.49mV	37.6mV				
				3	0.17mV	18.8mV				
				4	0.09mV	11.9mV				
CUK, High Vout	52% to 63%	0 μSec.	RPWM	1	3.0mV	143mV	24.98%	32.1%	-11.51 volts	-10.1 volts
				2	0.7mV	41.2mV				
				3	0.14mV	13.6mV				
				4	0.13mV	15.0mV				
CUK, High Vout	52% to 56%	0 to 2 μSec.	RPWM and RPPM	1	3.0 mV	143mV	22.40%	28.0%	-10.48 volts	-10.2 volts
				2	0.51mV	35.9mV				
				3	0.14mV	15.7mV				
				4	0.09mV	8.22mV				
CUK, High Vout	52%	0 to 3 μSec.	RPPM	1	3.0mV	150mV	21.94%	22.2%	-10.07 volts	-9.47 volts
				2	0.44mV	29.9mV				
				3	0.15mV	14.3mV				
				4	0.07mV	3.59mV				

The SEPIC simulation and experimentation results are shown in Table 6.2. The simulation FFT were shown in microvolts while the experimentation was shown in mV. Similar to the Cuk converter, the SEPIC had improvement with RPPM was incorporated but the THD was expected to increase.

Table 6.2, SEPIC Simulation and Experimentation Comparison Results

Converter Type	Duty Cycle	Phase Delay	PWM Type	Harmonic No.	FFT Value Sim.	FFT Value Exp.	THD Sim.	THD Exp.	Vout Sim.	Vout Exp.
SEPIC Converter, Low Vout Measurements										
SEPIC, Low Vout	23%	0 μSec.	PWM	1	140μV	74.1mV	14.87%	78.5%	8.38 volts	4.78 volts
				2	19μV	56.2mV				
				3	8μV	12.9mV				
				4	4μV	7.41mV				
SEPIC, Low Vout	23% to 56%	0 μSec.	RPWM	1	150μV	89.1mV	25.71%	25.4%	4.15 volts	8.80 volts
				2	26μV	19.5mV				
				3	12μV	8.51mV				
				4	7μV	7.76mV				
SEPIC, Low Vout	23% to 41%	0 to 5 μSec.	RPWM and RPPM	1	90μV	89.1mV	28.54%	26.0%	4.91 volts	6.92 volts
				2	10μV	21.4mV				
				3	6μV	5.89mV				
				4	1.8μV	6.76mV				
SEPIC, Low Vout	23%	0 to 11 μSec.	RPPM	1	107μV	25.2mV	57.80%	56.5%	3.9 volts	4.79 volts
				2	4.9μV	11.7mV				
				3	0.7μV	6.76mV				
				4	0.7μV	4.46mV				
SEPIC Converter, High Vout Measurements										
SEPIC, High Vout	52%	0 μSec.	PWM	1	231μV	155mV	16.86%	31.6%	8.9 volts	10.0 volts
				2	30μV	42.7mV				
				3	12μV	17.8mV				
				4	7μV	16.2mV				
SEPIC, High Vout	52% to 63%	0 μSec.	RPWM	1	243μV	148mV	24.19%	36.7%	12.1 volts	10.9 volts
				2	49μV	49.0mV				
				3	14μV	12.9mV				
				4	9μV	19.5mV				
SEPIC, High Vout	52% to 56%	0 to 2 μSec.	RPWM and RPPM	1	233μV	141mV	20.61%	35.0%	9.77 volts	10.48 volts
				2	38μV	42.7mV				
				3	11μV	18.6mV				
				4	6.8μV	16.2mV				
SEPIC, High Vout	52%	0 to 3 μSec.	RPPM	1	222μV	155mV	22.72%	27.0%	9.37 volts	10.07 volts
				2	28μV	37.2mV				
				3	11μV	17.0mV				
				4	4μV	8.91mV				

Application of Thesis Work

The Cuk and SEPIC can be used in industry if the flexibility of either higher or lower input voltage converter is needed. This flexibility can be harnessing various battery types and connections to communication equipment. Telecommunication equipment generate harmonics on a power line it is connected too[Singh] and this randomization technique could be utilized to adjust the discrete harmonic levels. If a range of battery voltage sources are available then the converters could accept those wide range of voltage inputs, adjust the discrete harmonic and supply the required voltage for the equipment connected to it. Evaluation of randomization PWM techniques could be utilized without having to purchase filters. This adds the flexibility of adjusting harmonics on the power line through a software change and does not the need to purchase a separate filter.

Future Work

The parameters for this thesis was 36kHz operating frequency, 7 volts input voltage, the randomization PWM techniques of RPWM, RPPM and both RPWM & RPPM and the basic circuit configuration of the Cuk and SEPIC converter. For future work, experiments could focus on increasing any of those parameters: frequency or voltage levels to determine if converters still behave similarly. Additionally, different randomized PWM techniques could be included to determine if the same results are witnessed when the Cuk and SEPIC converters are randomized.

References

Alexander, C. K., & Sadiku, M. N. O. (2007). *Fundamentals of electric circuits* (Third). Boston: McGraw-Hill.

Aminian, A., and Kazimierczuk, M. K. (2004). *Electronic Devices: a design approach.* Upper Saddle River (N.J.): Person Prentice Hall.

Arduino. (n.d.). Arduino Due. Retrieved May 4, 2020, from https://store.arduino.cc/usa/due

Arduino. (n.d.). Arduino Uno REV3. Retrieved May 4, 2020, from https://store.arduino.cc/usa/arduino-uno-rev3

Arduino. (February 2, 2019). Random(). Retrieved May 4, 2020, from https://www.arduino.cc/reference/en/language/functions/random-numbers/random/

Arduino. (June 21, 2019). delayMicrosecond(). Retrieved May 4, 2020 from https://www.arduino.cc/reference/en/language/functions/time/delaymicroseconds/

Arduino. (June 26, 2019). digitalWrite(). Retrieved May 4, 2020 from https://www.arduino.cc/reference/en/language/functions/digital-io/digitalwrite/

Dugan, R. C., Beaty, H. W., Santoso, S., and McGranaghan, M. F. (2012). *Electrical Power Systems Quality* (Third). McGraw Hill Professional Publishing.

Faisal, M., Yousaf., and Nah, W. (2019). Effect of Random Modulation Switching Schemes on Harmonics and CE Levels of a Buck Converter. *2019 International SoC Design Conference (ISOCC).* Doi: 10.1109/isocc47750.2019.902774

Fuchs, E. F., and Masoum, M. A. S. (2015). *Power Quality in Power Systems and Electrical Machines.* Amsterdam; Boston: Academic Press/Elsevier.

Hammerbauer, J., & Stork, M. (2013). State Space Study of the SEPIC Converter. *2013 International Conference on Applied Electronics*, 1-4.

Jadeja, R. Ved, A. & Chauhan, S. (2015). An Investigation on the Performance of Random PWM Controlled Converters. Engineering, Technology & Applied Science Research, 5(6), 876-884.

Kazimierczuk, M. (2016). *Pulse-Width Modulated DC-DC Power Converters (Second).* Chichester, West Sussex, United Kingdom:Wiley

Krein, P. T. (2016). *Elements of Power Electronics* (International 2nd ed.). New York: Oxford University Press.

Kushwaha, B. K., & Narain, A. (2012). Controller design for Cuk converter using model order reduction. *2012 2nd International Conference on Power, Control and Embedded Systems*. doi: 10.1109/icpces.2012.6508134

Langella, R., Testa, A., & Emanuel, A. E. (2012). Unbalance Definition for Electrical Power Systems in the Presence of Harmonics and Interharmonics. *IEEE Transactions on Instrumentation and Measurement,* 61(10, 2622-2631. Doi: 10.1109/tim.2012.2209909

MathWorks. (n.d.) Power_fftscope. Retrieved May 3, 2020, from https://www.mathworks.com/help/physmod/sps/powersys/ref/power_fftscope.html

Mathworks. (n.d.). powergui. Retrieved May 4, 2020, from https://www.mathworks.com/help/physmod/sps/powersys/ref/powergui.html

MathWorks. (n.d.). Fft. Retrieved May 3, 2020, from https://www.mathworks.com/help/matlab/ref/fft.html

MathWorks. (n.d.). Fourier Transforms. Retrieved May 3, 2020, from https://www.mathworks.com/help/matlab/math/fourier-transforms.html

Mihalič, F. (2012). Improved EMC of Switched-Mode Power Converters with Randomized Modulation. *Automatika*, 53(2), 173-183. DOI:10.7305/automatika.53-2.166

Mohan, N., Undeland, T. M., & Robbins, W. P. (1995). *Power electronics: converters, applications and design* (Second). Cañada: John Wiley & Sons.

Mutagi, R. (2004). Understanding the Discrete Fourier Transform. *R. F. Design, 27(1)*, 34, 36, 38, 40.

Nise, N.S. (2011). *Control System Engineering* (Sixth). Hoboken, NJ: Wiley

Singh, S., Bhuvaneswari, G., & Singh, B. (2011). Power Quality Improvement in Telecommunication Power Supply System using Buck Rectifier. 2011 Annual IEEE India Conference, doi: 10.1109/indcon.2011.6139526

Tektronix. *TDS1000- and TDS2000-Series Digital Storge Oscilloscope.* Beaverton; OR

Tse, K., Chung, H., Hui, S., & So, H. (2000). A comparative investigation on the use of random modulation schemes for DC/DC converters. IEEE Transactions on Industrial Electronics, 47(2), 253-263.

Zhang, B. (2015). *Sneak Circuits of Power Electronic Converters* (First, Vol. 9781118379943). John Wiley & Sons.